Politecnico di Torino

Politecnico di Torino

Master's Degree in Energy and Nuclear Engineering

A.a. 2025/2026

Graduation Session March 2026

Development of an Offshore Floating Photovoltaic System in Australia

Supervisor:

Giovanni Bracco

Wenhua Zhao

Cosupervisor:

Yunil Chu

Author:

Simona Scuccimarro

The University Of Queensland
AUSTRALIA
CREATE CHANGE

Abstract

This thesis investigates the feasibility, design requirements and techno - economic performance of a coastal floating photovoltaic (FPV) system proposed along the western shores of North Stradbroke Island, in Moreton Bay region of Brisbane (East Queensland). The research responds to increasing interest in floating solar technologies as a solution to land use constraints, rising electricity demand and the transition toward low carbon, climate resilient energy systems in high irradiance regions such as Australia. The study first defines the global and national context of renewable energy and examines the environmental characteristics of South East Queensland. A particular focus is given to North Stradbroke Island, a site that combines favorable solar resources and relatively sheltered coastal waters with engineering challenges, including wave loading, wind stresses, corrosion risks and ecological sensitivity. A comprehensive site assessment is conducted by analyzing solar irradiance, wind patterns, wave climate, bathymetry and marine conditions. These parameters inform the conceptual design of a modular, marine grade FPV system suitable for high UV and high salinity environments. The design framework addresses float materials, structural configuration, mooring and anchoring systems, hydrodynamic behaviour, electrical layout and scalability to ensure durability and operational reliability. Installation and maintenance strategies are evaluated, considering marine access, deployment logistics, inspection protocols, cable management and weather-related constraints. A techno-economic analysis is performed to estimate the Levelised Cost of Energy (LCOE), incorporating capital and operational costs, degradation rates, annual energy yield and sensitivity analyses. The results highlight key technical and economic factors influencing coastal FPV viability and demonstrate the potential contribution of floating solar systems to the renewable energy portfolio of Moreton Bay region.

Table of Contents

List of Tables VI

List of Figures VII

1 Introduction 1
- 1.1 Content of the Thesis . . . 1
- 1.2 Key Challenges . . . 3

2 Floating Photovoltaics: Context, Challenges and Opportunities 4
- 2.1 Why Floating Solar . . . 4
- 2.2 FPV Technology Overview . . . 6
- 2.3 Global and National Landscape . . . 12
- 2.4 Benefits and Challenges . . . 15

3 Sites selection for FPV Deployment 17
- 3.1 North Stradbroke Island: Ecological, Cultural and Strategic Context 17
- 3.2 [Strategic Site Selection for FPV system installation . . . 19

4 Data Collection and Analytical Assessment of Climatic and Marine Parameters 23
- 4.1 Climate Resource Assessment . . . 23
- 4.2 Marine Parameters . . . 28

5 Structural Design and Engineering Configuration of the FPV System 31
- 5.1 Selection of Floating Structure: Framed Offshore Platform with Perimeter Buoyancy . . . 32
- 5.2 PV Module Selection . . . 34
- 5.3 Floating Platform Materials . . . 36
- 5.4 Mooring and Anchoring System . . . 38
- 5.5 Electrical System and Grid Connection . . . 40

5.6 Installation, Accessibility and Maintenance Considerations 42

6 System Design and Hydrodynamic Modelling of the Offshore Floating PV Array 47
6.1 Design Basis and Sizing of system 47
6.2 Numerical model construction in AQUASIM Software 54
6.3 Environmental conditions and Hydrodynamic forces 63
6.4 Simulation results 67

7 Techno-Economic Evaluation of the FPV System 79
7.1 Economic Assessment Methodology 79
7.2 Components Cost Estimation 80
7.3 Annual Energy Production for Economic Evaluation 82
7.4 Capital Cost Estimation (CAPEX) 86
7.5 Operation and Maintenance Cost Estimation (OPEX) 88
7.6 Levelised Cost of Energy Analysis (LCOE) 89
7.7 Discussion of Techno-Economic Performance 90

8 Conclusions and Future Research Perspectives 92

Bibliography 95

List of Tables

4.1 Principal parameters governing photovoltaic performance for the proposed location in southeast Queensland (source [33]). 24

6.1 Main design parameters of the HDPE buoy element in AquaEdit . . 58
6.2 Main design parameters of the rigid platform in AquaEdit 59
6.3 Main design parameters of the synthetic rope in AquaEdit 61
6.4 Main design parameters of the steel chain in AquaEdit 62
6.5 Comparison between theoretical and simulation value 67

7.1 HDPE floater cost estimation 80
7.2 Aluminium platform cost estimation 81
7.3 Steel support cost estimation 81
7.4 Photovoltaic panel Jinko Solar Tiger Neo N-Type data 82
7.5 Estimation of the annual energy produced 83
7.6 Overall cost estimation of the floating platform 86
7.7 Capex, Opex and LCOE for the system studied 90

List of Figures

1.1 Overview of the methodological framework adopted in this project for the study of the offshore FPV system (adapted from [1]). 2

2.1 Data on future floating solar growth (source [3]) 5

2.2 Schematic representation of a floating photovoltaic plant and its principal components (source [6]) 7

2.3 Examples of individual floater units and interconnected floating island configurations used in semi-submerged rigid FPV systems (source [7]). 8

2.4 Interconnected flat-panel rigid floating photovoltaic modules (source: [7]). 9

2.5 Flexible floating photovoltaic system based on a tensioned membrane (source: [7]). 9

2.6 Principal anchoring typologies for FPV systems: (a) pile anchoring, (b) bank anchoring and (c) bottom anchoring (source [8]). 10

2.7 Example of helical anchor system (source [9]). 11

2.8 Floating solar farm equipped with a central inverter installed on a dedicated floating island and distributed string inverter mounted directly on the floating array (source [10]) 11

2.9 Renewable share of annual power capacity expansion (source [13]). . 12

2.10 Renewable Capacity Highlights (source [13]). 13

2.11 Cumulative installed renewable power capacity by continent at the end of 2024 (GW), including solar photovoltaic and wind power systems (source [13]). 13

2.12 Summary of key benefits, challenges and feasibility consideration for coastal FPV (author's elaboration). 15

3.1 Geographic extent of Moreton Bay and North Stradbroke Island, located along the eastern margin of the bay, considered in this study. The seaward boundary corresponds to the limits of the Moreton Bay Marine Park (highlighted area), while the landward boundary extends slightly inland from the highest tidal line (source [23]). . . . 18
3.2 Detailed view of Moreton Bay indicating the proposed FPV location along the western coast of North Stradbroke Island within the sheltered marine area (source [26]). 19
3.3 Geospatial assessment of the proposed FPV offshore site west of North Stradbroke Island, indicating relative distances to coastline, ferry route and Dunwich Port (source [26]). 20
3.4 Spatial distribution of Global Horizontal Irradiance (GHI) anomalies across Australia relative to the 2007–2020 baseline, highlighting positive deviations in South - East Queensland (source [32]). 21
3.5 Consequence of climatic stressor (source [75]). 22

4.1 Annual solar path and horizon diagram for the selected site, showing seasonal sun trajectories and daily solar elevation angles (source [33]). 25
4.2 Long term annual photovoltaic power output potential (PVOUT, kWh/kWp) across eastern Australia, highlighting the high yield solar resource (source [33]). 25
4.3 Annual wind rose representing direction and distribution for the selected site west of North Stradbroke Island (source [34]). 26
4.4 Monthly mean Significant Wave Height (Hs) recorded in Moreton Bay during 2024 (source [38]). 28
4.5 Bathymetric overview of Moreton Bay illustrating its semi enclosed morphology and connection to the Coral Sea (source [40]). 29

5.1 Conceptual illustration of the offshore floating photovoltaic system configuration considered in this thesis (author's elaboration). 32
5.2 Schematic representation of a glass–backsheet photovoltaic (PV) module, showing the layered arrangement of glass (source [51]). . . 34
5.3 Example of elevated support for PV above the deck (source[53]). . . 35
5.4 Blocks of HDPE material for offshore application (source [59]). . . . 36
5.5 Example of synthetic ropes for offshore application (source [63]). . . 38
5.6 Force decomposition in the adopted mooring configuration showing horizontal wind load, total line tension and vertical uplift component acting on the helical anchor (author's elaboration). 39
5.7 Overview of the electricity grid infrastructure in the Brisbane, Redland City and North Stradbroke Island area (source [66]). 40

5.8 Comparison between offshore and onshore inverter configurations for the 500 kWp FPV system (author's elaboration). 42
5.9 Trasport operation of a floating PV island by boats (source [55]). . 43
5.10 Illustration of O&M approach for FPV systems (source [75]). 44
5.11 Illustration of a FPV cleaning (source [46]). 45

6.1 Reduced AquaEdit model of the offshore FPV system in isometric view 54
6.2 Improvement AquaEdit model of the offshore FPV system in top view 55
6.3 Geometrical definition of the perimeter buoy element in AquaEdit . 56
6.4 Environment data simulation on AQUASIM Software 63
6.5 Most important wave measurement (source [90]). 64
6.6 Wave profile simulated on Software AQUASIM 65
6.7 Hydrodynamic simulation results on AQUASIM Software 67
6.8 3D results simulation in AquaView 69
6.9 Mass centre results on AQUASIM Software 69
6.10 4 nodes (NE - NW - SE - SW) fairlead mooring displacement along Z of model in AQUASIM 70
6.11 Spatial distribution of platform pitch, expressed in AQUASIM as rotation about the Y-axis, highlighting the angular gradient across opposite sides of the structure. 73
6.12 Time history of pitch response, expressed as rotation about the Y-axis, with oscillations approximately ranging from -1.0° to +1.9° in AquaView 73
6.13 Spatial distribution of rotation about the X-axis, representative of the wave induced roll motion of the floating platform in AquaView. 74
6.14 Time history of rotation about the X-axis in AquaView. 74
6.15 Time history of rotation about the X-axis in AquaView. 75
6.16 Time history of rotation about the X-axis in AquaView. 75
6.17 Local section stresses acting on SW mooring attachment node of model in in AquaView. 76
6.18 Von Mises [MPa] acting on mooring lines (NE - NW - SE - SW) model in in AquaView. 77

7.1 Mean daily production of solar panels in North Stradbroke Island (source [104]). 84
7.2 Average hourly profile during months in Global Solar Atlas (source [33]). 85
7.3 CAPEX Breakdown of the proposed FPV system (author's elaboration) 87
7.4 FPV O&M costs breakdown (source [75]). 88

1 Introduction

The global transition toward low carbon energy systems has accelerated the deployment of renewable energy technologies worldwide. Australia, characterised by exceptionally high solar irradiance, possesses substantial potential for large scale solar power generation. However, the expansion of ground mounted photovoltaic (PV) plants is frequently constrained by increasing land costs, ecological considerations and public sensitivity to landscape modification. Floating photovoltaic systems offer an alternative by utilising water surfaces rather than terrestrial land. Although FPV technology has expanded rapidly on inland reservoirs and hydropower dams, applications in marine environments remain limited due to greater engineering complexity, hydrodynamic loading, corrosion risks and environmental uncertainty. In Australia, FPV installations are predominantly located in protected freshwater bodies and coastal deployment has not been systematically evaluated. South East Queensland provides a relevant context for such investigation. The region combines increasing electricity demand with environmentally sensitive coastal ecosystems, particularly within Moreton Bay. North Stradbroke Island, located between Moreton Bay and the Coral Sea, represents a distinctive coastal environment where high solar irradiance coincides with moderate hydrodynamic exposure. The western shoreline, facing the sheltered waters of southern Moreton Bay, experiences lower wave energy than the exposed eastern coastline and therefore represents a potential candidate for early stage coastal FPV exploration. This thesis evaluates the feasibility of deploying a conceptual floating photovoltaic system along the western coastline of North Stradbroke Island under realistic environmental, technical and economic constraints. By focusing on a semi-sheltered marine setting, the study addresses a gap in the Australian literature, which has largely concentrated on freshwater FPV systems.

1.1 Content of the Thesis

The research defines clear geographical and thematic boundaries. Geographically, the investigation is restricted to the western shoreline of North Stradbroke Island, where partial protection from offshore wave action results in intermediate hydrodynamic conditions. The fully exposed eastern coastline is excluded due to higher wave heights, deeper bathymetry and structural requirements beyond the scope of a conceptual coastal study. From a thematic perspective, the thesis develops a site pecific conceptual system design rather than a fully detailed offshore engineering solution. The analysis considers the principal components of an FPV installation, including floating platforms, photovoltaic modules, mooring systems, anchoring strategies and electrical connections. Advanced structural dynamic simulations and

comprehensive extreme sea state analyses are not undertaken. The study first identifies suitable areas within the selected coastal zone by examining solar irradiance, wind exposure, wave climate, bathymetry and proximity to grid infrastructure. Environmental and meteorological data are collected and analysed to establish the design basis for the proposed system. A modular floating PV configuration is then proposed, with particular emphasis on structural stability, corrosion resistance, material durability and resilience to ultraviolet radiation and mechanical loading. Installation logistics, marine access, maintenance strategies and cable routing are also assessed to evaluate operational feasibility. The economic analysis assumes an operational lifetime of 20 – 25 years and incorporates capital expenditure, operational costs, projected energy yield, degradation rates, and decommissioning considerations. The Levelised Cost of Energy (LCOE) is calculated, and sensitivity analyses are performed to assess financial robustness. Finally, the thesis provides a preliminary environmental appraisal identifying potential interactions with intertidal habitats, seagrass meadows and nearshore ecosystems. Although not exhaustive, this component establishes a foundation for future detailed environmental assessments.

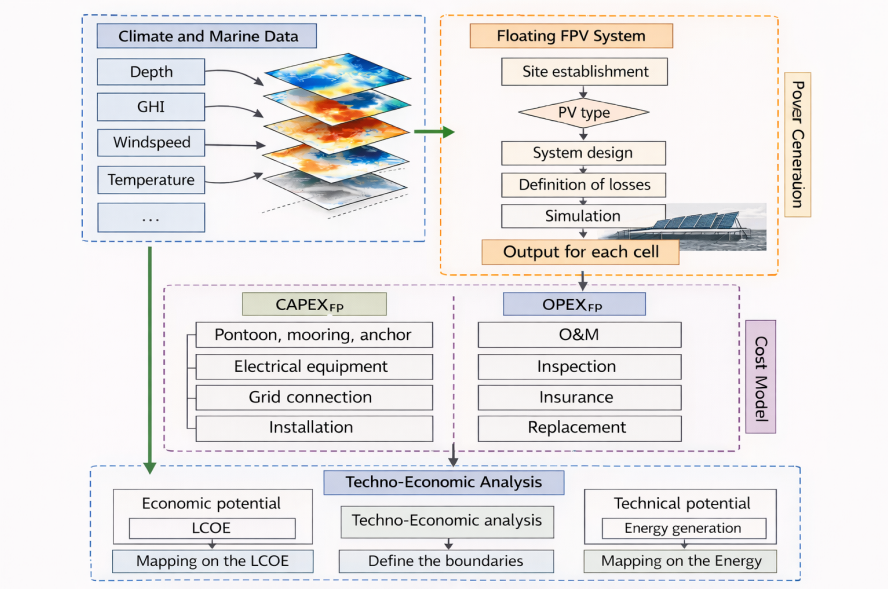

Figure 1.1: Overview of the methodological framework adopted in this project for the study of the offshore FPV system (adapted from [1]).

1.2 Key Challenges

The deployment of floating photovoltaic systems in coastal environments presents several technical and environmental challenges. Unlike freshwater installations, marine setting is characterised by saline conditions that accelerate corrosion and material degradation. Structural components must therefore be designed to withstand long term exposure to saltwater, ultraviolet radiation and cyclic mechanical loading. Hydrodynamic forces constitute a further challenge. Wave action, tidal currents and wind induced loads generate dynamic stresses on floating platforms and mooring systems. Even in semi-sheltered areas such as southern Moreton Bay, these forces require careful consideration in order to ensure structural stability and operational reliability over the system lifespan. Environmental sensitivity also represents a critical factor. Coastal ecosystems, including seagrass meadows and intertidal habitats, may be affected by shading, anchoring systems or construction activities. Any FPV deployment must therefore balance renewable energy generation with ecosystem protection. Finally, economic uncertainty remains a significant barrier to marine FPV expansion. Higher material specifications, installation complexity and maintenance requirements may increase capital and operational costs compared to inland systems. Evaluating whether such projects can achieve competitive LCOE values under realistic assumptions is therefore essential.

2 Floating Photovoltaics: Context, Challenges and Opportunities

This chapter provides an overview of floating photovoltaic (FPV) systems, examining their technical characteristics, deployment trends with the principal benefits and limitations associated with their adoption. The chapter first defines FPV technology outlining its core components and design considerations. Then the floating photovoltaic is placed within the broader global and Australian energy context, highlighting market development and strategic relevance. The chapter concludes with an assessment of the main technical, environmental and economic challenges associated with floating solar systems, thereby establishing the conceptual foundation for the site specific analysis developed in subsequent chapters.

2.1 Why Floating Solar

The growing interest in floating photovoltaic systems is closely linked to the rapid expansion of solar energy and the increasing need to deploy renewable electricity generation without intensifying land use. Continuous technological improvements, large scale manufacturing and economies of scale have significantly reduced the cost of photovoltaic modules and utility scale solar power over the past decade. As a result, solar energy has become one of the most competitive sources of electricity worldwide [2]. Within this evolving energy landscape, FPV systems represent an alternative to conventional ground mounted installations by enabling the productive use of water surfaces, including reservoirs, lakes, dams, irrigation basins and sheltered coastal areas. These surfaces, often underutilised from an energy perspective, offer spatial opportunities that do not compete directly with agricultural land, urban development or conservation areas. At global level, the FPV market is experiencing sustained growth. Recent industry analyses project in which global installed FPV capacity could reach approximately 77 GW by 2033, with the Asia - Pacific region accounting for the majority of this expansion [3]. This trend reflects increasing energy demand, declining capital costs and supportive renewable energy policies in several countries.

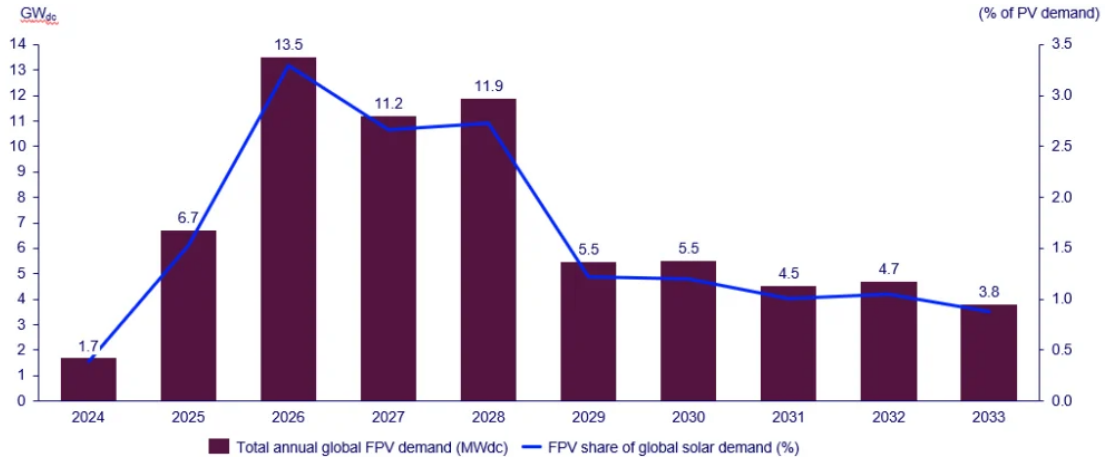

Figure 2.1: Data on future floating solar growth (source [3])

Historically, deployment has been concentrated in densely populated Asian nations such as China, India and Indonesia, where land scarcity has been a significant driver. However, interest in floating solar is expanding to other regions, including Australia [4]. Australian research has begun to evaluate the technical and economic feasibility of FPV systems. A feasibility study conducted on a hydropower reservoir in New South Wales reported that floating installations achieved slightly higher average efficiency compared to ground mounted systems, with module operating temperatures reduced by approximately 5 – 6 °C [5]. Although capital expenditure was estimated to be moderately higher than for ground installations, improved thermal performance and reduced land occupation contributed to favourable overall project performance. These findings suggest that FPV systems may offer tangible advantages within the Australian renewable energy context. One of the primary technical benefits of floating solar installations is the natural cooling effect provided by the underlying water body. The presence of water acts as a thermal buffer, reducing module operating temperature relative to ground systems. Since PV efficiency decreases with increasing temperature, this cooling effect can enhance energy yield and potentially reduce long term thermal degradation. Such behaviour is particularly relevant in regions characterised by high solar irradiance and elevated ambient temperatures, conditions typical of many Australian inland and coastal areas. In addition to performance related advantages, FPV systems contribute to more efficient spatial planning. By utilising water surfaces for energy generation, terrestrial land can be preserved for agriculture, infrastructure or environmental conservation. This consideration is increasingly important in regions experiencing population growth and expanding urbanisation. Furthermore, floating installations can often be located closer to electricity demand centres, particularly in coastal regions, thereby reducing transmission distances, infrastructure requirements with

associated losses. Within the specific context of this thesis, which investigates a potential installation along the western coast of North Stradbroke Island, FPV technology aligns with several favourable conditions. The site combines high solar resource availability, proximity to existing grid infrastructure and a partially sheltered marine environment characterised by moderate hydrodynamic exposure. These factors collectively support the consideration of FPV as a technically plausible and strategically coherent solution for integrating renewable energy generation within a sensitive coastal setting. Overall, declining photovoltaic costs, demonstrated performance benefits, global market expansion and strategic land use advantages position floating solar as an increasingly viable pathway for renewable energy development.

2.2 FPV Technology Overview

Floating photovoltaic (FPV) systems represent an evolution of conventional ground mounted solar installations. From an electrical perspective, their configuration remains similar: photovoltaic modules generate direct current (DC), which is collected through combiner boxes and converted into alternating current (AC) via inverters before being transmitted to the grid. The principal distinction lies in the structural arrangement, as FPV modules (in some configurations also inverters) are mounted on buoyant platforms deployed over water surfaces. A typical FPV system can be categorized into four main subsystems that work in synergy to generate and transmit power:

- Generation and Buoyancy Subsystem: The core of the plant consists of photovoltaic (PV) modules mounted on specialized floats or pontoons. These structures are engineered not only to support the weight of the panels but also to maintain an optimal tilt angle and facilitate passive cooling due to their close proximity to the water surface.
- Electrical and Conversion Subsystem: Direct current (DC) generated by the modules is collected through combiner boxes. As illustrated in the schematic, the power is then routed to a central inverter, which can be located on a dedicated floating platform or on the shore. The inverter converts the DC into alternating current (AC), making it suitable for distribution.
- Stability and Mooring Subsystem: Unlike land based systems, FPV designs must account for fluid dynamics. This is ensured by a complex system of mooring lines and anchors secured to the bed or the banks. These components allow the structure to withstand hydrodynamic loads, wind gusts and water level variations (such as tides or floods) while maintaining the integrity of electrical connections.

- Transmission and Protection Subsystem: Converted energy is transported to the shore via underwater cables to a substation or transformer, and then fed into the power grid through transmission lines. System safety is ensured by auxiliary devices, such as the lightning protection system visible on the platform.

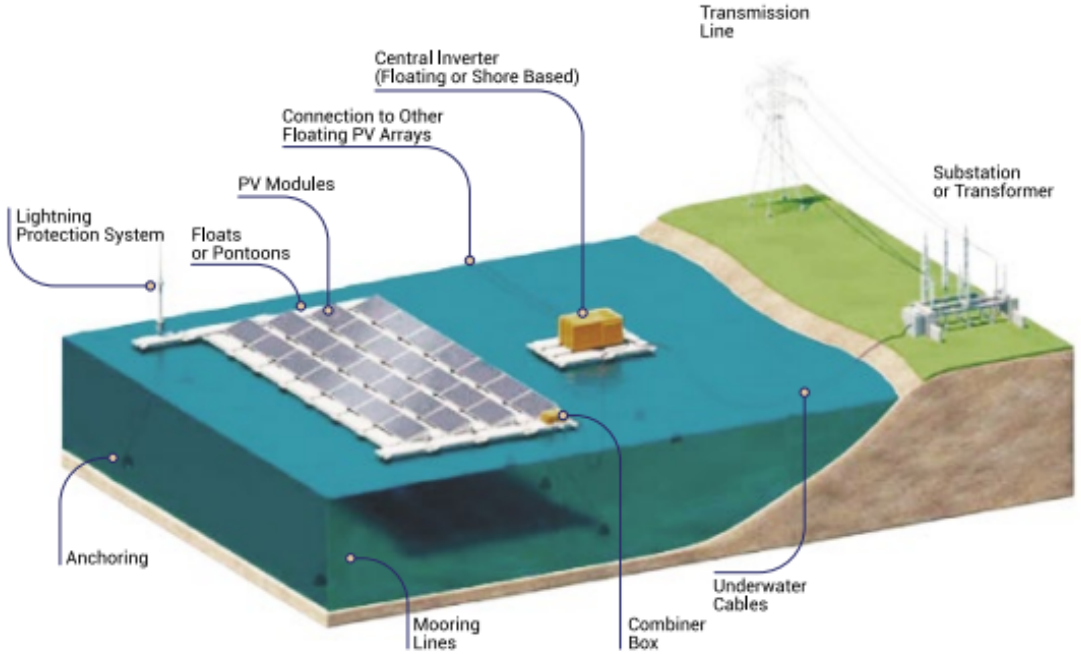

Figure 2.2: Schematic representation of a floating photovoltaic plant and its principal components (source [6])

.

From a hydrodynamic standpoint, floating photovoltaic platforms can be classified into three principal structural categories:

- Semi - submerged rigid multibody systems;
- Flat - panel rigid multibody systems;
- Flexible multibody or single body configurations.

The fundamental building block of a floating solar installation is the floater, a buoyant platform designed to support photovoltaic modules. The characteristic length of an individual floater is typically on the order of several tens of metres. Multiple floaters can be mechanically interconnected to form a larger aggregate structure, commonly referred to as an island. To ensure station keeping and

operational stability, each island must be secured through a suitable mooring system connected to the seabed or shoreline. A complete floating solar farm may consist of multiple interconnected islands arranged within the same site, forming a modular and scalable configuration. In semi - submerged systems, the photovoltaic platform is mounted on a tubular structural frame that provides buoyancy and maintains the modules above the water surface, regardless of wave elevation.The elevated configuration reduces the risk of direct seawater contact and contributes to lowering hydrodynamic loads through structural optimisation.

Figure 2.3: Examples of individual floater units and interconnected floating island configurations used in semi-submerged rigid FPV systems (source [7]).

This design offers several advantages (Figure2.3). The raised deck ensures that panels remain dry and provides accessible working space for inspection and maintenance. However, maintaining an elevated platform in rough sea conditions requires substantial structural reinforcement. Mooring loads are generally higher than in other configurations and interconnection forces between floaters can become significant due to the large mass of individual units, which may weigh several tonnes [7]. These interconnections must allow sufficient flexibility to accommodate wave induced motion while ensuring effective load transfer across the system. The second structural category consists of flat - panel rigid multibody systems (Figure2.4). In this configuration, photovoltaic modules are mounted on a flat floating base positioned slightly above the water level. Unlike semi - submerged systems, the panels are not elevated significantly to remain completely dry. The simplicity of this design results in reduced fabrication and installation costs.

Figure 2.4: Interconnected flat-panel rigid floating photovoltaic modules (source: [7]).

However, the limited freeboard increases the probability of direct contact with seawater during extreme conditions, potentially accelerating material degradation and reducing long term durability. The third category comprises flexible systems employing a tensioned membrane supported by a modular floating frame, typically manufactured from high-density polyethylene (HDPE) (Figure2.5). These structures may be interconnected or independently moored to the seabed.

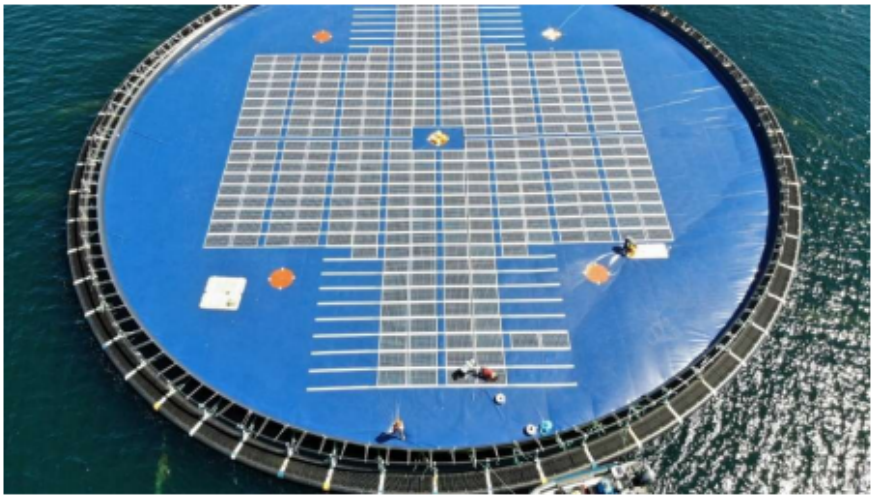

Figure 2.5: Flexible floating photovoltaic system based on a tensioned membrane (source: [7]).

Due to their structural characteristics, flexible systems can accommodate only lightweight or flexible photovoltaic modules. Their primary advantages include reduced structural weight, lower material costs, ease of transport and deployment

[7]. However, continuous exposure to seawater represents a significant limitation. Long term material degradation of membranes remains difficult to predict and dynamic behaviour under wave loading presents additional engineering challenges. Mooring systems are designed to restrict excessive movement of floating structures while allowing controlled response to environmental loads. Anchoring fixes the position of floating plant relative to the seabed or shoreline, preventing displacement due to wind, wave forces, currents or water level variations.

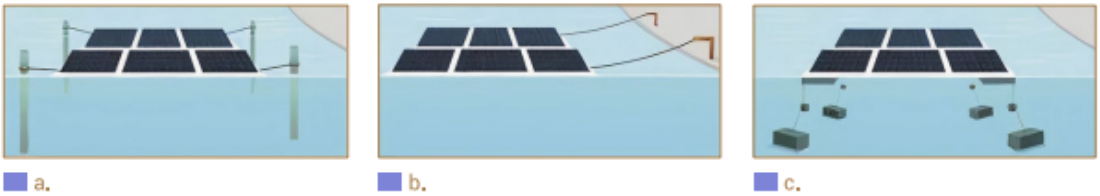

Figure 2.6: Principal anchoring typologies for FPV systems: (a) pile anchoring, (b) bank anchoring and (c) bottom anchoring (source [8]).

Three principal anchoring approaches are commonly adopted in FPV systems:

- Pile anchoring: consists of vertical piles around which the platform can slide in response to water level fluctuations. Although structurally effective, pile installation requires specialised equipment and civil works, resulting in higher costs.

- Bank anchoring connects the floating structure to the shoreline and is particularly suitable for small or shallow basins. It often represents a cost effective solution and facilitates access for installation and maintenance. However, feasibility depends on shoreline conditions and regulatory permissions.

- Bottom anchoring is the most widely used solution in existing FPV installations, ensuring long term station keeping. There are two main categories: gravity based anchors and installed anchors. Gravity based anchors include concrete sinkers, mushroom anchors and pyramid anchors, which rely primarily on weight and partial embedment. Installed anchors, such as helical anchors, are mechanically embedded into the substrate and provide a higher holding capacity, although at an increased installation cost and complexity.

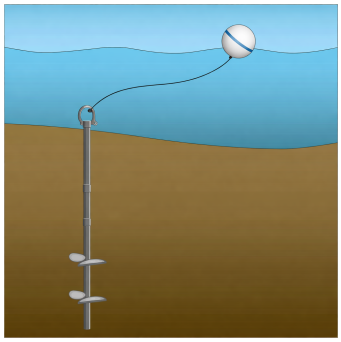

Figure 2.7: Example of helical anchor system (source [9]).

FPV systems can employ either monofacial or bifacial PV modules. In rigid floating configurations, double glass framed modules are generally preferred due to their superior mechanical robustness and enhanced resistance to high humidity environments. Conversely, frameless modules are typically reserved for specific applications, such as membrane based systems, where reduced weight and lower susceptibility to Potential Induced Degradation (PID) offer distinct advantages [11]. Currently, the majority of operational FPV plants utilize crystalline silicon (c-Si) technologies while polycrystalline modules are common in early installations, monocrystalline technology (such as PERC or n-type TOPCon) has become the industry standard due to its higher efficiency and declining costs [12]. From an electrical perspective, FPV plants typically adopt either centralised or decentralised (string) inverter configurations. In utility scale installations, deploying inverters directly on floating platforms minimizes resistive losses by shortening the DC cabling required to reach the shore. Containerised central inverters are often mounted on dedicated, reinforced floats (frequently integrated with transformers) and connected to the onshore substation via medium voltage (MV) submarine cables.

Figure 2.8: Floating solar farm equipped with a central inverter installed on a dedicated floating island and distributed string inverter mounted directly on the floating array (source [10])

Conversely, string inverters can be distributed across the floating array. While these may lead higher initial costs for large scale projects, they offer superior operational redundancy and fault isolation. A localized failure only impacts a small fraction of the total capacity and modular units allow for rapid replacement. To ensure maintenance accessibility, string inverters are strategically positioned at the array periphery, facilitating inspections and repairs via service vessels

2.3 Global and National Landscape

Global energy systems are undergoing an accelerated transformation driven by decarbonisation targets, technological innovation and declining renewable energy costs.

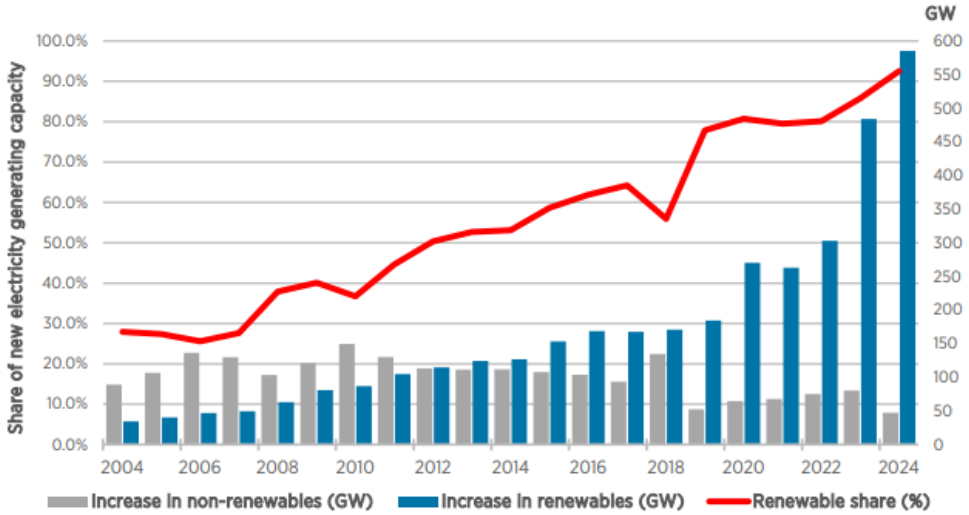

Figure 2.9: Renewable share of annual power capacity expansion (source [13]).

By the end of 2024, total global renewable power capacity reached approximately 4,448 GW, following a record annual increase of 585 GW [13]. Solar photovoltaic technology accounted for the largest share of new installations, with 452 GW added in 2024, bringing cumulative solar capacity to around 1,865 GW. Wind energy also expanded significantly, reaching approximately 1,13 GW after an annual increase of 113 GW. Together, solar and wind represented nearly all net additions to renewable power capacity in 2024.

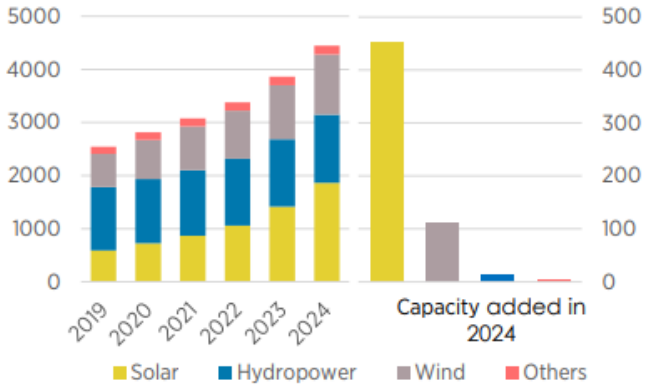

Figure 2.10: Renewable Capacity Highlights (source [13]).

Despite this rapid expansion, the dominance of ground mounted solar and onshore wind has intensified challenges related to land availability, grid integration and environmental constraints [14]. These pressures have stimulated growing interest in offshore and water based renewable technologies. Offshore wind capacity reached approximately 83 GW globally by the end of 2024, reflecting the increasing strategic importance of marine energy resources, particularly in regions characterised by high electricity demand and limited land availability.

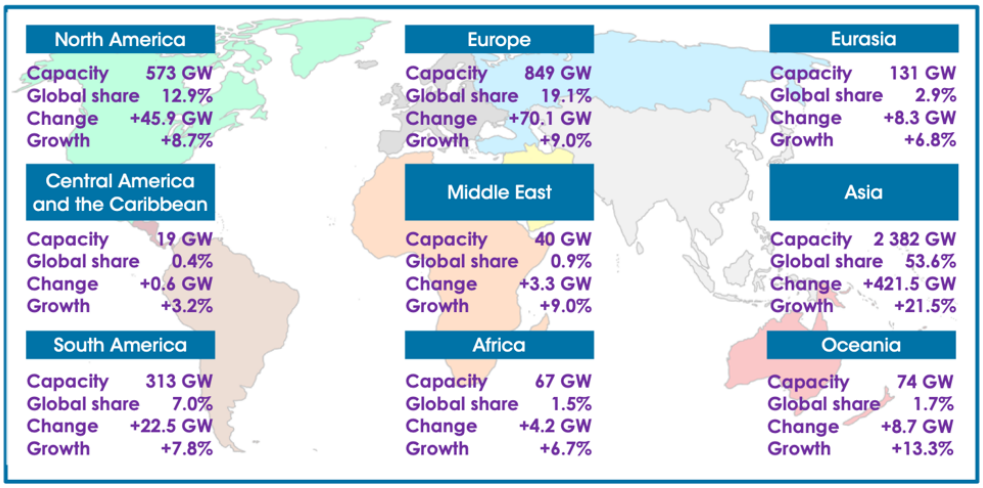

Figure 2.11: Cumulative installed renewable power capacity by continent at the end of 2024 (GW), including solar photovoltaic and wind power systems (source [13]).

Within this evolving landscape, floating photovoltaic (FPV) systems are emerging as a complementary technology capable of expanding solar deployment without

competing for ground land. By utilising reservoirs, lakes, irrigation basins and sheltered coastal waters, FPV offers a spatially efficient solution that may also benefit from reduced module operating temperatures due to water induced cooling effects. In parallel with the broader renewable energy expansion, the floating solar market has entered a phase of sustained acceleration. Recent industry estimates indicate that global FPV capacity additions surpassed 1.8 GW in 2024, marking a record annual increase. Future projections anticipate a compound annual growth rate (CAGR) exceeding 25% over the medium term [15]. Geographically, deployment remains centered in the Asia-Pacific (APAC) region as China, India, Japan and Southeast Asia where acute land scarcity and proactive policy frameworks have catalyzed adoption. From a technical standpoint, the long term potential of FPV is increasing. Continuous innovation in buoyant structures, mooring systems and hydro - solar hybridization is steadily bolstering reliability and narrowing the cost gap with conventional ground mounted PV, despite the lingering premium on capital expenditure (CAPEX). Early stage deployment has focused on wastewater treatment facilities, irrigation basins and agricultural reservoirs, proving the technology viability under local climatic extremes. Beyond electricity generation, these installations offer critical benefits, such as mitigating evaporation and enhancing module efficiency through passive thermal regulation. This momentum is reflected in growing industrial synergies between Australian developers and international technology providers, with a pivot toward advanced circular membrane platforms and hybrid configurations tailored for local conditions. However, water surface rights, rigorous ecological impact assessments and the technical demands of saline or high energy hydrodynamic environments remain pivotal challenges. Furthermore, the requirement for corrosion resistant materials and specialized mooring infrastructure contributes to higher upfront costs [16]. Within this national and global context, the feasibility assessment conducted in this thesis for a floating photovoltaic installation along the western coast of North Stradbroke Island is both timely and strategically aligned with emerging trends in water based renewable energy development.

2.4 Benefits and Challenges

Floating photovoltaic systems offer several advantages compared with conventional ground mounted photovoltaic installations, while also presenting distinct technical, economic and environmental challenges. A balanced assessment of these aspects is essential in order to determine their suitability for large scale deployment, particularly in coastal contexts.

Category	Key Benefits in Coastal Context	Key Challenges in Coastal Context	Implications for Feasibility
Land Use	• Avoids competition with limited coastal land; preserves terrestrial ecosystems and urban areas	• Potential spatial conflicts with marine uses (navigation, recreation, reatre-tion, fish)	• Careful spatial planning and stakeholder coordination
Thermal Performance	• Natural water cooling improves module efficiency under high irradiance conditions	• Salt spray and humidity may offset performance gains through material degradation	• Necessite careful spatial planning and stakehole-er coordination
Infrastructure Synergy	• Proximity to coastal demand centres and existing grid infrastructure	• Submarine cabling and marine installation increase technical complexity	• Electrical layout and grid connection must be optimized
Hydrodynamics	• Semi-sheltered waters may offer moderate wave climate suitable for FPV	• Exposure to waves, currents, tidal variation, and storm events	• Robust mooring and anchoring design required
Structural Durability	• Modular floating systems allow scalability and adaptability	• Saltwater corrosion, UV exposure, and cyclic loading accelerate fatigue	• Material selection and lifecycle analysis are critical
Environmental Impact	• Reduced terrestrial footprint compared to ground-mounted PV	• Potential impacts on marine ecosystems (shading, water stratification, biodiversity)	• Site-specific environmental
Water Management	• Possible reduction in surface evaporation	• Monitoring strategies required for long-term operation	• Monitoring strategies required for long-term operation
Operations & Maintenance	• Modular design facilitates phased deployment	• Access requires vessels, inspection of moorings and anchors more complex	• Maintenance logistrics into the meágn stage

Figure 2.12: Summary of key benefits, challenges and feasibility consideration for coastal FPV (author's elaboration).

One of the primary advantages of FPV lies in its capacity to mitigate land use constraints. In densely populated regions or areas characterised by competing land demands mounted solar plants may entail high acquisition costs and significant opportunity trade-offs. By contrast, FPV systems utilise existing water bodies, including reservoirs, irrigation basins and sheltered coastal areas, thereby preserving ground land for alternative uses [17]. This spatial flexibility represents a strategic advantage in regions experiencing rapid demographic and infrastructural growth. A further benefit derives from the thermal interaction between the floating array and the water surface [18]. The presence of water beneath the modules promotes heat dissipation, resulting in lower operating temperatures compared with conventional systems. Since PV efficiency decreases with increasing temperature, this natural

cooling effect can enhance energy yield, particularly in warm climates. Reported performance gains vary depending on environmental conditions and system configuration, but temperature reductions and efficiency improvements are observed in empirical studies. FPV installations may also contribute to water resource management. By partially covering the water surface, floating arrays reduce direct solar irradiation and wind driven evaporation [20]. In reservoirs used for irrigation, industrial supply or drinking water, this effect can generate measurable water savings. Additionally, FPV systems can be integrated with existing infrastructure, such as hydropower reservoirs or water treatment facilities where grid connection points already exist. Such integration can reduce transmission requirements and facilitate hybrid renewable energy systems. Despite these advantages, FPV technology involves higher capital and installation costs than conventional systems. The additional expenditure is primarily associated with floating structures, anchoring and mooring systems, corrosion resistant materials and more complex installation logistics. While module and inverter costs have declined significantly in recent years, the structural and marine components of FPV systems still introduce a cost premium. Structural stability represents a critical engineering challenge. Floating platforms must withstand wind loads, wave action, water level fluctuations and current induced forces over operational lifetimes typically ranging from 20 to 25 years. Mooring systems must be designed to limit excessive displacement while accommodating environmental loads and cyclic stresses. In coastal or near-shore environments, these demands become more severe due to saltwater corrosion, storm events and increased hydrodynamic exposure. Operational and maintenance considerations are also more complex than in land based PV plants [19]. Access to floating arrays may require vessels and periodic inspection of anchors and mooring lines is essential to ensure long term stability. Electrical components are exposed to elevated humidity and salinity, which can accelerate corrosion and reduce durability. Biofouling phenomena, including the accumulation of algae or marine organisms on structural elements, may further affect buoyancy and maintenance requirements. Environmental impacts, although generally lower in terms of land disturbance, must also be carefully evaluated. The shading of water surfaces may alter light penetration, temperature stratification and marine ecosystems. Potential effects on water quality, biodiversity and ecological balance remain areas of ongoing research. Regulatory approval processes may therefore require detailed environmental assessments, especially in multi use water or ecologically sensitive areas. In the specific case of coastal or semi-coastal deployment, such as the site examined in this thesis, both benefits and challenges are amplified. The combination of high solar irradiance, limited land availability and proximity to existing infrastructure strengthens the strategic rationale for FPV adoption. Conversely, anchoring complexity, corrosion risk, hydrodynamic loading and environmental sensitivity necessitate rigorous site specific design and risk assessment.

3 Sites selection for FPV Deployment

This chapter presents a focused geographical overview with initial characterisation of the proposed floating photovoltaic (FPV) installation site. The analysis outlines the principal physical, environmental and infrastructural attributes of the selected location, establishing the contextual basis for subsequent technical evaluation. The discussion is followed by a structured account of the selection criteria and the motivations underlying the choice of this site. Particular emphasis is placed on the alignment between specific characteristics of the site and the technical requirements of FPV deployment. These requirements include metocean conditions, bathymetric profile, proximity to grid infrastructure and accessibility. In addition to engineering considerations, broader contextual factors are examined. These include environmental sensitivity and spatial compatibility with existing coastal and marine activities. The objective is to demonstrate that the selected location satisfies both technical constraints and strategic planning criteria.

3.1 North Stradbroke Island: Ecological, Cultural and Strategic Context

North Stradbroke Island is located approximately 30 km southeast of Brisbane, Queensland, forming part of a large chain sand islands that separate Moreton Bay from the Pacific Ocean, together with South Stradbroke Island and Moreton Island. The island extends approximately 38 km in length and 11 km in width, with Main Beach stretching for over 30 km along the eastern ocean facing side [21], [24]. The island supports a wide range of interconnected terrestrial and marine ecosystems, including coastal dunes, freshwater lakes, wetlands and mangroves. The surrounding waters of Moreton Bay host diverse marine fauna, including turtles, sharks and migratory whales, reflecting the ecological significance of the region [22]. These environmental characteristics indicate a high level of ecological sensitivity that must be carefully considered in any infrastructure development. North Stradbroke Island also holds substantial cultural importance. Large portions of the island are subject to native title recognition and co-management arrangements aimed at preserving cultural heritage and ecological integrity. Any development initiative must therefore account for both environmental protection and Indigenous cultural values.

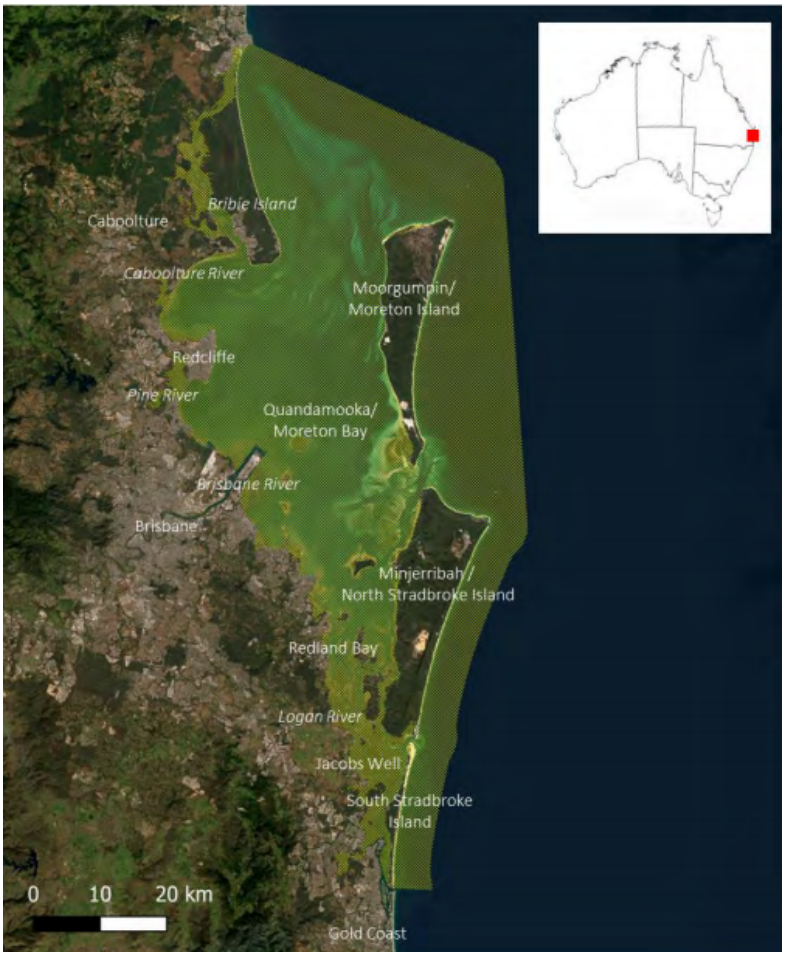

Figure 3.1: Geographic extent of Moreton Bay and North Stradbroke Island, located along the eastern margin of the bay, considered in this study. The seaward boundary corresponds to the limits of the Moreton Bay Marine Park (highlighted area), while the landward boundary extends slightly inland from the highest tidal line (source [23]).

From a strategic and technical perspective, the western coastline of the island, facing the sheltered waters of southern Moreton Bay, presents characteristics potentially compatible with floating photovoltaic deployment. Compared to the exposed eastern coastline, this area experiences reduced wave energy and lower swell intensity, offering relatively moderate hydrodynamic conditions. In addition, proximity to the Brisbane metropolitan area provides potential access to grid infrastructure and logistical support, facilitating installation and maintenance operations while enabling renewable generation close to demand centres. Overall, North Stradbroke Island represents a context in which ecological sensitivity, cultural

heritage and renewable energy development intersect. This dual environmental and strategic dimension reinforces the need for a site specific feasibility assessment capable of balancing technical viability with sustainability considerations.

3.2 Strategic Site Selection for FPV system installation

The selection of an installation site represents a decisive stage in the design of a coastal floating photovoltaic (FPV) system. The proposed site is located on the western coast of North Stradbroke Island (27° 33′ 19″ S, 153° 22′ 53″ E), within the waters of southern Moreton Bay [25].

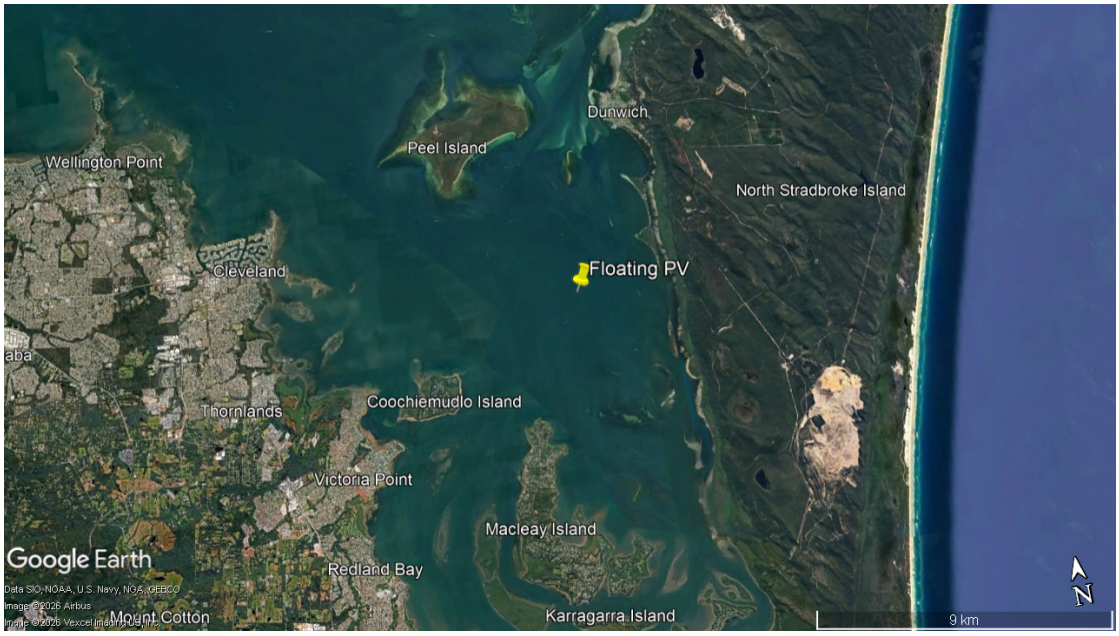

Figure 3.2: Detailed view of Moreton Bay indicating the proposed FPV location along the western coast of North Stradbroke Island within the sheltered marine area (source [26]).

One of the main advantages of this location is its relatively protected hydrodynamic setting. Unlike the exposed eastern coastline of the island, the western side benefits from the natural shelter provided by the morphology of Moreton Bay and by the presence of intermediate landforms such as Peel Island, Coochiemudlo Island and Macleay Island. These features reduce the effective wind fetch and attenuate swell propagation from the Coral Sea, resulting in lower wave heights and current velocities. Such moderate marine conditions are particularly favourable for FPV

deployment, as they reduce hydrodynamic loading on the floating structure, limit cyclic mechanical stresses, and mitigate fatigue effects on mooring lines, electrical connections and structural components. The bathymetric and seabed characteristics of the area further enhance site suitability. Western Moreton Bay is generally characterised by shallow to moderate water depths, typically ranging from 6 to 20 m, which are considered advantageous for coastal FPV systems [27]. These depths allow the adoption of anchoring solutions with relatively limited mooring line lengths and reduced underwater cabling complexity, thus contributing to a more practical and cost effective installation. In addition, available regional information suggests the presence of predominantly sandy or sandy - mud seabed conditions, which are generally compatible with gravity based or helical anchoring systems for soft sediments [27]. From an operational perspective, the selected site also offers favourable logistical conditions. The installation is located approximately 4 km offshore, representing a reasonable compromise between protection from nearshore disturbances and accessibility for inspection and maintenance. Its proximity to Dunwich Port, situated at approximately 5 km, provides a convenient base for vessel operations, personnel transfer and material transport [29]. In addition, the site is located outside the principal navigation corridors (around 1.5 km), including the main ferry route between Cleveland and Dunwich, thereby reducing potential conflicts with maritime traffic and limiting risks associated with vessel wake and collision.

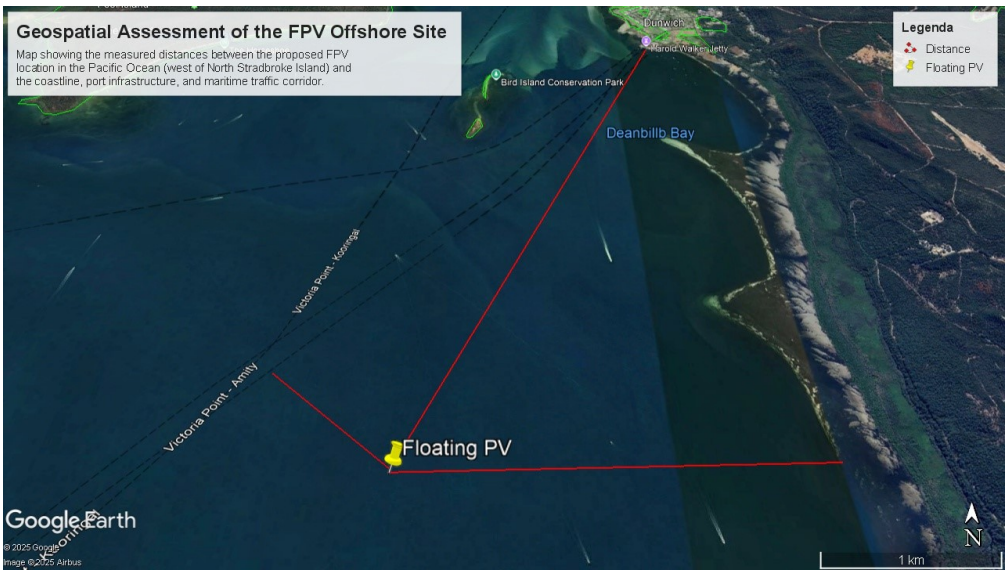

Figure 3.3: Geospatial assessment of the proposed FPV offshore site west of North Stradbroke Island, indicating relative distances to coastline, ferry route and Dunwich Port (source [26]).

Furthermore, the presence of electricity distribution infrastructure on the island creates the possibility of integrating generated electricity into the local network. At the same time, the relative proximity to mainland grid infrastructure in South - East Queensland supports the feasibility of submarine cable connection without excessive transmission distances, with consequent benefits in terms of resistive losses and balance of system (BoS) costs. The regulatory framework is also relatively favourable. According to the Marine Parks Zoning Plan (Moreton Bay) [30], the proposed site lies within a General Use Zone, where anchoring and marine activities are permitted subject to environmental and regulatory approval. This classification suggests a less restrictive permitting pathway than areas subject to higher protection levels. The solar resource available at the site provides a further strong argument in support of its selection. The area is characterised by high levels of Global Horizontal Irradiance (GHI), generally in the range of 1700 - 2000 kWh/m^2/year [31], which places the region among the most favourable in Australia for solar energy applications.

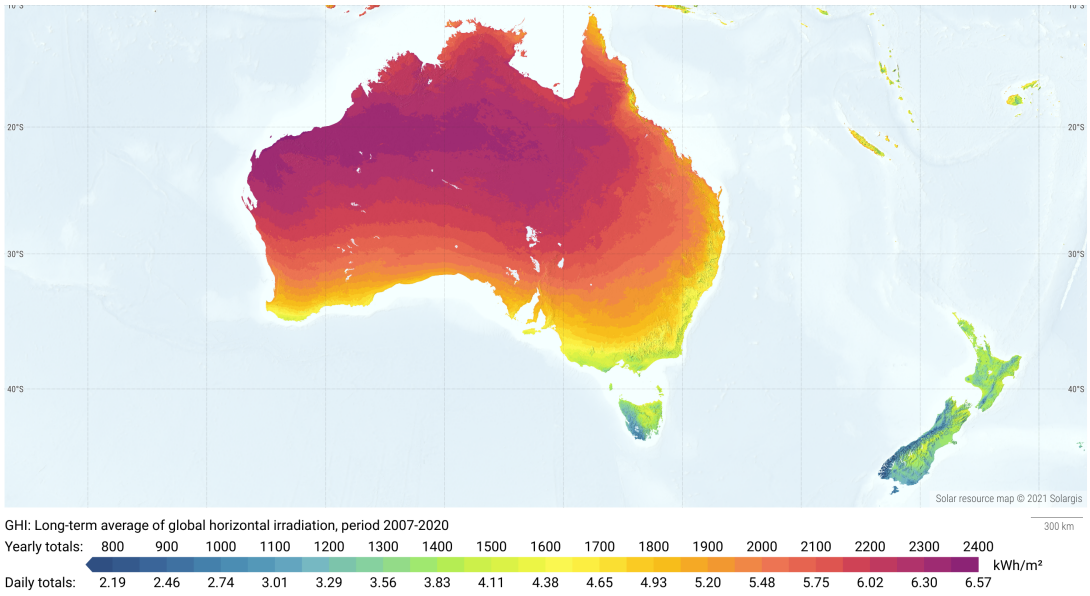

Figure 3.4: Spatial distribution of Global Horizontal Irradiance (GHI) anomalies across Australia relative to the 2007–2020 baseline, highlighting positive deviations in South - East Queensland (source [32]).

Recent anomaly analyses also indicate positive deviations from long term climatological averages, confirming the robustness of the local solar resource and its suitability for reliable annual electricity generation. Thermal conditions are similarly supportive: meteorological data from the Point Lookout station show moderate seasonal variability, with mean minimum temperatures ranging from

about 22 - 23 °C in summer to 13 - 15 °C in winter. Climatic conditions are also a key factor in FPV system assessment, as prolonged exposure to marine atmospheric stressors may influence component degradation, increase the likelihood of failure modes and reduce overall system performance over time.

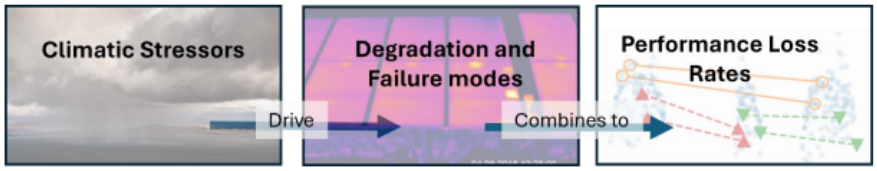

Figure 3.5: Consequence of climatic stressor (source [75]).

This climatic stability, combined with the thermal buffering effect of the surrounding seawater, is expected to lower module operating temperatures compared with conventional land based PV systems, thus reducing thermal efficiency losses and potentially limiting long term material degradation [75]. Overall, the selected site combines

- favourable solar availability;
- naturally sheltered hydrodynamic conditions;
- suitable bathymetry and seabed properties;
- good logistical accessibility and feasible grid connection options

Taken together, these characteristics support the preliminary feasibility of the proposed location for the deployment of a coastal FPV system in southern Moreton Bay.

4 Data Collection and Analytical Assessment of Climatic and Marine Parameters

This chapter presents the systematic collection and analytical evaluation of the climatic and marine parameters characterising the site selected for the proposed floating photovoltaic installation. The purpose of this analysis is to quantify the environmental conditions that govern system performance, structural response, operational reliability and long term feasibility. In coastal FPV applications, environmental forcing constitutes a primary design driver, influencing energy yield estimation, anchoring requirements, material durability, and maintenance strategies. The assessment encompasses the principal environmental variables relevant to both energy production and structural integrity, including:

- Solar resource, expressed through its irradiance components
- Wind regime, considering both annual averages and potential extreme conditions
- Wave and tidal characteristics, which determine hydrodynamic loading and mooring design constraints
- Ambient temperature, which affects photovoltaic conversion efficiency and long term material performance

By integrating these datasets, the chapter establishes the environmental design basis necessary for subsequent technical modelling, economic evaluation and structural considerations. The analysis therefore serves as the quantitative foundation upon which the feasibility of the proposed FPV system is assessed. The present section begins with a detailed evaluation of solar irradiance, as this parameter directly determines the theoretical and expected photovoltaic energy production at the site. Subsequent sections will address wind, wave, tidal and thermal conditions, thereby providing a comprehensive environmental framework for the proposed installation.

4.1 Climate Resource Assessment

The long term solar and climatic characteristics of the selected offshore site are obtained from the Global Solar Atlas database. The principal parameters governing photovoltaic performance are summarised in the Table 4.1, which reports the annual irradiation components for the proposed FPV location.

MAP DATA	SIMBOL	VALUES PER YEAR
Direct Normal Irradiation	DNI	2013.9 kWh/m^2
Global Horizontal Irradiance	GHI	1861.5 kWh/m^2
Diffuse Horizontal Irradiance	DIF	621 kWh/m^2
Global Tilted Irradiation at optimum angle	GTIopta	2051.9 kWh/m^2

Table 4.1: Principal parameters governing photovoltaic performance for the proposed location in southeast Queensland (source [33]).

The site is characterised by an high level of annual solar availability, typical of coastal subtropical regions of Australia. The Global Horizontal Irradiation (GHI), equal to 1861.5 kWh/m^2/year, represents the total solar radiation incident on a horizontal surface and includes both direct beam and diffuse components [33]. It is commonly expressed as:

$$GHI = DNI \cdot \cos(\theta_z) + DIF$$

where DNI is the direct normal irradiation, θ_z is the solar zenith angle and DIF is the diffuse horizontal irradiation. A GHI value above approximately 1700 kWh/m^2/year is generally considered highly favourable for photovoltaic deployment [33]. The recorded value therefore places the selected site within the upper range of productive Australian locations, supporting strong annual energy yield potential. The Direct Normal Irradiation (DNI), equal to 2013.9 kWh/m^2/year, quantifies the solar radiation received by a surface always perpendicular to the rays of sun and represents only the direct beam component. Although DNI is primarily relevant for concentrated solar power systems, high values also indicate frequent clear sky conditions and strong beam radiation, reflecting overall atmospheric clarity. The magnitude observed at the site confirms the presence of intense solar resource conditions. The Diffuse Horizontal Irradiation (DIF), equal to 621.0 kWh/m^2/year, represents the portion of solar radiation scattered by atmospheric constituents such as clouds, aerosols and humidity. This value suggests moderate atmospheric scattering and seasonal cloud variability, typical of coastal Queensland [33]. Photovoltaic modules convert both direct and diffuse radiation. Consequently, the presence of a substantial diffuse component contributes to energy yield stability under partially cloudy conditions.

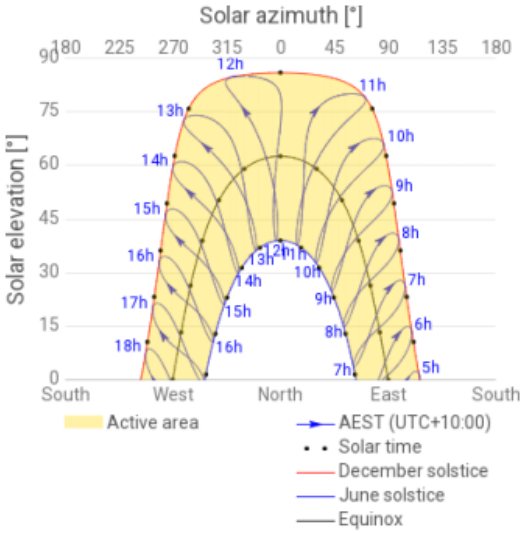

Figure 4.1: Annual solar path and horizon diagram for the selected site, showing seasonal sun trajectories and daily solar elevation angles (source [33]).

The Global Tilted Irradiation at the optimum angle ($GTIopta$) is 2051.9 kWh/m^2/year, corresponding to a fixed tilt of 27° facing the Equator (azimuth 0°) [33]. The higher value relative to GHI reflects the improved interception of direct radiation achieved by optimising module inclination. In ground systems, this tilt would maximise annual production.

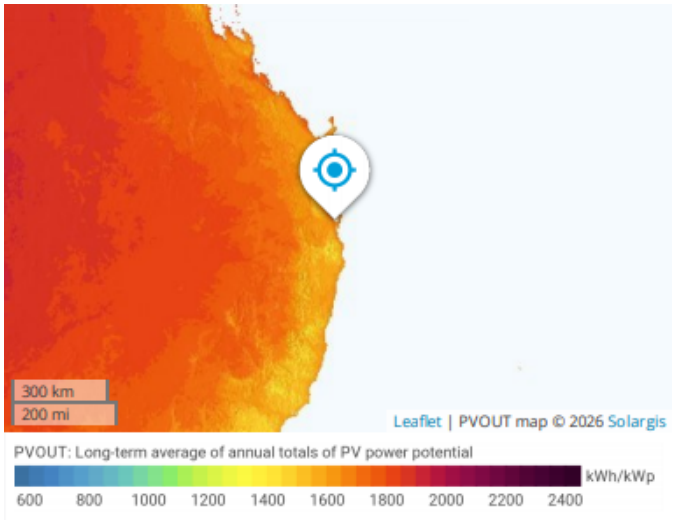

Figure 4.2: Long term annual photovoltaic power output potential (PVOUT, kWh/kWp) across eastern Australia, highlighting the high yield solar resource (source [33]).

However, floating photovoltaic installations typically adopt lower tilt angles (commonly around 10°) to reduce aerodynamic loads and structural stresses induced by wind, implying a moderate trade off between peak energy yield and structural resilience. The average annual air temperature at 2m height is 21°C, consistent with a warm but stable coastal climate [33]. Elevated temperatures generally reduce PV conversion efficiency, with typical performance losses ranging between -0.35% and -0.45%/°C above 25°C temperature. Nevertheless, FPV systems may benefit from natural cooling effects provided by surrounding seawater and sea breezes, which can reduce module operating temperature relative to comparable land based systems and partially offset thermal efficiency losses. Overall, the combination of high GHI, strong DNI, substantial GTI at optimum inclination and moderate thermal conditions confirms that the selected site exhibits a highly favourable solar resource profile. From an energy resource perspective, the climatic characteristics of the offshore zone west of North Stradbroke Island are well suited to support efficient and reliable long term FPV operation. To characterise the wind regime of Moreton Bay, the statistical distribution of wind direction and frequency is analysed through a wind rose representation for the selected site.

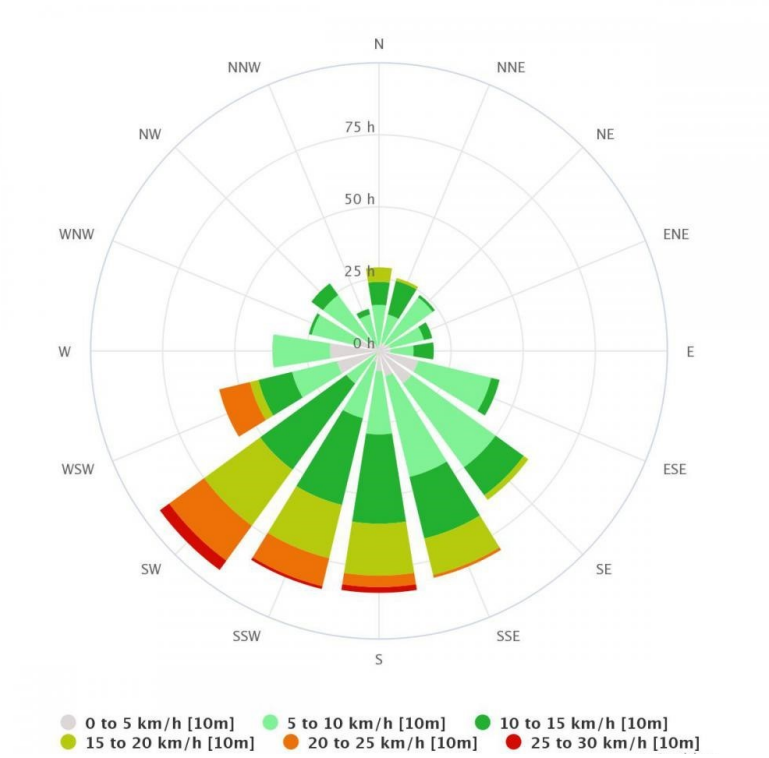

Figure 4.3: Annual wind rose representing direction and distribution for the selected site west of North Stradbroke Island (source [34]).

The wind rose shows that the most recurrent winds at the selected site come from the eastern sector, mainly between East and South - East and are generally characterised by low to moderate wind speeds [35]. Stronger wind events are instead associated with the South - Western sector, although they occur less frequently. This distribution is consistent with subtropical trade wind circulation and the influence of high pressure systems over the South Pacific. The presence of North Stradbroke Island acts as a natural barrier between the open Coral Sea and the sheltered waters of Moreton Bay, significantly reducing the effective fetch and attenuating incoming ocean swell [36]. In a wind wave coupled system, wind direction, duration and fetch jointly determine wave energy. Therefore, the morphological shielding provided by the island limits the development of high energy wave conditions at the selected coordinates. This reduced hydrodynamic exposure represents a favourable condition for FPV deployment.

4.2 Marine Parameters

The marine environment constitutes a fundamental design constraint for offshore and near shore floating photovoltaic (FPV) systems. The wave climate at the selected site west of North Stradbroke Island has been assessed using monthly mean values of Significant Wave Height (Hs) recorded during 2024 at the North Moreton Bay monitoring station [37]. Significant Wave Height is defined as the average height of the highest one third of waves measured during each sampling interval and represents the standard engineering parameter adopted in coastal and offshore applications to characterise wave conditions [89].

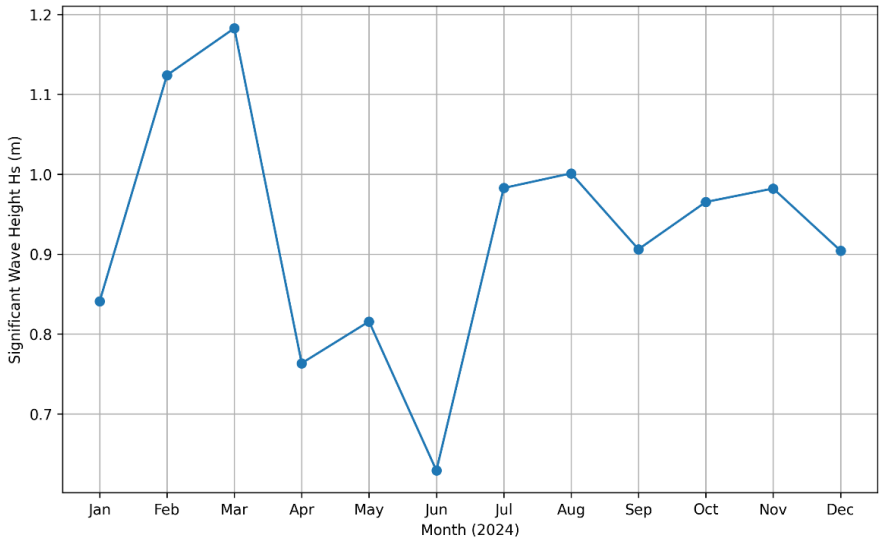

Figure 4.4: Monthly mean Significant Wave Height (Hs) recorded in Moreton Bay during 2024 (source [38]).

The 2024 dataset indicates moderate wave heights typical of a semi sheltered embayment, with monthly averages remaining within a relatively narrow range and without pronounced seasonal oscillations. Slight increases in Hs are observed during periods associated with stronger wind regimes, whereas calmer conditions correspond to more stable atmospheric phases. The limited variability and absence of extreme values reflect the protective influence of Moreton Island and the geomorphological configuration of Moreton Bay, which attenuate incoming open ocean swell and reduce wave energy penetration into the bay. From an engineering perspective, wave height is directly linked to hydrodynamic loads acting on floating platforms and mooring systems. Even moderate wave climates generate cyclic loading that may contribute to long term fatigue effects in structural components and anchor lines. Furthermore, wave induced platform motions influence cable

tension, mechanical connectors and potential inclination variations of photovoltaic modules, thereby affecting both structural integrity and operational reliability over the system design life. In the absence of a fully consolidated 2025 dataset, the 2024 annual record is adopted as a representative reference, as interannual variability in South Moreton Bay is generally limited under typical climatic conditions [38]. The broader hydrodynamic regime of Moreton Bay is primarily governed by tidal forcing, modulated by local wind stress and basin morphology. Moreton Bay is a semi enclosed embayment connected to the Coral Sea through defined entrances and tidal passages, with internal morphology characterised by shallow shoals, sandbanks and deeper central basins.

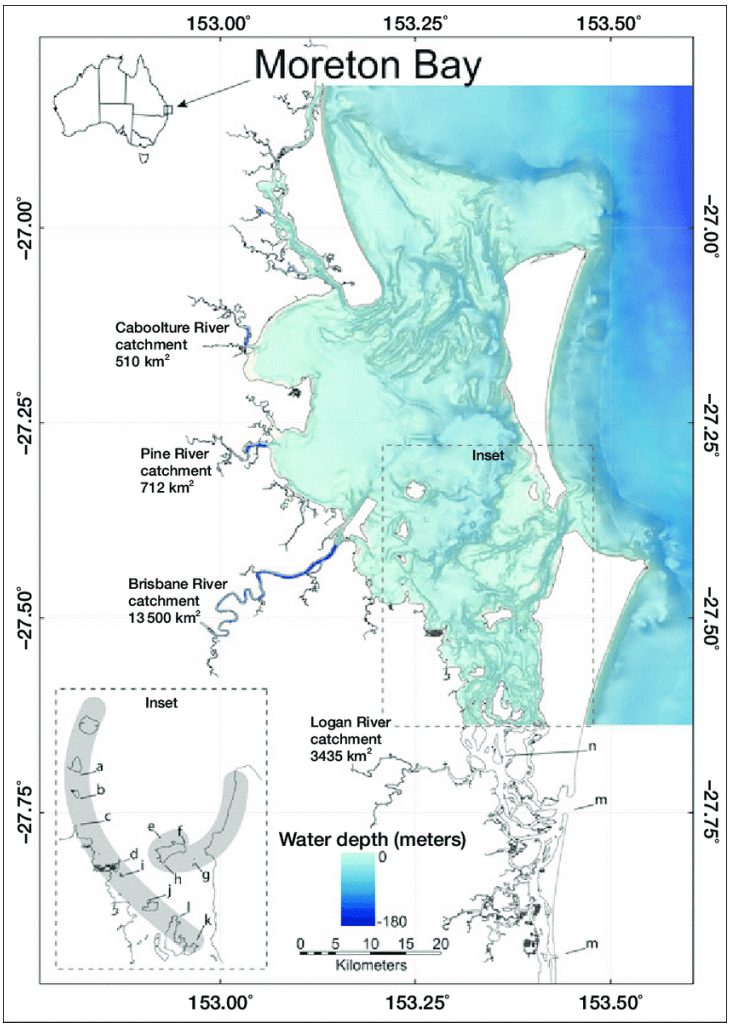

Figure 4.5: Bathymetric overview of Moreton Bay illustrating its semi enclosed morphology and connection to the Coral Sea (source [40]).

This geomorphological structure plays a decisive role in shaping circulation patterns and energy dissipation. The tidal exchange between the Coral Sea and the bay produces a predominantly semidiurnal regime, generating periodic inflows and outflows through the main entrances. Current velocities increase within constricted channels and passages due to bathymetric narrowing and depth gradients, while broader and deeper sections exhibit more moderate flow conditions. Available coastal process studies indicate that peak tidal currents in major passages typically range between approximately 0.5 and 1.0m/s (in localized constricted sections may exceed during peak tidal phases) [41]. Conversely, in the broader and deeper central portions of the bay, velocities are generally more moderate, often remaining below 0.5 m/s under normal tidal conditions. These spatial variations reflect the influence of bathymetric controls on tidal momentum distribution and energy dissipation across the embayment. The interaction between tidal currents and wind forcing defines the overall hydrodynamic environment in the vicinity of the proposed installation site and constitutes a key input for mooring design, anchor sizing and long term station keeping assessment. Salinity conditions in the waters surrounding North Stradbroke Island are also relevant for engineering evaluation. Moreton Bay exhibits a spatial salinity gradient influenced by tidal mixing with the Coral Sea and freshwater inputs from river catchments. Eastern sectors closer to the open ocean maintain salinity levels near typical oceanic values of approximately 35%, while western and inner regions may experience modest dilution during wet season runoff events [42]. From an engineering standpoint, such salinity levels imply sustained exposure to corrosive marine environments, necessitating the use of marine grade materials, corrosion resistant components and appropriate protective coatings for structural elements, mooring systems and electrical connections [43]. Overall, the combined assessment of wave climate, tidal and current regime and salinity conditions indicates that the selected site is characterised by moderate hydrodynamic exposure within a fully marine environment.

5 Structural Design and Engineering Configuration of the FPV System

This chapter presents the engineering configuration of the proposed Floating Photovoltaic (FPV) system, translating the site specific environmental, climatic and marine boundary conditions analysed in the previous chapters into a coherent technical design framework. The purpose is to define a technically consistent system layout capable of operating safely and efficiently under the hydrodynamic and atmospheric conditions characterising the offshore area west of North Stradbroke Island. The design process is structured around the integration of multiple constraints. Solar resource availability determines the theoretical energy production potential of the system, while wind regime, wave climate, tidal currents, bathymetry and salinity influence structural stability, station keeping requirements and material durability. Consequently, the FPV configuration must reconcile photovoltaic performance optimisation with marine engineering reliability. An installed capacity of approximately 500 kWp is proposed for the present configuration. This scale is selected to ensure compatibility with the spatial constraints of the identified offshore area while providing a technical reference case for performance evaluation. The chosen capacity enables the assessment of system behaviour under real marine exposure conditions, including structural response to environmental loads and operational performance under coastal climatic variability. The chapter is organised into dedicated sections addressing the principal components of the system. First, the floating support concept is introduced, defining the typology of structure adopted for offshore deployment. Subsequently, the photovoltaic module selection is discussed in relation to efficiency, durability and environmental suitability. The configuration of the floating platform and associated materials is then examined, followed by the description of the mooring and anchoring strategy required to ensure long term positional stability. Finally, the electrical connection is outlined, including the integration of the floating array with the island distribution infrastructure.

5.1 Selection of Floating Structure: Framed Offshore Platform with Perimeter Buoyancy

The floating structure selected for the proposed FPV system is a framed offshore platform with distributed perimeter buoyancy, conceived for deployment in shallow coastal marine waters West of North Stradbroke Island, where the local design basis assumes a water depth of approximately 12 m and persistent exposure to saline conditions, tidal currents, wind action and wave loading. In this context, the structural concept must be treated as a fully marine shallow water solution rather than as a conventional inland floating arrangement, since marine FPV systems are subjected to more demanding requirements in terms of corrosion resistance, structural reliability and dynamic response under environmental forcing [44].

Figure 5.1: Conceptual illustration of the offshore floating photovoltaic system configuration considered in this thesis (author's elaboration).

The figure 5.1 is intended to provide an illustrative overview of the floating system model that is conceived and investigated in the present work. The proposed configuration, represents a prototype concept developed in the framework of this thesis. It consists of a continuous load bearing deck supported by perimeter HDPE

buoyancy elements, raised PV mounting frames, a peripheral service walkway with guardrails and a mooring system connected to seabed anchors. This architecture is consistent with offshore oriented FPV literature, where floating platforms are commonly described as structural frameworks supported by floats and retained in position by dedicated anchoring and mooring systems sized according to water depth, metocean loading and seabed conditions [45]. From a structural perspective, the frame and substructure act as the primary load transfer system, distributing the weight of the PV modules and auxiliary equipment together with wind, wave and current induced actions toward the buoyant perimeter and the mooring connection points. This is important in offshore field, where the floating body must ensure not only buoyancy but also adequate global stiffness, geometric continuity and controlled motion response during operation [47]. The choice of HDPE for the floating elements is introduced already at this stage because it is widely adopted in FPV systems thanks to its low density, corrosion resistance and suitability for long term water exposure. Offshore case studies and design reviews also show that HDPE based flotation is frequently combined with steel structural frames and elevated module supports to achieve the stiffness and durability required in marine applications. The adoption of a continuous deck is functionally important because it provides both a structural base for load redistribution and a practical operating surface for inspection and maintenance, which are more complex in FPV systems. In this regard, FPV guidance [47] explicitly identifies the anchoring and mooring system as essential and states that maintenance walkways should be provided, since access routes and service corridors improve O&M efficiency and reduce operational difficulty. The raised PV support frames maintain the module plane above the deck and above the immediate splash zone, improving maintainability and helping to limit direct exposure of electrical components to marine spray, while low tilt mounting remains compatible with established FPV practice because it reduces wind induced loading and preserves a compact overall geometry. Finally, the mooring arrangement is an integral part of the selected floating structure rather than an external accessory, because in shallow coastal water the station keeping system must be designed together with the platform geometry and mass distribution in order to ensure stability, durability and acceptable line loads over the project lifetime. Accordingly, the proposed platform is best interpreted as a marine grade framed FPV unit with perimeter HDPE flotation, continuous accessible deck and offshore compatible mooring, selected to provide a technically coherent balance between buoyancy, accessibility, structural robustness and environmental compatibility at the chosen site.

5.2 PV Module Selection

For the proposed system, the PV module selection must satisfy not only conventional electrical requirements but also the constraints associated with marine floating applications, including low structural mass, robust encapsulation, corrosion resistance, reliable sealing and compatibility with low tilt mounting configurations. As noted in the literature [48], in marine environments module selection cannot be separated from platform design, since panel weight, tilt angle, aerodynamic loading, and durability directly affect buoyancy demand, structural response and long term operability. For this reason, high efficiency monocrystalline silicon technology is adopted. Compared with polycrystalline alternatives, monocrystalline modules generally provide higher conversion efficiency and therefore higher installed capacity per unit area, which is advantageous where the usable deck footprint and allowable structural loading are limited. This is particularly relevant for the present platform, where the available deck area must be used efficiently while keeping total mass and support reactions within acceptable limits. In addition, studies [49] report better practical energy performance for monocrystalline modules, supporting their use in compact and performance oriented floating systems [50]. A conventional monofacial glass - backsheet module is considered more appropriate for this application than a bifacial alternative. While glass - glass modules can offer advantages in moisture protection and mechanical durability, they also introduce a weight penalty and higher procurement costs, which become more critical in offshore floating applications. Given the selected low tilt configuration and the expected limited bifacial gain over seawater, a high quality glass - backsheet module certified for marine environments represents a more balanced technical and economic solution [52].

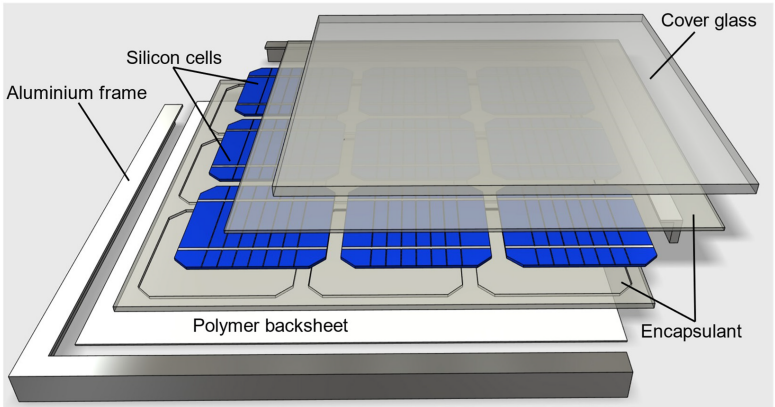

Figure 5.2: Schematic representation of a glass–backsheet photovoltaic (PV) module, showing the layered arrangement of glass (source [51]).

Accordingly, the reference module is assumed to consist of

- a tempered front glass layer;
- a polymeric encapsulant sheets;
- monocrystalline silicon cells;
- polymeric backsheet;
- an anodised aluminium frame;
- sealed rear junction box.

This layered architecture corresponds to the standard construction of crystalline silicon PV modules, where the front glass provides environmental and mechanical protection, the encapsulant ensures electrical insulation and laminate bonding, the backsheet acts as a rear protective barrier and the frame provides stiffness and mounting continuity. Modules in the 500 W power class are selected as the design reference. For a nominal installed capacity of 500 kWp, approximately 1000 modules are required under standard test condition ratings. The use of relatively high power modules reduces the total number of individual units, thereby limiting the number of mounting interfaces, electrical interconnections and potential failure points in the marine environment. This simplification is particularly beneficial in floating systems, where access for inspection and maintenance is more complex than in ground mounted installations.

Figure 5.3: Example of elevated support for PV above the deck (source[53]).

In terms of array layout, the modules are arranged in regular low tilt rows mounted on elevated support frames above the continuous deck. This configuration is

consistent with the selected floating platform, as it allows efficient use of the available deck surface while maintaining orderly load transfer to the supporting frame and perimeter buoyancy system. The raised installation also improves drainage, rear ventilation and maintenance accessibility, while keeping the modules further from direct splash exposure. The limited tilt angle (10°), consistent with floating platform constraints, reduces wind loads while maintaining adequate irradiance interception [54]. At the same time, the regular row arrangement promotes a more uniform distribution of loads across the deck and supporting structure, improving the overall mechanical behaviour of the floating unit under combined wind and wave action. Module frames are required to be manufactured in marine grade anodised aluminium to mitigate chloride induced corrosion while preserving structural lightness. Junction boxes and connectors must comply with high ingress protection ratings, such as IP67 [56], to prevent moisture intrusion. Furthermore, compliance with IEC 61701 [97] salt mist corrosion testing is specified to ensure verified resistance to saline exposure.

5.3 Floating Platform Materials

In the selected FPV configuration, buoyancy is primarily provided by perimeter floating elements made of UV stabilised High Density Poly Ethylene (HDPE), while the continuous deck and the supporting frame act as the main load carrying components for the photovoltaic array and maintenance walkway. This material choice is consistent with FPV engineering practice, where HDPE is widely adopted for floating elements because of its high resistance to corrosion, ultraviolet radiation, low maintenance demand, recyclability and adequate mechanical strength [58].

Figure 5.4: Blocks of HDPE material for offshore application (source [59]).

This material is particularly suitable because it is not subject to electrochemical corrosion and therefore does not suffer the chloride degradation mechanisms typically associated with metallic floating bodies in seawater. Its low density provides intrinsic buoyancy, while its relatively high toughness and deformation capacity allow it to accommodate limited cyclic movements and local impact loads without brittle failure. This is advantageous in shallow coastal marine conditions, where the platform is continuously exposed to wave induced motions and saline water. The requirement for UV stabilisation is especially important. Studies [60] on FPV float materials show that untreated HDPE can harden and become more brittle under prolonged UV exposure, whereas HDPE with carbon black or equivalent UV additives retains mechanical integrity far more effectively. In particular, testing up to 1152 h of artificial UV exposure found that HDPE/carbon black composite floats showed only limited reductions in tensile strength and elongation at break, while virgin HDPE degraded much more rapidly. The study concludes that HDPE with about 2% carbon black remains suitable to bear PV loads after accelerated weathering. In the proposed platform, however, the HDPE elements are not intended to provide the full global stiffness of the structure. Their role is primarily to supply distributed reserve buoyancy along the perimeter, while the overall rigidity and load redistribution of the platform are governed by the continuous deck and metallic structural frame. This design philosophy is consistent with FPV guidance and with DNV practice [76], which recognises configurations based on structural frameworks supported by floats rather than fully plastic self supporting floating bodies. A further advantage of HDPE is its manufacturability [61]. Floaters can be produced as sealed hollow bodies with controlled geometry and integrated connection details, enabling lightweight buoyancy units with good durability and limited maintenance requirements. At the same time, the smooth polymeric surface reduces corrosion issues and is generally less problematic than exposed metallic flotation in long term seawater service. Overall, the combination of perimeter HDPE floaters and a corrosion protected metallic support structure provides a robust and technically coherent solution for the selected offshore FPV platform, supporting the design target of long service life under marine exposure.

5.4 Mooring and Anchoring System

A semi - taut mooring configuration with compliant synthetic rope elements is adopted as the reference station keeping solution. This choice is consistent with the shallow water characteristics of the selected site, where the local water depth is approximately 12 m and with the need to control the horizontal excursions of a lightweight floating platform. In floating PV design, mooring line material and configuration must be selected by considering durability, corrosion, fraying, biofouling and the interaction between mooring system with the floating structure. In addition, where water level variations and dynamic motions are relevant, elastic mooring lines with adjustable or compliant behaviour can reduce sudden peak loads at the float attachment points, while taut systems help maintain positional control under variable environmental loading [62]. Compared with conventional catenary arrangements based mainly on heavy chains, a semi - taut system limits excessive line length in the water column and reduces the seabed footprint. This is particularly relevant for the present case, since long ground chain contact can increase seabed interaction and alter the intended restoring response, whereas this kind of layout provides a more compact station keeping geometry and reduced horizontal excursion. In addition, the use of synthetic ropes, such as polyester or nylon segments, introduces useful compliance into the mooring system, reducing dynamic line loads and improving fatigue behaviour compared with stiffer line systems [64].

Figure 5.5: Example of synthetic ropes for offshore application (source [63]).

The mechanical behaviour of the adopted mooring system is illustrated in Figure 5.6.

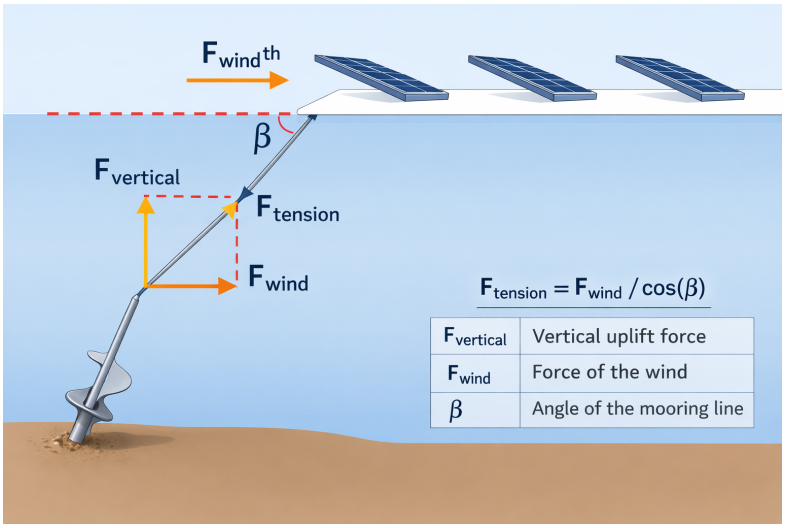

Figure 5.6: Force decomposition in the adopted mooring configuration showing horizontal wind load, total line tension and vertical uplift component acting on the helical anchor (author's elaboration).

The floating platform is primarily subjected to horizontal wind force F_{wind}, which generates tension in the inclined mooring line. The total tension F_t in the line can be expressed as

$$F_t = \frac{F_w}{\cos(\beta)}$$

where F_w is the horizontal wind load and β is the inclination angle of the mooring line relative to the horizontal plane. The vertical component transmitted to the anchor is therefore:

$$F_{vertical} = F_t \sin(\beta)$$

As the inclination angle increases, the total line tension rises for a given horizontal load due to the reduction of $\cos(\beta)$. Mooring lines should be kept as horizontal as possible in order to avoid excessive tensile stress under wind loading and that larger tilt angles lead to higher line tension for the same applied wind force. Consequently, careful optimisation of the line geometry is required to balance restoring stiffness and anchor loading. The vertical component contributes directly to uplift demand on the anchor system and must therefore be considered in anchor capacity design. The introduction of compliant segments improves fatigue performance and limits stress concentration at structural connection points, while auxiliary buoys or localised weights may be used where necessary to refine line geometry and reduce jerks associated with abrupt platform motion [64]. Anchoring is achieved through helical anchors installed in the predominantly sandy seabed. Helical anchors are selected due to their predictable load bearing behaviour in

granular soils and their ability to resist combined horizontal and vertical load components associated with taut mooring action [65]. Unlike catenary systems with ground chains, the proposed configuration minimises continuous seabed contact reducing potential disturbance to benthic habitats within Moreton Bay. Overall, the selected concept combines controlled platform positioning, reduced seabed footprint, improved dynamic compliance and compatibility with the structural philosophy of the proposed FPV system. Within this arrangement, the synthetic taut lines provide the required restoring action, while the helical anchors provide reliable holding resistance in sandy seabed conditions. Appropriate safety factors must therefore be included in both rope and anchor design to account for cyclic fatigue and dynamic amplification.

5.5 Electrical System and Grid Connection

The electrical configuration of the proposed FPV system has been defined by considering both the marine constraints of the offshore site west of Dunwich and the existing electrical infrastructure on North Stradbroke Island. The infrastructure assessment indicates the presence of 11 kV, 33 kV and 110 kV networks, with the 110 kV line providing transmission interconnection to the mainland grid.

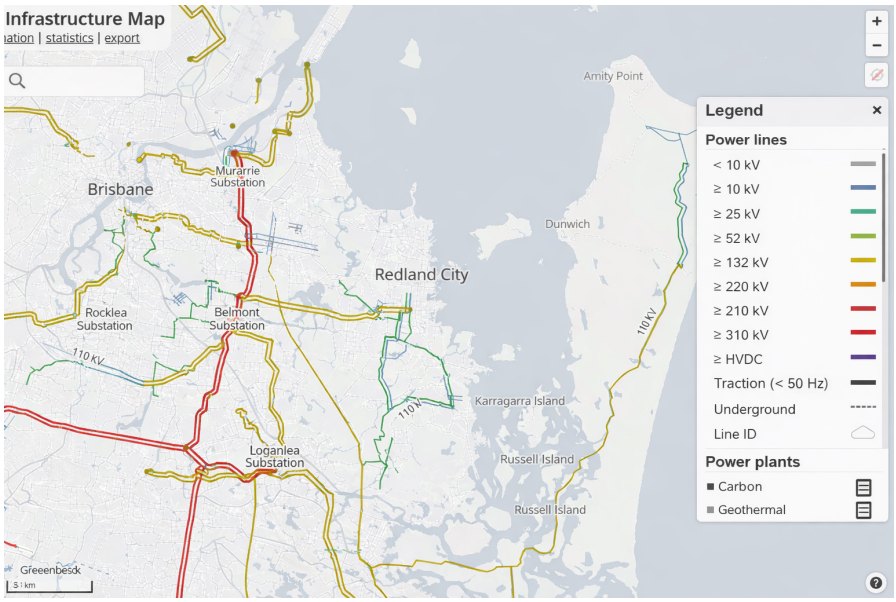

Figure 5.7: Overview of the electricity grid infrastructure in the Brisbane, Redland City and North Stradbroke Island area (source [66]).

However, given the relatively modest installed capacity of the proposed plant,

equal to 500 kWp, direct connection at transmission level would be technically disproportionate and economically unjustified. For this reason, connection at the 11 kV medium voltage distribution level is considered the most appropriate solution. During the design phase, two alternative electrical architectures were evaluated: (i) an onshore inverter configuration with DC submarine export, and (ii) an offshore inverter configuration with AC submarine export at 11 kV. The comparison was mainly driven by the current that would need to be transmitted over the approximately 4 km submarine cable route between the floating platform and the shore. In the first option, the DC power generated by the PV array would be exported to land at approximately 1.5 kV and converted to AC only after landfall. In this case, the transmitted current is given by

$$I = \frac{P}{V}$$

For a rated power of 500 kW and a DC voltage of 1.5 kV, the resulting current is approximately 333 A. Such a current level over a 4 km submarine route would require conductor cross sections in the order of 250 mm^2 to maintain acceptable voltage drop and thermal performance. This implies increased copper mass, higher installation complexity and larger cable diameters. Conversely, in the offshore inverter configuration, DC/AC conversion is performed directly on the floating platform and power is exported at 11 kV three phase AC. The transported current is therefore:

$$I = \frac{P}{\sqrt{3}\,V}$$

For P = 500 kW and V = 11 kV, the current is approximately 26 A. The reduction from 333 A to 26 A significantly decreases conductor cross section requirements, resulting in lower resistive losses, reduced cable weight and simplified submarine installation [68]. Although medium voltage insulation is required, the overall electrical efficiency and material optimization strongly favor the offshore inverter solution for the considered transmission distance. Based on this analysis, the offshore inverter configuration is selected. The inverters feed an offshore step up transformer (0.8 kV to 11 kV), enabling medium voltage AC export directly from the floating structure. The 11 kV armored submarine cable is routed toward the western shoreline of Dunwich. Shore crossing is implemented using Horizontal Directional Drilling (HDD) [69] to avoid disturbance to coastal dune systems and seagrass habitats. A compact onshore switching compound provides medium voltage switchgear, grid interface protection and revenue grade metering before connection to the nearest 11 kV feeder serving the Dunwich area. For the selected configuration, a 3 - core armored XLPE insulated submarine cable with conductor cross section of 40 mm^2 is adequate [70]. Considering insulation, armoring and mechanical protection layers, the external cable diameter is expected to range between 70 and

90 mm [71]. Where protective conduits are required near shore, HDPE ducts with internal diameter of approximately 140 mm is sufficient to accommodate installation tolerances and thermal dissipation requirements. A comparative assessment of the offshore and onshore inverter configurations is presented in Figure 5.8.

Criterion	Offshore Inverter Configuration	Onshore Inverter Configuration
Copper cross-section	Minimal (≈ 35–50 mm²) due to 11 kV AC export	Large (≈ 240–300 mm²) due to low-voltage DC export
Submarine cable cost	Lower conductor material demand, but requires 11 kV insulation and marine-rated MV protection	Higher conductor material cost due to large copper section, despite lower insulation voltage
Maintenance accessibility	More complex, as offshore inspection and servicing require marine access and suitable sea-state conditions	Simpler, with full land access for inspection and servicing
Electrical equipment integration	More complex, since inverter and transformer must be integrated on the floating platform under marine exposure	Simpler, since all main conversion equipment are located onshore
Floating platform structural load	Increased due to inverter and transformer mass supported by the framed deck and perimeter buoyancy system	Reduced, since only the PV array and associated support structure are carried offshore
Environmental risk	Presence of high-voltage and heat-generating equipment offshore	Electrical conversion fully located onshore, reducing marine operational risk

Figure 5.8: Comparison between offshore and onshore inverter configurations for the 500 kWp FPV system (author's elaboration).

Although offshore placement of inverters increases marine exposure of the power electronics and introduces additional integration requirements on the floating structure, these disadvantages are outweighed by the marked reduction in transmitted current, cable cross section and long distance resistive losses. The electrical architecture represents an effective compromise between marine engineering constraints, electrical efficiency and installation feasibility considering it as a suitable configuration for the proposed offshore FPV installation.

5.6 Installation, Accessibility and Maintenance Considerations

Site accessibility and proximity to support infrastructure are key factors in the feasibility and long term operability of the proposed coastal FPV system. The

selected site is located only 4 km from the western shoreline of North Stradbroke Island and 5 km from Dunwich Port, allowing relatively rapid marine transfer of personnel, materials and equipment. In addition, the nearby Moreton Bay Research Station (MBRS) in Dunwich represents a valuable logistical and technical support point, offering small vessel access, environmental monitoring expertise and operational assistance for inspections and maintenance campaigns [67]. This favourable accessibility reduces navigation time and facilitates recurrent servicing activities. Since no site specific FPV regulation is identified for North Stradbroke Island, coordination with local maritime and environmental authorities should be considered during project development. To reduce offshore risks and improve construction quality, the rigid platform with the peripheral HDPE buoyancy elements should be prefabricated and partially assembled onshore before marine deployment. A realistic installation strategy would involve fabrication of the main steel deck, support frames and buoyancy units at a coastal staging area, followed by transport offshore by barge or crane assisted marine equipment with final launch at the selected site. The installation sequence should include onshore assembly of the primary structural components, offshore transport and initial positioning, progressive connection of the HDPE perimeter buoys, verification of buoyancy balance and final connection of the mooring system.

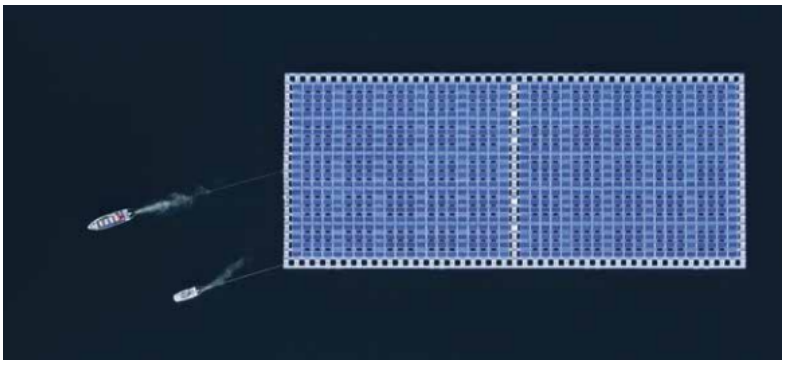

Figure 5.9: Trasport operation of a floating PV island by boats (source [55]).

Particular attention is required during this phase to ensure uniform buoyancy distribution in order to avoid asymmetric draft, uncontrolled rotations or local over stressing of the platform [72]. Anchors can be pre installed on the seabed before final positioning in order to reduce offshore working time. All marine operations should be scheduled within favourable weather windows, with calm sea state and moderate wind conditions, to minimise offshore exposure and improve the reliability of structural and mechanical connections. The anchoring and mooring system must ensure positional stability under wind, wave and current actions. A practical strategy consists of installing helical anchors and fixed seabed connections first

and subsequently connecting the mooring lines to the launched platform. This approach improves alignment accuracy with reduction of the duration and cost of offshore activities [73]. Because the site is relatively shallow, the final connection of synthetic ropes may be performed using light marine equipment, with diver or ROV assistance where necessary, thereby limiting operational risk and avoiding heavy underwater intervention. The rigid platform configuration also enables a more controlled electrical layout through dedicated cable trays, conduits and mechanical protections fixed to the supporting frame. Compared with low freeboard floating systems, this arrangement improves cable management and reduces the number of sections continuously exposed to motion. All electrical components should be selected for marine service, including UV and salt resistant cables, watertight connectors and high protection enclosures. Exposed metallic elements should be protected through robust anti corrosion systems, such as galvanisation combined with epoxy coatings to ensure durability over the project lifetime. In accordance with IEC recommendations, periodic inspection of the electrical system should include cable integrity, junction tightness, inverter panels and grounding continuity, while submerged or water exposed sections should be monitored carefully for corrosion, cracking or insulation degradation. Reinforced cable to platform transitions and adequate slack lengths should also be incorporated at the design stage to reduce bending concentration and abrasion.

Figure 5.10: Illustration of O&M approach for FPV systems (source [75]).

The figure 5.10 summarises the main operation and maintenance (O&M) strategies applicable to floating photovoltaic systems, distinguishing between preventive, corrective and predictive approaches. Preventive maintenance includes scheduled inspections and periodic recommissioning activities aimed at preserving system reliability over time. Corrective maintenance refers instead to unscheduled interventions carried out in response to faults or malfunctioning components, where rapid response is essential to limit downtime and associated costs. Predictive maintenance is based on real time monitoring and early warning systems, allowing potential failure modes to be identified in advance and improving the overall effectiveness of maintenance planning. Operational maintenance should be based on a structured inspection and servicing programme covering the floating structure, electrical equipment and mooring system.

Figure 5.11: Illustration of a FPV cleaning (source [46]).

The maintenance framework adopted should be regarded as an indicative estimate developed on the basis of the World Bank document [47]. Routine inspections should be carried out monthly by qualified personnel, either directly from the platform or from small service vessels, including visual checks of PV modules, structural joints, support frames and electrical connections. Inverters and junction boxes should be inspected in accordance with IEC 62446-2 [74], including verification of operating temperatures and electrical performance. More detailed structural inspections should be conducted quarterly, with particular focus on buoy to structure connections, mooring attachments, fasteners, corrosion, local

deformation and possible loss of tension in the anchoring lines. Underwater inspections by diver or ROV may be required to document submerged components and anchor conditions [75]. Module cleaning must also be included in the maintenance plan, with frequency depending on dust, salt deposition and bird activity. The HDPE buoyancy elements should be checked regularly for cracking, deformation, UV ageing, loss of buoyancy and loosening at mechanical interfaces, while mooring lines and chains should be managed through preventive inspection and periodic replacement, typically within a 5 – 10 year interval depending on material and environmental severity [76]. Following severe weather events, an emergency inspection is essential to verify the integrity of submerged and exposed components. In such cases, experienced divers or specialised ROV systems should be employed to assess potential underwater damages. Given the accessibility of the site, support from UQ MBRS and local marine operators could facilitate rapid intervention [77]. Any faults should be addressed immediately to avoid prolonged downtime or progressive damage. Although a detailed maintenance budget is not included in the present study, it is advisable to allocate an emergency reserve, typically on the order of 5–10% of the initial budget, to cover unexpected repair actions [47]. From a design perspective, long term maintainability should be integrated from the earliest development stage. Dedicated cable trays, accessible junction points and sufficient slack lengths should be incorporated to simplify inspection and replacement operations. Exposed metallic details should receive high quality corrosion protection in order to achieve the intended service life. Likewise, all HDPE buoyancy elements should be UV stabilised and selected for a design life exceeding 20 years, while electrical components should comply with relevant IEC standards to ensure safety and durability in the marine environment. Overall, the integration of logistical planning, robust installation procedures, marine grade materials and a preventive maintenance strategy is essential to ensure the operational reliability of the proposed coastal FPV system over its lifetime.

6 System Design and Hydrodynamic Modelling of the Offshore Floating PV Array

The preliminary system design is defined according to a conservative engineering approach in which the governing sizing conditions are associated with the most severe metocean loads expected at the selected deployment site, rather than with mean operating conditions. This is consistent with offshore structural practice, where platform configuration, reserve buoyancy and station keeping requirements are primarily dictated by wind and wave induced actions. The site west of North Stradbroke Island is characterised by prevailing winds mainly originating from the eastern and South-Eastern quadrants and by a semi sheltered hydrodynamic regime due to island shielding, which reduces effective fetch and attenuates incoming swell. The wave climate assessment based on the 2024 record indicates moderate significant wave heights in Moreton Bay and highlights that wave height directly drives cyclic hydrodynamic loading, influencing fatigue, platform motions and mooring demand. Therefore, the following sizing is presented as a design basis estimate purposely including explicit safety with reserve factors and it is subsequently verified and refined through AQUASIM Software simulations under the selected extreme sea state and wind forcing. In offshore FPV applications, module tilt is typically constrained by structural and aerodynamic considerations, commonly maintained at $\leq 15^{\circ}$ to reduce wind induced uplift and overturning moments on the floating structure, thereby limiting global stresses and mooring demand. At the same time, a tilt of $\geq 10^{\circ}$ is often adopted as a practical lower bound to promote rainfall driven self cleaning and mitigate soiling accumulation. For this reason, a tilt of 10° is chosen that represents a balanced compromise between energy capture and offshore survivability, as it reduces aerodynamic loads and associated structural stresses while supporting acceptable operational performance.

6.1 Design Basis and Sizing of system

The system design presented is formulated for defining a coherent geometric layout and a first order mass–buoyancy–mooring balance prior to numerical modelling. Unlike conventional inland FPV plants based on modular plastic pontoons, the configuration proposed in this work consists of a marine grade framed offshore platform with a continuous accessible deck supported by discrete cylindrical HDPE buoyancy elements distributed along the perimeter and within the internal area of

the structure. This solution is considered more appropriate for the present case because the selected site is a marine environment subject to wave action, wind exposure, saline corrosion and offshore maintenance constraints. In such conditions, a rigid framed deck supported by distributed flotation elements provides a more coherent balance between structural robustness, accessibility, maintenance operability, and compatibility with offshore mooring loads than a modular pontoon matrix. At this stage, several quantities (e.g., single module mass, auxiliary structural mass and reserve buoyancy) are based on representative values from typical 500 W class monocrystalline modules and cylindrical HDPE floating structures. The purpose is twofold: (i) to provide a physically consistent baseline configuration for model implementation and (ii) to justify that the adopted parameters are realistic in order of magnitude. The final validation and refinement of the assumed distributions (mass, buoyancy, stiffness and mooring pretension) are then performed in the subsequent AQUASIM hydrodynamic simulations [78], where dynamic response under representative sea states are evaluated. AQUASIM is a numerical simulation software used to model the hydrodynamic behaviour of floating and moored marine systems under environmental loads such as waves, wind and currents. It allows the analysis of motions with structural response, supporting the assessment of stability, loading conditions and overall system feasibility. The target plant size is 500 kW and a conservative DC oversizing is adopted to compensate for practical losses and long term degradation. The installed DC power is therefore computed as

$$P_{\mathrm{DC}} = N_{\mathrm{m}}\, P_{\mathrm{m}} = 550\mathrm{kWp}$$

where N_m is the number of PV modules and P_m is the rated power of a single module. With N_m=1100 and P_m=500 W. Compared to ground mounted, floating PV operates in a harsher environment that increase degradation rates and failure modes. Consequently, the selected DC oversizing and the explicit reserve margins (e.g., reserve buoyancy, robust material selection, suitable ingress protection ratings for electrical components) are justified not only for performance conservatism but also for long term reliability and maintainability in offshore conditions. Relative to a 500 kW target, the oversizing factor is approximately 10% DC oversizing.

$$k_{\mathrm{os}} = \frac{P_{\mathrm{DC}}}{P_{\mathrm{target}}} = \frac{550}{500} = 1.10$$

A representative geometry for 500 W class monocrystalline modules is adopted for preliminary footprint calculations, with module length L_m=2.20 m and width W_m=1.10 m. The projected plan area of one module is

$$A_{\mathrm{m}} = L_{\mathrm{m}}\, W_{\mathrm{m}} = 2.42\ \mathrm{m}^2$$

and the total projected module area is

$$A_{\mathrm{PV,tot}} = N_{\mathrm{m}}\, A_{\mathrm{m}} = 2662\ \mathrm{m}^2$$

The floating platform envelope is defined as L_p=65 m and W_p=50 m, hence the platform plan area is

$$A_{\mathrm{p}} = L_{\mathrm{p}}\, W_{\mathrm{p}} = 3250 \text{ m}^2$$

A compactness indicator is the plan area packing ratio

$$\eta_A = \frac{A_{\mathrm{PV,tot}}}{A_{\mathrm{p}}} = \frac{2662}{3250} = 0.82$$

meaning that about 82% of the platform plan area is occupied by PV projections, while the remaining 18% is available for structural members, clearances, corridors, buoyancy modules and cable routing. The adopted layout uses N_m=20 rows. The average number of modules per row is

$$n_{\mathrm{row}} = \frac{N_{\mathrm{m}}}{N_{\mathrm{row}}} = 55 \text{ modules/row}$$

An average row pitch across the platform width is

$$p_{\mathrm{row}} = \frac{W_{\mathrm{p}}}{N_{\mathrm{row}}} = 2.50 \text{ m}$$

which is consistent with a compact offshore arrangement (low tilt and limited inter row spacing), while still allowing local clearances depending on the structural framing. Row spacing is preliminarily defined to minimise inter row shading, adopting an "unshaded" criterion commonly used in PV layout design. In particular, shading avoidance can be assessed by imposing no mutual shading within the time window 09:00–15:00 at the winter solstice [79], which represents the most critical solar elevation condition over the year. Consistently, a conservative layout constraint can be expressed as a shading factor requirement such as $FactorShadow \geq 0.99$ indicating that shading related losses are kept below approximately 1% under the critical design condition [80]. This supports the selection of the adopted 20 row arrangement and associated row pitch as compatible with low shading objectives, noting that the low tilt offshore configuration further reduces shading sensitivity compared to steeper ground mounted arrays. If modules are aligned with their width along the platform length, a first order check of row occupancy along L_p is

$$L_{\mathrm{row,PV}} \approx n_{\mathrm{row}}\, W_{\mathrm{m}} = 60.5 \text{ m}$$

leaving approximately 65 - 60.5= 4.5 m to be distributed between end clearances, perimeter corridors and structural margins. The water surface primarily occupied by the array corresponds to the platform plan footprint

$$A_{\mathrm{water}} \approx A_{\mathrm{p}} = 65 \times 50 = 3250 \text{ m}^2$$

If an operational buffer band of width b is included around the platform (navigation clearance and mooring safety), the effective occupied area becomes

$$A_{\text{water,eff}} = (L_{\text{p}} + 2b)(W_{\text{p}} + 2b) = 5950 \text{ m}^2$$

It is noted that the project water footprint is not limited to the platform plan area alone. In practical offshore deployment, additional sea surface must be allocated to account for the mooring spread, safety clearances and navigation zones. Therefore, the effective occupied area $A_{\text{water,eff}}$ should be interpreted as a minimum planning envelope that incorporates not only the deck footprint but also the lateral clearance required for station keeping and line geometry. Buoyancy sizing follows the principle of Archimede. Let ρ_w be the seawater density and g the gravitational acceleration. The buoyant force is

$$B = \rho_w g \, V_{\text{disp}}$$

where V_{disp} is the displaced water volume. Static equilibrium requires $B = W$, where W is the system weight. Hence:

$$\rho_w g \, V_{\text{disp}} = M_{\text{des}} g$$

$$V_{\text{disp}} = \frac{M_{\text{des}}}{\rho_w}$$

Using ρ_w= 1025 kg/m^3, a preliminary mass budget is formed. A typical 500 W module mass is assumed $m_m \approx 27kg$

$$M_{\text{PV}} = N_{\text{m}} \, m_{\text{m}} = 29700 \text{ kg}$$

A conservative estimation for the supporting structure is taken:

- HDPE Floaters, whose function is to guarantee the buoyancy of the system $M_{\text{HDPE}} \approx 8700$ kg;
- Deck frame on which the photovoltaic panels are located $M_{\text{deck}} \approx 7000$ kg;
- Joints and support that connect the floaters to the frame $M_{\text{joint}} \approx 12500$ kg.

The proposed mass distribution appears technically reasonable for the Queensland case study. An estimated HDPE floater mass of approximately 310 kg is consistent with the buoyancy requirement associated with the displacement of about 88–90 m^3 of water, including an appropriate reserve buoyancy margin. Such a value is compatible with the use of floaters having wall thicknesses on the order of 20 mm, which is particularly relevant in the Australian coastal context, where the floating structure must withstand repeated mechanical stresses induced by wave action as well as long term thermal and ultraviolet degradation. For deck is chosen to adopt

a marine grade aluminium alloy 5005 provides a favourable compromise between low weight, corrosion resistance and structural stiffness. For a platform of this scale, corresponds to a relatively moderate distributed structural mass, sufficient to ensure adequate rigidity of the supporting frame while avoiding an excessive increase in the total displacement requirement. In practical terms, this allows the platform to remain sufficiently stiff under operational loads, including maintenance access and localised live loads, without compromising buoyancy performance. Steel joints and connection elements mass is justified by the large plan area of the structure and by the high number of load transfer points between the aluminium frame and the HDPE floaters. The adoption of stainless steel components, such as AISI 205 in marine environments, is appropriate to ensure both mechanical reliability and durability under saline exposure. The total mass estimated becomes:

$$M_{\text{tot}} = M_{\text{PV}} + M_{\text{HDPE}} + M_{\text{deck}} + M_{\text{joint}} + M_{\text{aux}} = 61900 \text{ kg}$$

Where $M_{\text{aux}} \approx 4000$ kg includes framing, local reinforcements, cables and junction boxes. To ensure reserve buoyancy (uncertainty, fouling, water ingress risk and dynamic freeboard), a reserve factor k_r is applied

$$M_{\text{des}} = k_r \, M_{\text{tot}} = 71185 \text{ kg}$$

With $k_r = 1.15$. The required displacement volume is then

$$V_{\text{disp}} = \frac{M_{\text{des}}}{\rho_w} = 69.45 \text{ m}^3$$

This value represents the minimum total displacement that must be provided by the cylindrical buoyancy units supporting the deck. At this stage, a finite number of structural cylindrical HDPE buoys connected to the framed platform is defined. A realistic preliminary arrangement for a deck measuring 65x50 m consists of:

- 18 perimeter buoys, distributed around the external frame: 7 on longer side and 4 on shorter side;
- 10 internal buoys, they support the weight where the flexing moment is maximum improving load distribution.

for a total number of buoyancy units equal to $N_b = 28$. The average displaced volume required for each buoy is therefore

$$V_b = \frac{V_{\text{disp}}}{N_b} = \frac{69.45}{28} = 2.48 \text{ m}^3$$

Assuming each flotation unit is modelled as a partially submerged cylindrical buoy, the displaced volume of one buoy is

$$V_b = \frac{4}{\pi} D^2 h_{\text{imm}}$$

where D is the buoy diameter and h_{imm} is the effective immersed height under design loading. If a representative buoy diameter of $D = 1.70m$ is selected, the required immersed height becomes

$$h_{\text{imm}} = \frac{4V_b}{\pi D^2} = 1.09\text{m}$$

This preliminary buoyancy solution consists of 28 cylindrical HDPE buoys, each providing an effective displaced volume of approximately $2.48m^3$, corresponding to a representative diameter of 1.7 m and an immersed height of about 1.09 m. The total geometric buoy height would be significantly greater than the immersed height, so as to preserve buoyancy reserve and ensure an adequate freeboard under both operational and extreme environmental conditions, such as those typical of the Queensland region. The extreme sea state is introduced through the wave height $H \approx 1.2m$ for the most severe conditions considered. In paragraph 6.3 the wave amplitude (Amp) will be introduced that rapresent a useful linear wave parameterrequest in AQUASIM Software. It provides a consistent magnitude for free surface elevation forcing in simplified formulations. Wind forcing is treated through the 10 m wind speed U_{10}. Assuming the upper wind speed class indicated for the site corresponds to $U_{10} \approx 30$ km/h, the conversion gives:

$$U_{10,\text{max}} = 30 \cdot \frac{1000}{3600} = 8.33 \text{ m/s}$$

The associated dynamic pressure is

$$q = \frac{1}{2}\rho_{\text{air}} U_{10}^2 = 42.5 \text{ Pa}$$

where $\rho_{\text{air}} = 1.225\text{kg/m}^3$ is air density. For PV module structural integrity, practical design limits are often expressed in terms of allowable pressure loading. The maximum values adopted in industry practice are approximately $5400Pa$ for front side loading and $2400Pa$ for back side. They represent the test requirements of the international standard IEC 61215 [81]. In the present preliminary assessment, the aerodynamic pressure estimated from the site wind class is orders of magnitude lower than these ultimate module pressure capacities. However, extreme gusts, local flow acceleration and dynamic amplification effects can substantially increase peak pressures. For a site depth $h_{\text{depth}} \approx 12$ m and a line lenght L, the geometric relation for a semi - taut line can be expressed by

$$\sin\beta = \frac{h}{L}$$

where β is the inclination angle at the fairlead with respect to the horizontal. With $L = 30m$

$$\beta = \arcsin\left(\frac{12}{30}\right) = 23.6^\circ$$

$$\cos\beta = 0.917, \qquad \sin\beta = 0.400$$

If T denotes the fairlead line tension, the horizontal and vertical components are

$$T_H = T\cos\beta, \qquad T_V = T\sin\beta$$

For example, with $T = 150kN$

$$T_H = 150 \times 0.917 = 137.5 \text{ kN}, \qquad T_V = 150 \times 0.400 = 60.0 \text{ kN}$$

These relations are important because corner and side buoy positions are preferable locations for reinforced mooring attachments, thereby avoiding excessive force concentration at local deck joints and improving load transfer into the primary framed structure. Overall, the above calculations constitute a realistic preliminary sizing for a compact 65 m $\times$ 50 m offshore FPV unit at 550 kWp providing: (i) a conservative DC oversizing margin, (ii) an internally consistent plan area packing and (iii) a buoyancy requirement $V_{\text{disp}} \approx 69.45$ m^3. This formulation supports the subsequent dynamic verification in AQUASIM, where the selected extreme H and wind forcing are applied to quantify platform motions and peak mooring tensions and to iteratively refine buoyancy reserve, stiffness distribution and mooring pretension to satisfy both survivability and operability requirements.

6.2 Numerical model construction in AQUASIM Software

The hydrodynamic model of the proposed offshore floating photovoltaic system was developed in AquaEdit (a modelling tool of AQUSIM Software) in order to reproduce the main geometric, structural and boundary characteristics of the conceptual design under marine conditions of the chosen site. The sectional and distributed properties assigned to the elements in AquaEdit are not adopted arbitrarily, but are progressively calibrated through an iterative process aimed at achieving the final hydrostatic equilibrium of the FPV system. In order to keep the numerical model computationally manageable and to improve the stability of the simulation process, only a quarter of the full floating platform is represented in AQUASIM. This choice is adopted because the computational burden increases significantly with the size of the simulated structure, as a larger platform requires a greater number of discretised elements and corresponding numerical calculations that may lead to increased run times, numerical instability and possible convergence difficulties at the end of the simulation. The reduced model therefore shows a portion of 16 x 12.5 m of the real system, allowed the essential structural and hydrodynamic behaviour.

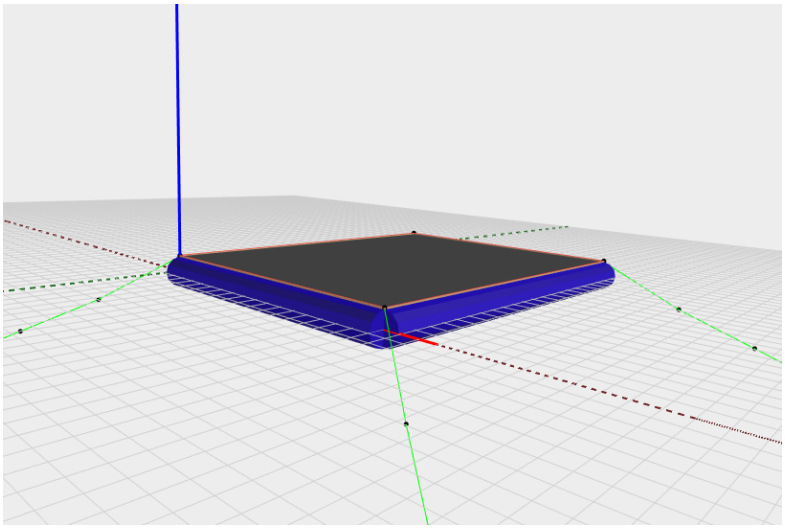

Figure 6.1: Reduced AquaEdit model of the offshore FPV system in isometric view

As shown in Figure 6.1, the model includes the rigid platform, floater system, mooring lines and the support elements that connects the floater with the frame. This one is represented through a combination of beam and membrane elements,

where the membrane is introduced mainly for the graphical and geometrical representation of the continuous rigid platform surface (no hydrodynamic parameters), while the structural mass and load transfer are assigned to the beam elements. Initially, the deck beam arrangement is defined only along the perimeter of the platform. However, during the preliminary simulations, this configuration showed limitations in terms of load distribution with local numerical issues related to the transfer of structural actions as torsional and bending deformation of the upper platform.

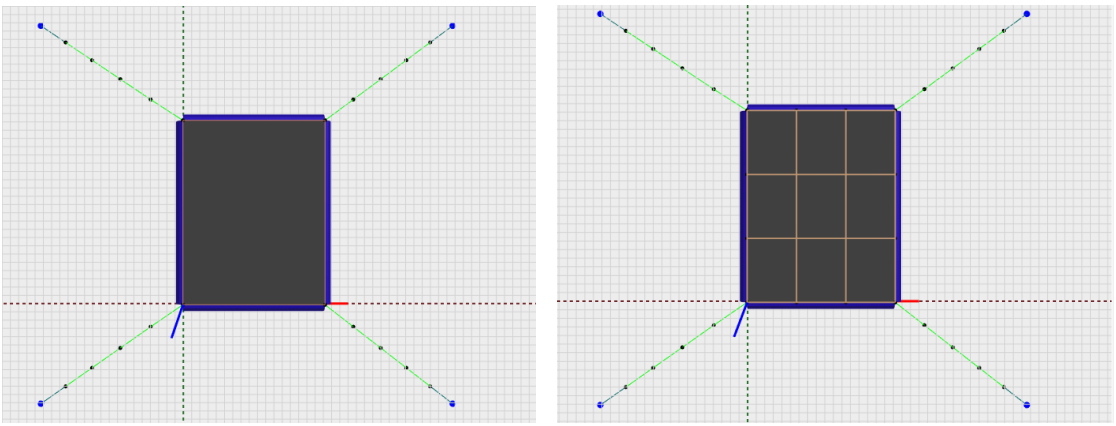

Figure 6.2: Improvement AquaEdit model of the offshore FPV system in top view

For this reason, the beam layout is refined by introducing additional internal longitudinal and transverse members, allowing the loads platform to be redistributed more effectively improving the overall stiffness and numerical stability of the model. In addition, the weight contribution of the photovoltaic modules, cables and auxiliary equipment is not modelled as separate structural components but is included as part of the equivalent distributed mass assigned to the rigid platform. The buoyant bodies, shown in blue, represent the floating support structure placed along the perimeter of the modelled platform. The mooring system is modelled through truss elements and subdivided into two main portions: a light green segment representing the synthetic rope and a dark green segment representing the steel chain section. To reproduce the anchoring condition at the seabed, the outer ends of the four mooring lines are fixed by restraining all six degrees of freedom. In addition, joint elements are introduced between the deck and the floating structure in order to reinforce the structural connection and improve load transfer continuity between the supported deck and the buoyant bodies.

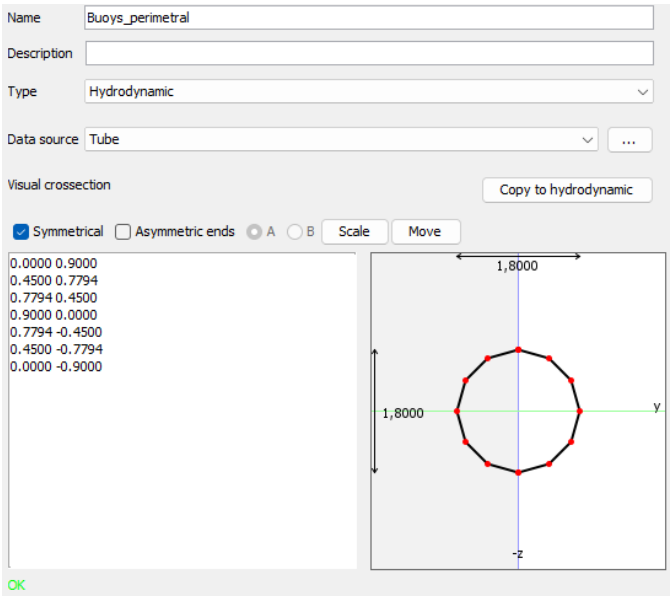

Figure 6.3: Geometrical definition of the perimeter buoy element in AquaEdit

For the buoyant support system, the perimeter floats are modelled using a Hydrodynamic beam element with tube geometry. In AquaEdit, the Hydrodynamic load formulation is used to represent the interaction between water and floating or partially submerged beam like structural elements. According to the official Aquastructures documentation, this option combines Morison type loading with strip theory. In this way, the member response is influenced not only by viscous drag, but also by inertia and hydrostatic effects. In order to evaluate the strip theory contribution, a calculation cross section must be defined in AquaEdit. This section is required because the software derives the relevant hydrodynamic and hydrostatic properties from the defined geometry and submerged volume of the element [83]. More specifically, this option treats the structural member as a floating or partially immersed component whose time dependent response is governed by several water actions. These include:

- viscous drag: is the viscous resistance associated with the relative motion between the fluid and the structure. It depends mainly on the fluid velocity and represents the dissipative part of the hydrodynamic loading.;
- Froude–Krylov: is the force generated by the undisturbed wave pressure field acting on the submerged body. It represents the direct effect of the incident wave pressure on the structure
- diffraction forces: when the incoming waves are locally disturbed by the structure and this produces an additional hydrodynamic force.

- added mass: is the apparent increase in inertia of a body moving in water, due to the fact that part of the surrounding fluid must also be accelerated together with the structure;
- hydrodynamic damping: represents the energy dissipation associated with the motion of the body in water and with wave radiation effects. It contributes to reducing the amplitude of structural oscillations over time.

The drag contribution is taken from the Morison formulation that is commonly used for slender submerged members, such as tubes or cylindrical elements. It expresses the hydrodynamic load as the sum of an inertia term, associated with fluid acceleration and a drag term, associated with the relative velocity between fluid and structure. It is especially suitable when the structural diameter is small compared to the wavelength. The Froude – Krylov force, diffraction effects, added mass and hydrodynamic damping are evaluated through strip theory in which a long floating body is divided into a series of transverse sections. The hydrodynamic forces are then evaluated on each individual section and integrated along the body length. This method is particularly useful for slender or elongated floating structures, since it provides an efficient approximation of added mass, damping and wave induced forces. In addition, AquaSim computes the hydrostatic stiffness in heave and roll from the section shape and submerged configuration defined in AquaEdit [83]. A generalized expression reported in the Aquastructures validation documentation for the wave force acting on a hydrodynamic beam element in the horizontal or vertical direction is:

$$F_i = \frac{1}{2}\rho C_D L D\, u\sqrt{u^2+w^2} \;+\; \rho V_S(1+C_a)\, a_i \;+\; \rho C_a V_S a_i^{(\text{beam})}$$

where:

- F_i is the wave force in i =[x,y,z] directions;
- $_D$ is the drag coefficient;
- L is the beam length;
- D is the beam diameter;
- u and w are the horizontal and vertical fluid particle velocities;
- ρ is the water density;
- V_s is the wetted volume of the beam defined as:

$$V_S = \frac{\pi D^2 L}{4}$$

- C_a is the added mass coefficient;
- a_i is the fluid particle acceleration according to linear wave theory:

$$a_1 = \omega^2 \zeta_{AR} e^{kz} \cos(\omega t - kx)$$

- $a_i^{(\text{beam}}$ is the beam acceleration.

In this formulation, the first term represents the drag force, the second term the Froude–Krylov with diffraction contribution and the third term the added mass and damping related contribution. The user defines the beam geometry, the external diameter used for hydrodynamic loading, the displaced volume and the drag coefficients in the local directions, so that the software can evaluate the distributed wave induced forces acting along the element. A circular tubular cross section is assigned to the buoy element, with an external diameter of 1.7 m, as extimated with the preliminary sizing developed in the previous section. The buoy material is defined with High Density Poly Ethylene (HDPE) material for the floating support structure. A representative mass density of $950 kg/m^3$ is assigned, ensuring a realistic description of the material behaviour in a marine environment. It has a wall thickness of 20 mm, while the internal cavity is set as air filled from the default software settings, since the program did not provide the option for foam filling. Although the conceptual design, the assumption of an air filled internal volume remains acceptable for the present hydrodynamic representation, as it preserves the main buoyancy mechanism of the cylindrical float.

PARAMETER	VALUE
E-modulus	9.0e8 N/m^2
G-modulus	3.4615 N/m^2
Poisson's number	0.3
Density	950 kg/m^3
Volume	0.04 m^3/m
Weight in air	53 kg/m
Weight in water	12 kg/m
Rayleigh damping mass	0.025
Rayleigh damping stiffness	0.025

Table 6.1: Main design parameters of the HDPE buoy element in AquaEdit

The elastic properties assigned to the material included the Young's modulus, Shear modulus and Poisson's ratio. The value of $0.04 m^3$ does not represent the volume of water that the system must displace to float but corresponds to the structural volume per unit length of the tubular element used by the software to

define the Morison beam. The value of 53 kg/m in air represents the weight of the HDPE tubular buoy element, which over the 57 m perimeter of the reduced model corresponds to about 3.02 ton. When submerged, the value decreases to 12 kg/m, corresponding to 0.68 ton over the same perimeter due to the buoyancy force generated by the displaced water. This means that the buoy behaves as structural support with strong hydrostatic efficiency. Rayleigh damping is introduced to account for a simplified dissipation of energy during the dynamic response of the floating structure. In this formulation, the damping matrix is expressed as a combination of the mass and stiffness. The mass related coefficient affects the low frequency global motions of the platform, while the stiffness coefficient mainly damps higher frequency local oscillations. This choice is to limit unrealistic oscillation amplification in the hydrodynamic simulation. As previously introduced, the rigid platform is represented in AquaEdit through a combined beam and membrane for a graphic and modelling strategy to reproduce a geometrical continuity. In particular, the beam elements are used to represent the main structural support of the deck and the membrane element is used to cover up and down the beams to create a rigid platform. The platform is modelled as a Morison submerged beam formulation for the numerical rapresentation with a rectangular section. The chosen material is aluminium alloy because

- conducts the cooling effect of the water more effectively, helping to reduce panel temperature
- form a protective oxide layer that provides good resistance to saline environments
- suitable for describing the equivalent mechanical response of the rigid platform

PARAMETER	VALUE
E-modulus	7e10 N/m^2
G-modulus	2.6e10 N/m^2
Poisson's number	0.3
Density	2700 kg/m^3
Moment of Inertia I_y	9.7169e-4 m^4
Moment of Inertia I_z	7.7789e-4 m^4
Torsional Constant I_t	1.4513e-4 m^4
Volume	9.9e-3 m^3/m
Weight in air	48 kg/m
Weight in water	37.85 kg/m

Table 6.2: Main design parameters of the rigid platform in AquaEdit

The Moment of Inertia I_y, I_z are relatively high, as they represent the bending resistance of the deck in the two principal directions: the first one governs the resistance to vertical bending (preventing the platform from sagging downward under the weight of the photovoltaic modules), the second one governs the resistance to lateral bending, counter balancing the horizontal action of the wind acting on the side of the panels as well as the lateral impact of wave loading. By contrast, I_t is a critical parameter in offshore design, as it governs the torsional resistance of the structural section and therefore limits the tendency of the platform to twist about its own longitudinal axis. Since the adopted deck beam is defined by a closed section, its torsional stiffness is high, which makes it effective in resisting rotational deformation under combined environmental loading. Unlike the HDPE buoy elements, the deck beam does not behave as a highly buoyant component. Rather, it represents a significant downward load contribution that must be supported by the floating structure. In the construction of floating photovoltaic systems, the aluminium deck cannot be directly welded to the HDPE buoyant elements. For this reason, the connection is typically achieved through dedicated metallic connectors often manufactured from AISI 205 stainless steel, which provides adequate mechanical strength together with high corrosion resistance in marine environments. In this numerical model, direct connection between the rigid aluminium platform and HDPE buoyant element may lead to mathematical inconsistencies or local instabilities at the interface, owing to the significant difference in stiffness between the two materials. In the adopted model, the joints represent a localised connection members intended to improve structural continuity and to avoid unrealistic discontinuities at the interface between platform and buoys. The mooring system is represented in AquaEdit using truss elements, since the mooring lines are intended to carry axial tensile forces. In the adopted numerical scheme are presents 4 mooring line, each of which is subdivided into two different parts with distinct mechanical functions: an upper part in synthetic rope (that is 4/5 of the total lenght) (polyester) with 50 mm diameter, connected to the floating platform and a lower part in steel chain with 40 mm diameter, located close to the seabed and to the anchoring point. This combined arrangement is selected in order to reproduce a realistic semi - taut mooring behaviour for the proposed offshore FPV platform.

PARAMETER	VALUE
E-modulus	2.0e9 N/m^2
Area	1.9365e-3 m^3/m
Mass density	356.5 kg/m^3
Diameter Y (drag loads)	0.09 m
Diameter Z (drag loads)	0.09 m
Drag coefficient Y, Z	1.2
Volume	1.9635e-3 m^3/m
Weight in air	0.7 kg/m
Weight in water	-1.3125 kg/m
Breaking load	7e5 N

Table 6.3: Main design parameters of the synthetic rope in AquaEdit

In shallow water depths, the use of a synthetic fibre segment (characterised by high buoyancy) integrated with a bottom chain, represents a standard strategy for offshore floating photovoltaic systems. Experimental studies have shown that the hybrid polyester chain configuration is superior to all chain systems in controlling surge motion (horizontal movement), as it maintains a catenary geometry capable of preventing impulsive loads on the anchoring system [85]. These synthetic lines exhibit low axial stiffness, which allows them to elongate elastically, absorb part of the kinetic energy induced by wave motion and significantly reduce peak tensions (snap loads) compared with rigid steel chains. The negative effective submerged weight observed in the model $-1.3125kg/m$ is an intentional design property. Academic literature [82] highlights that the low density of synthetic fibres reduces the dead load acting on the floating platform, thereby improving the overall equilibrium of the buoyant support system. Moreover, unlike metallic components, polyester is immune to electrochemical corrosion which makes it suitable for long term marine applications [86]. Nevertheless, it must also be recognised that biofouling, may progressively alter both its hydrodynamic section and its effective weight over time. The diameters used for the calculation of hydrodynamic drag loads are equal to 0.09 m, obtained by multiplying the nominal rope diameter (0.05 m) by a corrective factor of 1.8 [87]. In offshore applications, the physical diameter of a synthetic rope does not coincide with its effective hydrodynamic diameter. Owing to the structure deformation under load and the inevitable accumulation of biofouling (such as algae and barnacles), the effective projected area exposed to currents can increase significantly. The adoption of an enlarged diameter represents a conservative standard practice intended to simulate the worst case scenario. The drag coefficients set to the default value of 1.2 (typical for braided mooring ropes [88]), are dimensionless parameters that quantify the resistance offered by the rope to fluid flow. Within the software, this coefficient is used in the Morison equation

to calculate the drag forces exerted by waves and currents on the line. Finally, the breaking load represents the maximum tensile force that the rope can withstand before structural failure occurs. The adopted value of 700 kN defines the critical safety threshold: during the simulations, the maximum tension developed in the mooring line should remain within this fraction.

PARAMETER	VALUE
E-modulus	1.1e11 N/m^2
Area	2.51e-3 m^3/m
Mass density	1.247e4 kg/m^3
Diameter Y (drag loads)	0.072 m
Diameter Z (drag loads)	0.072 m
Drag coefficient Y, Z	1.2
Volume	2.51e-3 m^3/m
Weight in air	31.3 kg/m
Weight in water	28.727 kg/m
Breaking load	9e5 N

Table 6.4: Main design parameters of the steel chain in AquaEdit

For the final part of the mooring line there is adopted a steel chain because is the zone most exposed to concentrated tensile transfer, abrasion, local impact against the seabed and mechanical interaction with the anchor connection. In such conditions, a steel chain provides greater robustness and wear resistance than a synthetic rope. From a mechanical perspective, the steel chain also contributes additional local weight, which helps stabilise the lower part of the mooring line and improves the reliability of the load transfer to the anchor. In other words, while the upper polyester rope provides compliance and reduces dynamic peak tensions, the lower steel chain ensures local durability and a more stable terminal connection with the seabed restraint. The connection between the rigid upper platform and the HDPE buoyant perimeter elements was represented in AquaEdit through dedicated joint elements. These components are introduced in order to reinforce the numerical connection between the deck and the floating structure, thereby ensuring a more reliable transfer of forces between the upper rigid platform and the buoyant support system. In the adopted model, the joints do not represent an independent floating or load bearing subsystem, but rather localised connection members intended to improve structural continuity and to avoid unrealistic discontinuities at the interface between rigid platform and buoys.

6.3 Environmental conditions and Hydrodynamic forces

The environmental loading adopted in the AQUASIM simulations reproduce a representative extreme hydrodynamic condition for the selected offshore FPV site, located west of North Stradbroke Island, within the waters of southern Moreton Bay. As discussed in Chapter 3 and 4 of this thesis, the site is characterised by a moderate marine climate thanks to its partial natural protection, with lower wave energy than fully open coastal conditions, but still subject to cyclic wave loading and tidal forcing that remain structurally relevant for the floating system. Due to the local bathymetry is assumed an installation depth of approximately 12 m, which is used as the reference seabed level in the numerical model indentifing the site as shallow water.

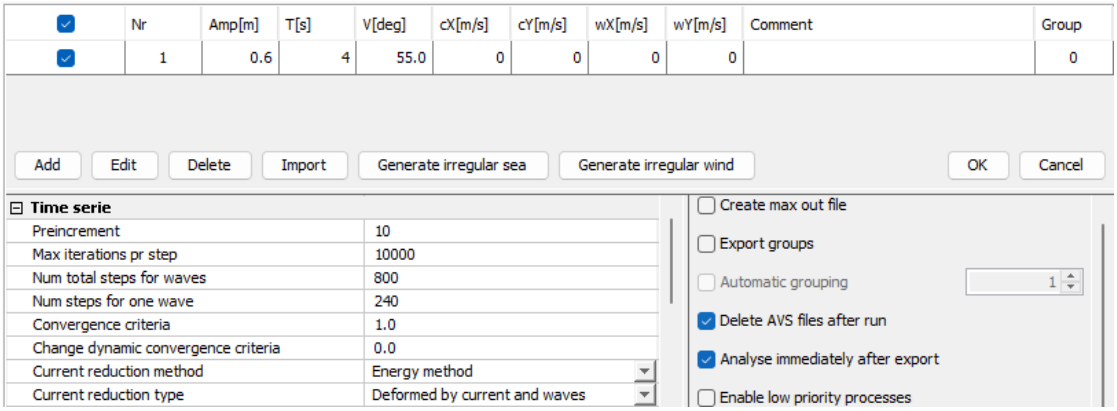

Figure 6.4: Environment data simulation on AQUASIM Software

In principle, a more realistic offshore representation would require the adoption of an irregular wave spectrum, since real sea states are characterised by a statistical distribution of wave heights, periods and directions rather than by a single sinusoidal component. However, in the present study, the use of irregular waves would have required a much more detailed metocean characterisation together with a more complex numerical setup, making convergence of the coupled floating, platform and mooring model considerably difficult. For this reason, the environmental forcing is simplified through a regular wave representation, which still allows the main hydrodynamic response of the system. The selected propagation direction of 55° is adopted to reproduce an oblique environmental forcing condition with respect to the principal axes of the platform. This choice is consistent with the annual wind rose presented in the previous chapter 4.3, showing that the most energetic directional contributions occur predominantly from the South - West.

In the numerical model, this prevailing directional exposure is translated into an equivalent input angle, according to the directional calibration convention used in AQUASIM. In ocean engineering and naval architecture, it is fundamental to distinguish between deterministic and statistical wave parameters [89]:

- Wave Height (H): This is a deterministic value defined as the vertical distance from a specific crest to the preceding trough. In linear wave theory (Airy theory), H is a constant value used to define the water surface elevation

$$\eta(x,t) = \frac{H}{2}\cos(kx - \omega t) = A\cos(kx - \omega t) \tag{6.1}$$

  where:

  - $\eta(x,t)$ is the elevation of the water surface relative to the mean sea level;
  - H is the wave height (distance between crest and trough);
  - A is the wave amplitude, with $A = \frac{H}{2}$;
  - k is the wave number, defined as $k = \frac{2\pi}{\lambda}$;
  - ω is the angular frequency, defined as $\omega = \frac{2\pi}{T}$;
  - x is the spatial coordinate;
  - t is time.

- Significant Wave Height (Hs):This is a statistical parameter defined as the average height of the highest one third of waves in a given sea state. Hs is the standard measure used to characterize the energy content of a stochastic sea state.

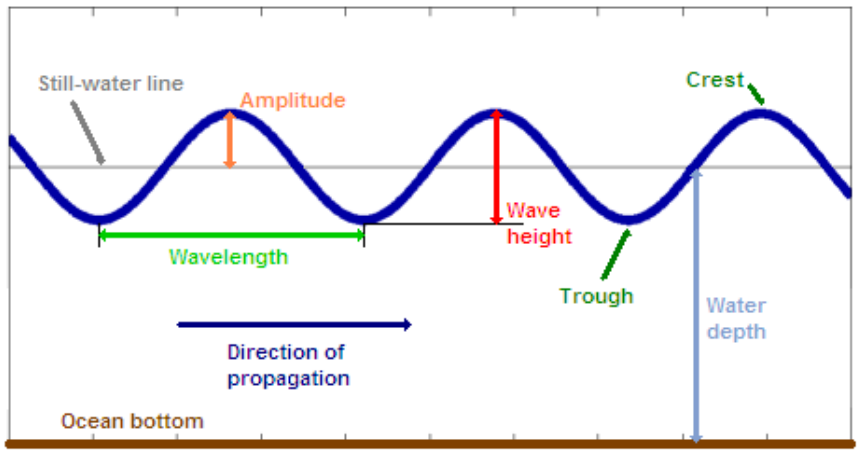

Figure 6.5: Most important wave measurement (source [90]).

Observing the meteocean conditions of the chosen site 4.4, is adopted $Hs = 1.18m$ as the design wave height (H) in the simulation, although these two parameters represent different concepts. This approach is justified by several considerations. In common practice, when a full spectral stochastic analysis is replaced by a regular wave simulation, the Significant Wave Height is often used as the representative height to ensure the system is tested against the most energetic waves typically present at the installation site. This choice [91], allows for a conservative estimation of the hydrodynamic forces acting on the floating structures by focusing on the upper tier of the wave distribution. Furthermore, following linear wave theory, the Wave Amplitude (Amp on AQUASIM) is defined as $H/2$ [92]. Therefore, the resulting amplitude is approximately $A = 0.59m$ (rounded to $A = 0.6m$). This value represents the maximum vertical displacement from the mean water level, providing a rigorous and safe boundary condition for the analysis of the FPV stability of platform and mooring tension.

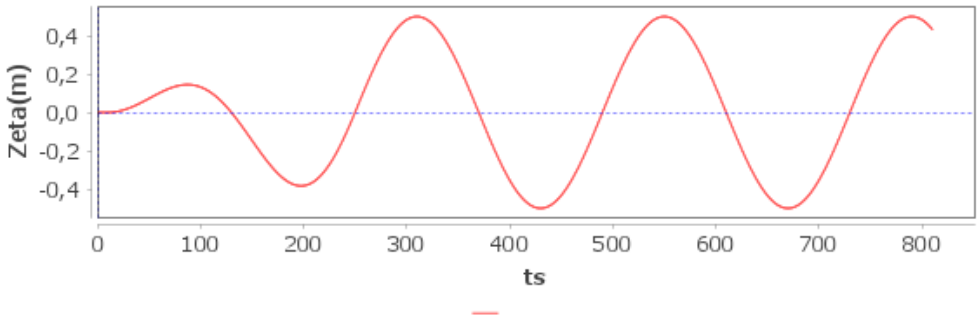

Figure 6.6: Wave profile simulated on Software AQUASIM

The hydrodynamic simulation is performed in the time domain using a transient time series approach. In this framework, the environmental loads and the structural response of the floating platform are computed step by step over a discretised time interval ensuring numerical stability and accuracy of the dynamic solution. The time increment (Preincrement) defines the temporal resolution of the simulation. It represents the time step used to update the system response and environmental forcing during the calculation. The max iterations parameter step represents the maximum number of numerical iterations allowed at each time step for the solver to reach equilibrium. During each increment the solver iteratively updates forces, displacements and velocities until convergence is achieved. The "Number of time steps for waves" defines the total duration of the simulation expressed as a sequence of discrete increments. In this study a value of 800 steps is selected, allowing the model to simulate several wave cycles (harmonic state represented in Figure 6.6) and to observe the transient behaviour of the platform. The "Number of steps" for one wave indicates how many time increments are used to discretise a single

wave period. Additional numerical options control the interaction between waves, currents and floating structure. The current reduction method, set as "Energy method", accounts for the energy exchange between the current field and the wave motion. The current reduction type, defined as "Deformed by current and waves", considers the modification of the current field caused by both wave propagation and structural deformation. Overall, the adopted time series configuration allows the numerical model to reproduce the transient hydrodynamic behaviour of the floating photovoltaic platform under the selected environmental loading conditions, while ensuring stable convergence of the nonlinear solver.

6.4 Simulation results

This section discusses the simulation results, taking into account that the present model refers to approximately a quarter of the full scale system, corresponding to a reduced platform of about 16 x 12.5 m. Therefore, all simulated quantities must be interpreted with reference to the scaled numerical configuration introduced in the previous sections.

```
 Total, all elements
Weight in air  [N]                                  167975.27074
Weight in water [N]                                    488.77275
Buoyancy [N]                                        167486.49800
Diffac = Weight/buoyancy of all elements                 1.00292
Total mass [kg]                                     17122.89039
buoyancy non Hydrodyn beams and trusses [kg]         5030.91800
Weight elements [N] / Mass elements [kg]                9.80998
Total mass of beam elements [kg]                    11622.03613
```

Figure 6.7: Hydrodynamic simulation results on AQUASIM Software

Parameter	Theoretical value 1/4 model	Simulated value	Difference
Total Mass [kg]	17796.25	17122.89	-3.78%
Displaced Volume $[m^3]$	17.36	16.66	-4.03%
Mass Beam Elements (including floater + pv + auxiliary) [kg]	11850	11622.04	-1.92%
Weight/Buoyancy Ratio	1	1.0029	+0.29%

Table 6.5: Comparison between theoretical and simulation value

The comparison reported in Table 6.5 shows that the simulated values remain in satisfactory agreement with the theoretical estimates derived in Section 6.1, despite the expected differences associated with the simplified numerical representation of the system. The total mass obtained from the simulation is slightly lighter than the theoretical one. Such result is plausible because part of the real system geometry is simplified, some local construction details are not explicitly represented and the distributed equivalent properties used in the model may lead to a modest reduction

in the overall simulated mass. The deviations observed between theoretical and simulated values are interpreted as physically acceptable. For the displaced volume is give a difference of -4.03%, coherent with the lower simulated mass, since a lighter floating system requires a smaller displaced water volume in order to satisfy hydrostatic equilibrium. The reduced displacement is not a separate anomaly but the direct consequence of the slightly lower simulated structural weight. Regarding the mass of beam elements, the theoretical value is determined by aggregating the structural frame mass (aluminum and steel) and the estimated weight of the photovoltaic modules (for the model). In the simulation, the PV modules and auxiliary components are modeled by distributing their equivalent mass into the structural beams. The resulting simulated value shows a limited deviation -1.92% which confirms the accuracy of the modeling approach: integrating the PV weight within the beam elements provided a fit between the theoretical sizing and the simulated structural response. The most important result is given by the Hydrostatic balance:

$$\text{Diff} = \frac{\text{Total Weight}}{\text{Total Buoyancy}} = \frac{167975.27}{167486.50} = 1.0029$$

where:

$$TotalBuoyancy = \rho\, g\, V_{\text{disp}}$$

The parameter Diff represents the ratio between the total structural weight and the total buoyancy force acting on the floating system. The small deviation +0.29% is an excellent outcome and shows that the iterative tuning of the numerical model successfully achieved the intended hydrostatic equilibrium. In practice, the difference between gravitational load and hydrostatic support is extremely small, meaning that the platform is very close to neutral flotation. From an engineering viewpoint, this is the most significant indicator of the validity of the model, because it demonstrates that the global balance between structural weight and buoyancy has been correctly reproduced.

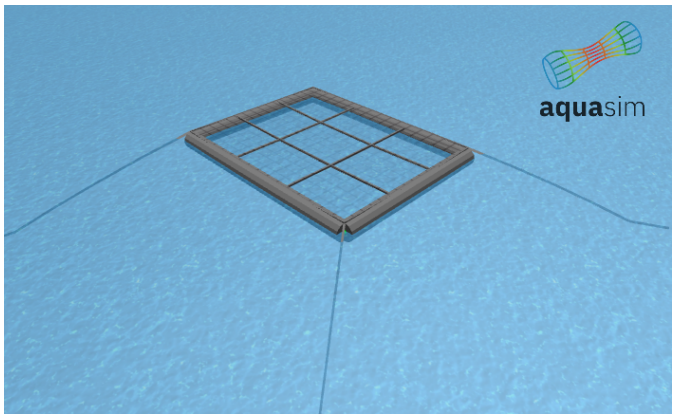

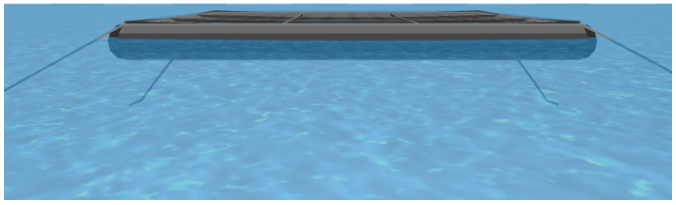

Figure 6.8: 3D results simulation in AquaView

This is also visually confirmed by the 3D view exported from AquaView, where the deck is shown floating above the still water level while the mooring lines remain tensioned and connected to the seabed. The platform images shown in the following figures were obtained by extracting selected frames from the video files generated by AQUASIM as part of the simulation output. This allows representative configurations of the dynamic response of the structure to be visualised more clearly.

```
Mass centre beams and trusses
    x          , y           , z
  6.167358       7.981287      -0.2819235

Mass centre beams only
    x          , y           , z
  8.500000       11.00000      0.2922877
```

Figure 6.9: Mass centre results on AQUASIM Software

From this results can be noticed that the beam mass centre is centred in plan and located above the still water reference, reflecting the position of the deck structure. When truss and submerged support components are included, the overall mass centre shifts downward, indicating the influence of the immersed buoyant and mooring elements. This lowering of the global structural mass centre is favourable from the point of view of static stability.

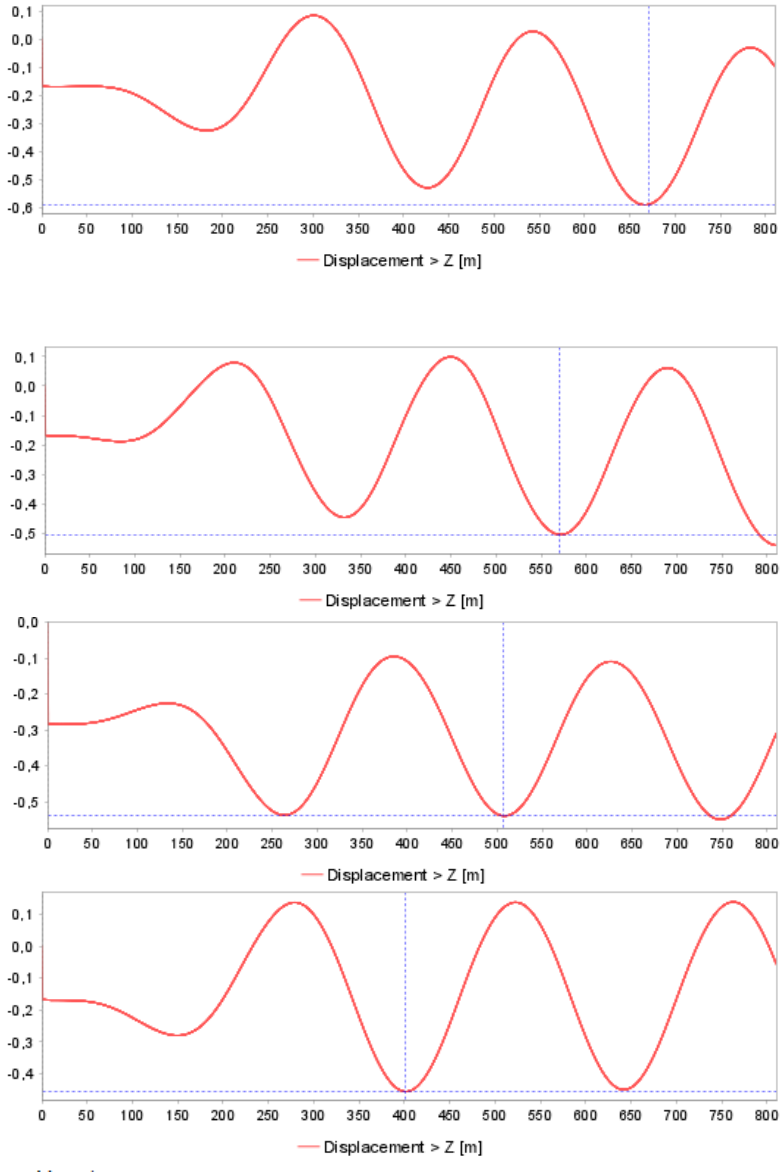

Figure 6.10: 4 nodes (NE - NW - SE - SW) fairlead mooring displacement along Z of model in AQUASIM

The vertical displacement histories of the four mooring attachment points show a regular oscillatory behaviour under wave loading. The negative values observed in the z-direction should be interpreted as downward motion relative to the initial equilibrium position of each node. As shown in the Figure 6.10, all signals exhibit a quasi sinusoidal trend with comparable amplitudes and no evidence of abnormal peaks or numerical instability. The overall response remains within a moderate range, indicating that the mooring connection points follow the wave induced

motion of the floating platform. Although the four displacement histories are similar in magnitude, they are not perfectly in phase. This behaviour is expected, since the attachment points are located at different positions along the platform perimeter and their vertical response is influenced not only by global heave, but also by the combined effects of roll and pitch. The Centre Of Buoyancy B is the point through which the resultant buoyant force acts where, in the present hydrostatic output, is located at:

$$B = -0.1874222 \text{ m}$$

The negative sign depends on the local reference system adopted in the software and indicates that the buoyancy centre lies below the selected origin. This is physically consistent for a partially submerged cylindrical buoy, since the buoyant force acts on the immersed portion of the body. When the floating body inclines, the geometry of the submerged volume changes, the position of B shifts and a restoring moment is generated. According to DNVGL-RP-0584 [84], "the stability requirements for floats are based on righting moment curves with acceptance criteria expressed in terms of requirements for the area of the righting moment curve relative to the area of the wind heeling moment curve and, in special cases, in terms of a simple requirement for the location of the metacentric height, GM". The Metacentric height can be calculated as:

$$GM = KB + BM - KG$$

where:

- GM is the distance between the centre of gravity and the metacentre;
- KB is the vertical position of the centre of buoyancy;
- BM is the metacentric radius;
- KG is the vertical position of the centre of gravity.

The metacentric radius is given by:

$$BM = \frac{I_{wp}}{V_{\text{disp}}}$$

where I_{wp} is the second moment of area of the waterplane and V_{disp} is the displaced volume. In the present case, the output gives:

$$GM = 0.081592292 \text{ m}$$

It is moderate and plausible for the floating photovoltaic platform: it is sufficiently positive to ensure restoring capability but not so large as to suggest an unrealistically stiff behaviour in roll, because:

- $GM > 0$: the floating body exhibits positive initial stability.
- $GM = 0$: the floating body is in neutral equilibrium.
- $GM < 0$: the floating body is hydrostatically unstable.

The GM distance from COG to metacentre is a relevant hydrostatic quantity for evaluating the small angle roll stability of the component. For a floating body subjected to a small angular displacement ϕ, the restoring moment is:

$$M_R = \Delta\, GM\, \sin\phi$$

and, for small rotations:

$$\sin\phi \approx \phi$$

so that:

$$M_R \approx \Delta\, GM\, \phi$$

where Δ is the displacement of the body. This shows that the restoring action is directly proportional to the metacentric height. The roll stiffness represents the rotational restoring stiffness in roll, that is, the restoring moment generated per unit rotation angle. For small angular motions it can be written as:

$$K_\phi = \Delta\, GM$$

and therefore:

$$M_R = K_\phi\, \phi$$

In the present output, the roll stiffness is

$$K_\phi = 84.56742 \text{ N/rad}$$

This value indicates a moderate roll restoring capacity, consistent with the hydrostatic behaviour expected for the reduced floating PV configuration. Overall, the combination of a submerged buoyancy centre located below the reference axis, a positive metacentric height of about 0.082 m and a roll stiffness of about 84.6 N/rad supports the conclusion that the model exhibits a realistic and physically consistent initial hydrostatic stability. Once this condition is verified, the analysis can be extended to the wave induced rotational response of the platform. The pitch motion represents the rotation of the platform about the transverse Y-axis, describing the wave induced ongitudinal angular motion of the floating system. According to the AquaView output, the angular response exhibits a clearly defined periodic oscillation, with values ranging approximately between 1.0° and 1.9°.

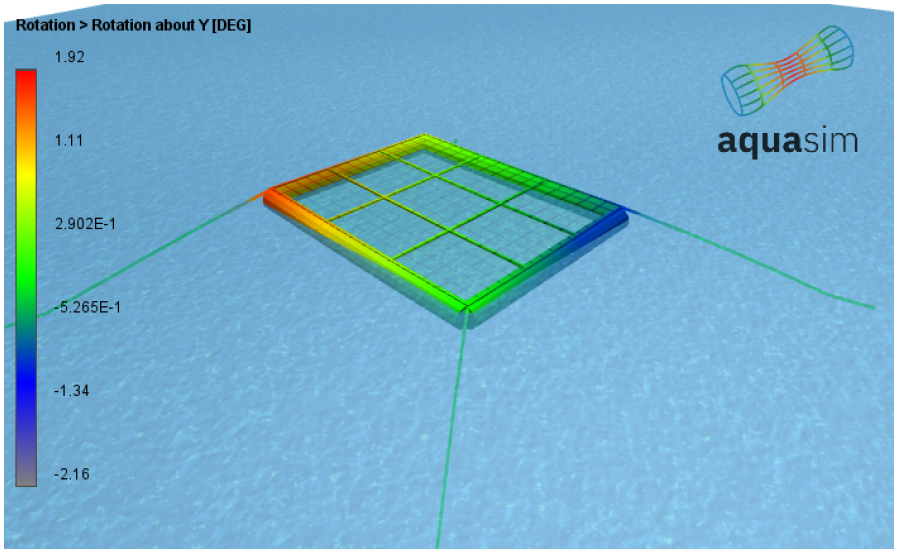

Figure 6.11: Spatial distribution of platform pitch, expressed in AQUASIM as rotation about the Y-axis, highlighting the angular gradient across opposite sides of the structure.

The colour distribution shown in the "Rotation about Y [DEG]" plot indicates that the rotation is not uniform over the structure, but develops with a clear gradient between opposite sides of the platform.

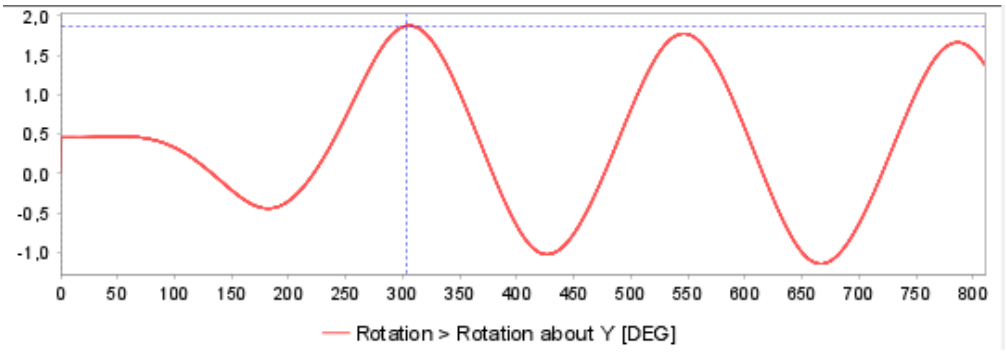

Figure 6.12: Time history of pitch response, expressed as rotation about the Y-axis, with oscillations approximately ranging from -1.0° to +1.9° in AquaView

The limited angular amplitude (Figure 6.12) indicates that the platform preserves a satisfactory hydrodynamic stability while still responding to wave action in a physically meaningful way. This aspect is particularly relevant for a floating photovoltaic platform, since restrained angular motions are beneficial both for maintaining regular operating conditions and for limiting the loads transmitted to

the structural members, joints and mooring system. The roll motion represents the rotation of the platform about the longitudinal X-axis, and therefore describes the wave induced lateral angular motion of the floating structure.

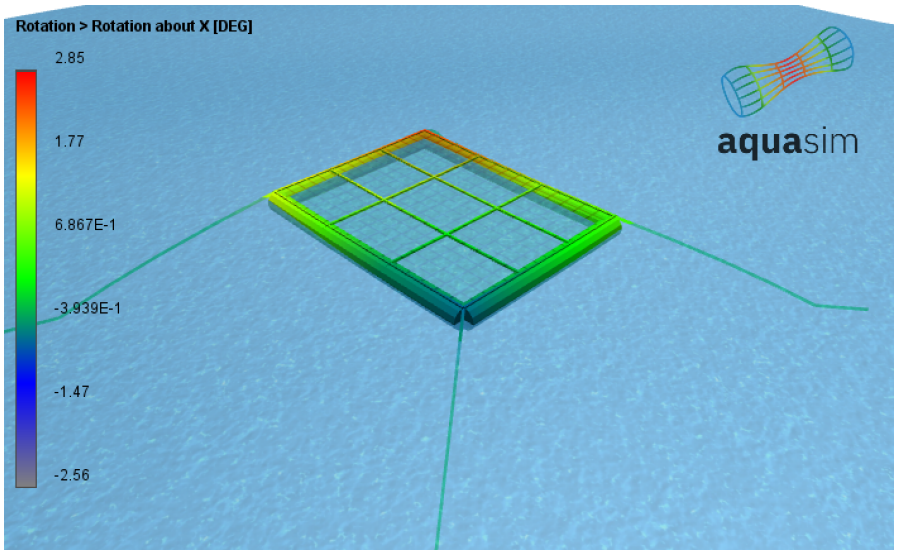

Figure 6.13: Spatial distribution of rotation about the X-axis, representative of the wave induced roll motion of the floating platform in AquaView.

The colour distribution shown in the "Rotation about X [DEG]" plot highlights a clear rotational gradient between opposite sides of the platform. This pattern is consistent with a roll motion, in which one side of the platform rises while the opposite side moves downward with respect to the equilibrium position.

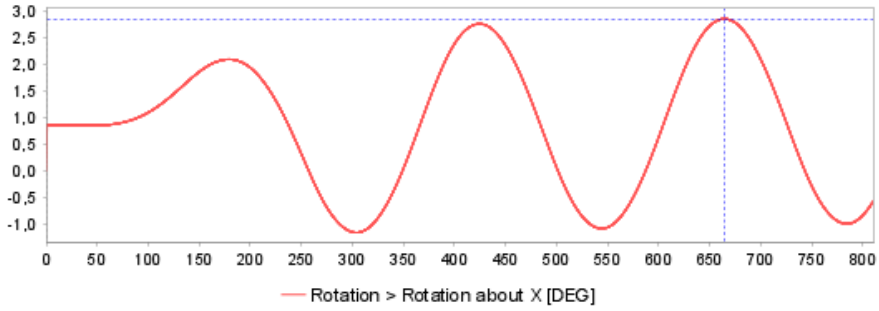

Figure 6.14: Time history of rotation about the X-axis in AquaView.

According to the AquaView output, the angular response exhibits a regular oscillatory pattern, with values ranging approximately between -1.1° and +2.9°. Compared with pitch, the roll response shows a slightly larger angular amplitude,

suggests that roll is more relevant remaining, at the same time, moderate with a stable floating configuration. Finally, The yaw motion represents the rotation of the platform about the vertical Z-axis, and therefore describes the wave induced heading variation of the floating structure.

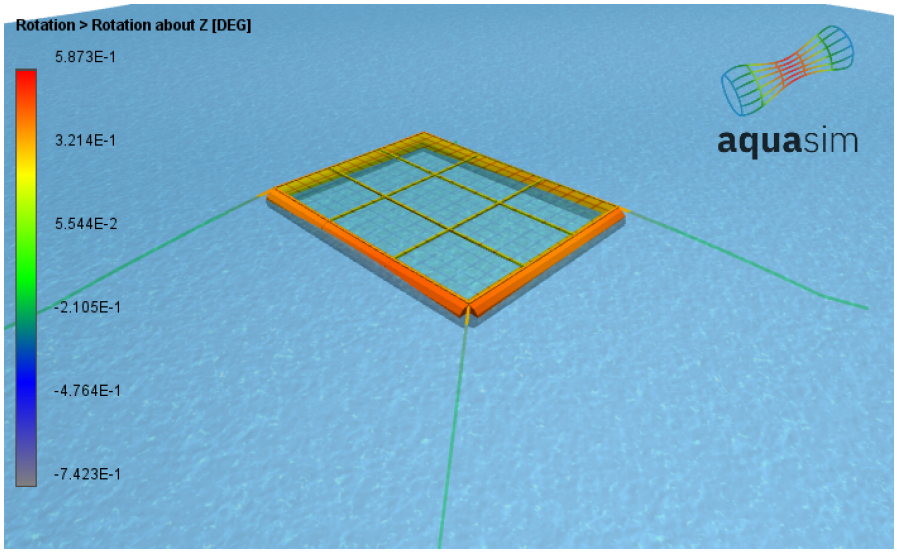

Figure 6.15: Time history of rotation about the X-axis in AquaView.

The colour distribution shown in the Rotation about Z [DEG] plot confirms this behaviour, as the values remain relatively uniform over the whole platform.

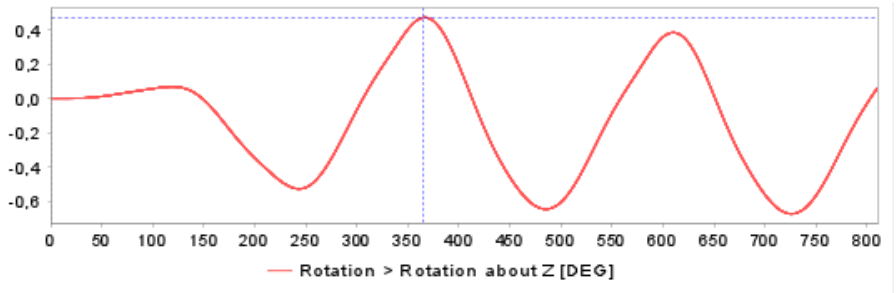

Figure 6.16: Time history of rotation about the X-axis in AquaView.

According to the AquaView output, the angular response exhibits limited oscillations, with values ranging approximately between -0.6° and +0.45°. Compared with pitch and roll, the yaw amplitude is significantly smaller. This suggests that, although the platform experiences a slight in plane rotation, yaw does not represent a dominant response mode. The following discussion refers to the South West (SW) mooring attachment node, selected as a representative point for analysing since it

is located at the interface between the taut mooring line and rigid deck structure, providing a meaningful reference for evaluating how the environmental loading is locally transferred to the platform under wave action.

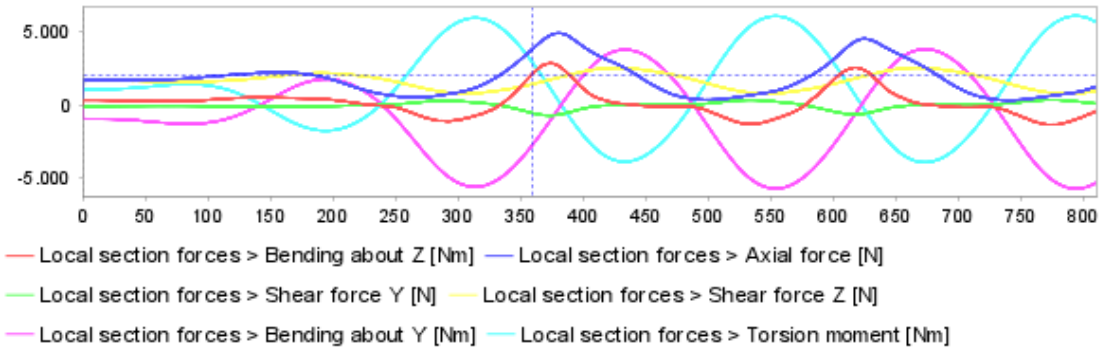

Figure 6.17: Local section stresses acting on SW mooring attachment node of model in in AquaView.

The local section forces 6.17 show a dynamically stable response under wave loading in which the amplitudes of the internal actions are limited and remain within a moderate range, indicating a favourable transfer of the environmental load to the deck structure. The axial force remains positive throughout the simulation, showing that the mooring line remains continuously in tension and does not undergo significant slackening. This is beneficial from a structural and operational point of view, as it prevents the occurrence of snap load phenomena associated with sudden retensioning of the line. The load transfer is therefore smooth and continuous. The shear forces in the local Y and Z directions remain moderate and oscillate in a regular way. These components represent the transverse and vertical local force transfer at the attachment point. This represent that the mooring does not act only in pure tension, but also introduces local transverse actions due to the motion of the floating platform. Their limited amplitude suggests that the system does not experience abnormal local shear concentrations. The bending moment about the Y axis represents the main local bending action at the mooring connection. Its oscillatory behaviour indicates that the attachment point is subjected to cyclic bending as a consequence of the combined effect of line tension, wave induced platform motion and local eccentricity of the load transfer. The torsional moment also shows a regular oscillatory behaviour and appears closely coupled with the bending response. The specular trend between torsion and bending about Y suggests that the mooring attachment is subjected to a combined bending and torsional action, which is physically consistent with the 3D motion of the platform. After a short transient phase, all force and moment components evolve in a periodic manner, which confirms that the model has reached a steady state response under

regular wave forcing. The resulting internal actions remain within a low structural demand range, supporting the validity of the adopted structural configuration and the adequacy of the mooring deck connection design. Although the detailed discussion is presented for a single representative node, the behaviour observed at the other mooring attachment points is similar in both trend and magnitude.

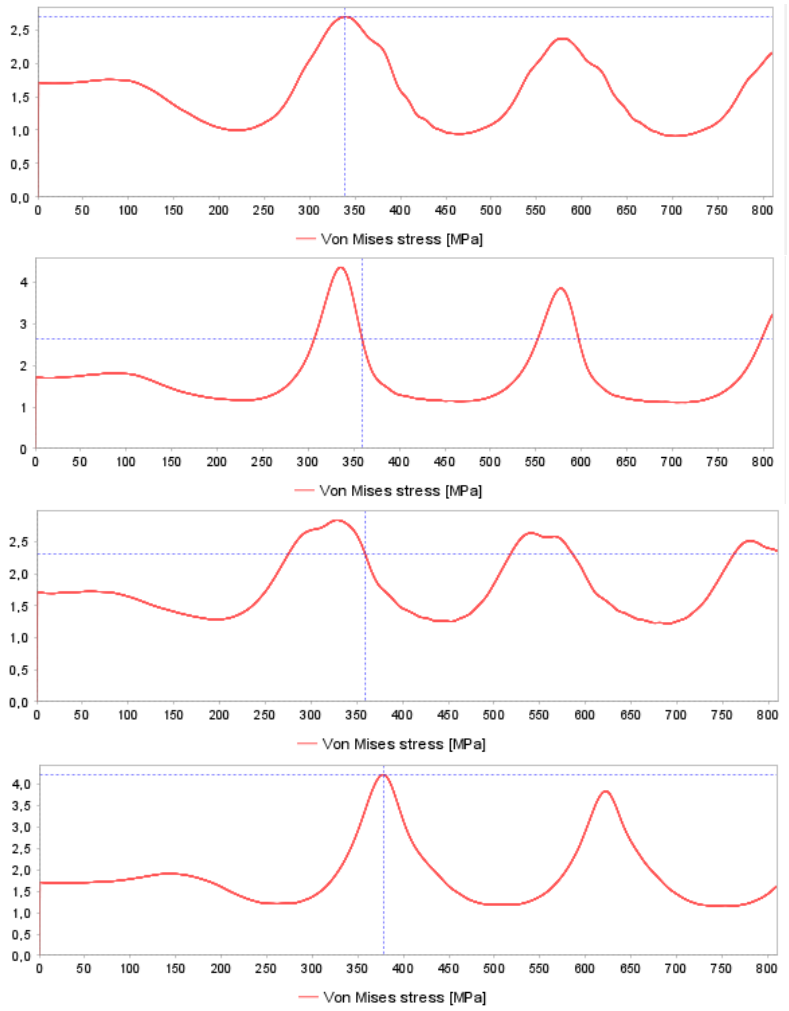

Figure 6.18: Von Mises [MPa] acting on mooring lines (NE - NW - SE - SW) model in in AquaView.

The Von Mises stress histories evaluated along the four mooring lines 6.18 show a stable and periodic response under the imposed wave loading. In all cases, the equivalent stress remains within a relatively low range, which indicates that the mooring system operates under structurally moderate demand conditions.Two mooring lines show slightly lower peak values, of the order of 2.5 – 2.8 MPa,

whereas the other two reach maximum stresses of about 4.0 – 4.3 MPa. This difference is physically expected, since each line is subjected to a slightly different combination of tension, platform motion and wave induced load transfer. In particular, due to the imposed environmental forcing acts from the South - West direction, some mooring lines are more directly engaged in resisting the incoming wave action than others. From a structural point of view, the resulting Von Mises levels are very low and remain far below typical material strength limits, thereby indicating that the adopted mooring configuration is adequate for the considered loading condition. Overall, the numerical results obtained from the AQUASIM simulations indicate that the proposed FPV model reproduce a physically and mechanically stable floating response under the selected environmental loading conditions. With satysfying hydrostatic balance between total weight and buoyancy, the platform remained afloat throughout the simulation and the dynamic response of the buoyant structure, deck and mooring system followed a regular oscillatory behaviour. In addition, the stress levels observed in the mooring lines remained within a moderate range, confirming that the station keeping system is able to transfer the wave induced loads without reaching critical structural demand. At the same time, the results also highlight that some aspects of the model could be further refined in future developments. In particular, the local internal forces at the mooring platform connection points suggest that the structural detailing of these interfaces may be improved in order to achieve a more uniform load transfer and reduce local bending torsional demand. Additional refinements could also include a more detailed representation of the connection geometry, a more advanced calibration of the structural stiffness distribution and the extension of the analysis to a wider range of irregular sea states and combined wind wave loading scenarios.

7 Techno-Economic Evaluation of the FPV System

In terms of economics, the floating photovoltaic installation has an important impact on the system's economic performance. The profit of such energy production plants is considered by the cost of generation and the production intensity. Regardless of the superiority of other energy generation systems, the economic evaluation would make the final decision to ensure the profits for the government, which is why decision makers rely on the economic assessment to emphasize particular energy production technologies.

7.1 Economic Assessment Methodology

The assessment is referred to the State of Queensland (Australia), a region characterised by high solar resource availability and a liberalised electricity market context. The analysis is developed over a time of 25 year consistent with the expected service life of the photovoltaic modules, while the discount rate is assumed to be equal to approximately 6%, representing a typical value for renewable energy investments. From a geographical and regulatory perspective, it is assumed that the system is connected to the National Electricity Market (NEM) and developed in compliance with the applicable Australian standards and regulations governing photovoltaic installations. The economic performance of the system is evaluated through a set of standard financial indicators.

- Net Present Value (NPV) is used to compare the discounted cash flows generated over the project lifetime with the initial investment, providing a direct measure of project profitability [93];
- Internal Rate of Return (IRR) identifies the discount rate at which the NPV becomes zero and allows the profitability of the investment to be compared with the assumed cost of capital;
- Levelised Cost of Energy (LCOE), defined as the ratio between the discounted lifetime costs and the discounted electricity generation, is adopted to express the average cost of electricity production in €/kWh;
- Payback Period, considered in both simple and discounted terms, is used to estimate the time required to recover the initial investment.

The chapter presents the economic assessment methodology adopted for the case study FPV system introducing the main input parameters and modelling the

annual cash flow. The subsequent sections present the economic assumptions related to capital expenditure, operation and maintenance costs. To this follow a discussion on LCOE resulting values, the sensitivity analysis and an evaluation of the Annual Energy Production. Throughout the chapter, the adopted assumptions are supported where possible, by reference values from the literature, technical reports and institutional sources, while parameters not directly available from the project definition are introduced through justified assumptions consistent with the Australian context.

7.2 Components Cost Estimation

In order to estimate CAPEX, OPEX and LCOE, several preliminary assumptions must be established regarding both the cost of the floating unit and the expected annual solar energy production. The analysis begins with the evaluation of the cost of the individual floating module, including both the supporting platform and the photovoltaic panels. Then, the additional costs associated with the mooring system and the subsea electrical cable are taken into account. The support structure can be divided into three main components:

- the floaters, which ensure the buoyancy of the system;
- the frame supporting the photovoltaic panels;
- the connecting structure linking the floaters to the main frame.

For the floaters, High-Density Poly Ethylene (HDPE) is selected because of its excellent resistance to ultraviolet radiation and saline exposure, combined with satisfactory mechanical strength and relatively low cost. The estimated cost associated with the HDPE component (in Queensland context [94]) is reported, considering a single floater:

HDPE Material	VALUE	UNIT OF MEASURE
Mass	310	kg
Density	950	kg/m^3
Volume	0.33	m^3
Material cost	1.8	€/kg
Total cost	558	€

Table 7.1: HDPE floater cost estimation

To optimize logistics and simplify the manufacturing process, the aluminum mounting surface with a total mass of 5000 kg is designed as a modular system. This

structure is subdivided into 18 prefabricated modules that are subsequently transported to the site and assembled onto the primary steel frame, significantly reducing installation time and labor costs on the water.

Aluminium 5005	VALUE	UNIT OF MEASURE
Mass	388.88	kg
Density	2700	kg/m^3
Volume	0.14	m^3
Material cost	2.43	€/kg
Total cost	944.78	€

Table 7.2: Aluminium platform cost estimation

The 14500 kg primary steel grid is organized into 14 standardized structural blocks. In technical terms, the design transitions from a Single Buoy mono-block to a Twin Buoy Module configuration. By integrating two buoyancy units into a single steel frame, the platform achieves higher global stiffness and significantly reduces the number of critical connection points to be assembled on site. This configuration is also designed to streamline both the fabrication phase and logistical handling, allowing each unit to serve as a high strength connection node for the buoyancy system.

Steel AISI 205	VALUE	UNIT OF MEASURE
Mass	982.8	kg
Density	7800	kg/m^3
Volume	0.11	m^3
Material cost	3	€/kg
Total cost	2678.4	€

Table 7.3: Steel support cost estimation

The choice of the photovoltaic panel aims to minimize the platform cost and maximize the panel power output, preferring the highest possible efficiency. The panel chosen in this study is Jinko Solar Tiger Neo N-Type 500W (72HL4-V). It is one of the most widely sold and installed solar panels in Queensland, owing to its proven reliability and cost effectiveness compared to premium models. Key advantages for this specific application:

- N-Type TOPCon Technology: highly resistant to Light Induced Degradation (LID) and Light and elevated Temperature Induced Degradation (LeTID) compared to older P-type modules. This is crucial for the intense solar radiation typical of the Queensland environment [95], [96];

- Marine Certifications: Certified according to IEC 61701 (Salt Mist Corrosion) at the maximum level (Severity 6). This ensures the panel can operate in close proximity to salt water without internal circuit corrosion [97];
- Dimensions: Measuring approximately 2278 × 1134 × 35 mm, this 72-cell panel is ideal for covering extensive areas like the 65x50m platform, effectively reducing the required number of clamps and supporting structural elements [98].

Jinko Solar Tiger Neo N-Type	VALUE	UNIT OF MEASURE
Nr of element	1100	-
Mass	27.1	kg
Length	2278	mm
Width	1134	mm
Nominal Power	500	W
Power Tolerance	+/-3	%
Panel Efficiency	23.17	%

Table 7.4: Photovoltaic panel Jinko Solar Tiger Neo N-Type data

7.3 Annual Energy Production for Economic Evaluation

The annual energy yield of the floating PV system is calculated by considering the technical specifications of the modules and the solar resource available at the site. The energy production of a single panel is determined by its surface area, its nominal efficiency and the Global Tilted Irradiation (GTI). Furthermore, a second efficiency is considered, taking into account the efficiency of the conversion process from Direct Current (DC) to Alternating Current (AC) and the losses due to inefficiencies of the transport of energy. The fundamental equation describing the energy yield is:

$$E = A \cdot r \cdot H \cdot PR \tag{7.1}$$

where A is the panel area, r is the efficiency or solar panel yield, H is the global tilted irradiation, and PR is the performance ratio, indicating losses overall effect on the PV system output due to the temperature, system inefficiencies or failures [99]. The energy supplied by a single panel in a day is then multiplied by the number of panels on the platform to obtain the actual energy yield. In order to estimate the energy yield is used technical characteristics of the N-Type modules for the 1100 panel platform and data from Global Solar Atlas for the installation site selected North Stradbroke Island:

- PR (performance ratio) = 75% (assumption [45])
- r (panel efficiency) = 23.17%
- A (area single panel Jinko) = 2.278m x 1.134m = 2.5832m^2
- N (panel number) = 1100
- H (average GTI from Global Solar Atlas) = 5.62 kWh/m^2/day

Finally, Table 7.5 shows the calculation of the actual annual energy yield of the plant:

FEATURES	VALUE	UNIT OF MEASURE
Nr of panel on platform	1100	
PV panel nominal power	500	W
Energy produced/platform/day	2775.1	kWh/day
Energy produced/platform/year	1012.9	$MWh/year$

Table 7.5: Estimation of the annual energy produced

Based on data [100], North Stradbroke Island has a total of 1976 private dwellings. During the peak summer season in December, energy demand escalates significantly due to the influx of tourists, tripling the population on island and the intensive use of air conditioning. In this period, the average daily consumption per household is estimated at approximately 20–22 kWh (factoring in high load vacation rentals and hospitality services), leading to a total island peak demand of roughly 40–45 MWh per day. On an annual scale, considering the fluctuations between low and high seasons, the average daily requirement stabilizes at around 31 MWh, resulting in a total annual energy consumption of approximately 11.3 GWh. These estimation is aligned with the regional consumption profiles provided by Energex and the Distribution Network Service Provider (DNSP) for South East Queensland [101], [104]. Furthermore, the island features a penetration of residential solar photovoltaics. This local generation drastically reduces the demand from the mainland grid during peak sunlight hours (9:00 AM – 3:00 PM), creating a pronounced "duck curve" profile [103].

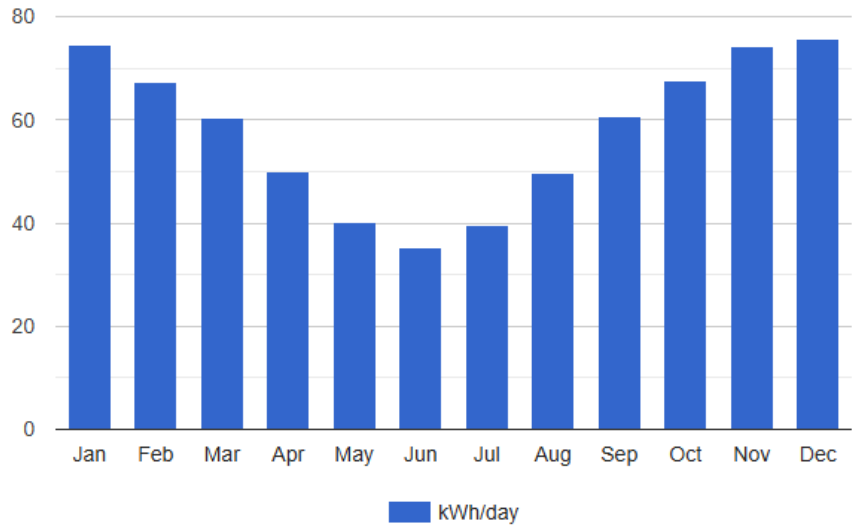

Figure 7.1: Mean daily production of solar panels in North Stradbroke Island (source [104]).

In this context, Figure 7.1 shows that the existing residential solar PV installations on North Stradbroke Island generate approximately 75.692 kWh/day in December, corresponding to only 0.19% of the total island electricity demand during the high season. By comparison, the proposed offshore FPV system analysed in this study is expected to produce about 2775 kWh/day, covering approximately 9% of the same daily demand. This difference highlights the contribution that the proposed system could provide, despite still remaining limited with respect to the total island load. However, this result should be interpreted in light of the specific nature of the installation considered in this work. The proposed FPV system is intentionally conceived as a theoretical and experimental design case, rather than as a utility scale commercial plant. The purpose is not to meet a dominant share of the island electricity demand, but rather to assess the feasibility of an offshore floating photovoltaic solution under realistic site with specific environmental and technical conditions. The energy yield of the FPV system, preliminary estimated, is then verified through simulations made with the Global Solar Atlas. The Global Solar Atlas provides interactive maps to visualize the solar resource potential worldwide. Moreover, a PV yield calculator estimates the energy yield in different time scales for different solutions, such as small residential rooftops, medium size commercial, ground mounted large scale and floating large scale systems. The simulation considers a floating PV system of 0.5 MWp installed capacity, with a 10° tilt angle and 0° azimuth angle (due to southern hemisphere).

	Jan	Feb	Mar	Apr	May	Jun	Jul	Aug	Sep	Oct	Nov	Dec
0 - 1												
1 - 2												
2 - 3												
3 - 4												
4 - 5												
5 - 6	6.074	1.546							0.134	7.773	17.784	15.639
6 - 7	54.214	37.735	23.512	15.864	3.909	1.006	1.067	7.128	35.599	69.242	81.344	73.172
7 - 8	121.330	108.778	94.597	89.618	68.181	44.698	48.817	83.464	121.506	147.683	154.149	142.986
8 - 9	183.308	176.124	163.470	164.746	143.468	122.826	132.498	165.667	198.027	216.296	216.143	202.521
9 - 10	235.444	228.720	212.202	218.595	196.118	176.478	191.801	227.472	253.461	267.089	265.411	247.596
10 - 11	263.814	258.327	242.201	250.658	227.664	208.173	226.761	263.096	290.426	295.311	289.446	273.971
11 - 12	282.040	277.667	261.895	262.780	239.979	223.456	246.537	284.415	310.665	308.792	305.250	291.109
12 - 13	281.910	279.558	263.643	261.171	234.907	216.277	241.510	281.138	302.093	302.760	304.227	291.189
13 - 14	265.876	263.923	245.257	236.362	209.618	192.091	215.965	254.336	273.674	276.303	274.756	271.558
14 - 15	230.432	227.439	204.519	191.563	162.029	147.224	169.033	207.176	220.469	225.972	224.390	228.132
15 - 16	180.634	173.133	150.359	129.850	98.113	86.494	107.843	138.801	150.402	156.055	163.876	169.156
16 - 17	115.079	108.266	83.828	51.980	22.791	14.790	26.047	52.536	67.087	74.678	88.700	100.811
17 - 18	45.916	39.367	17.591	1.585				1.025	4.396	10.148	20.909	35.404
18 - 19	2.942	1.750										1.902
19 - 20												
20 - 21												
21 - 22												
22 - 23												
23 - 24												
Sum	2,269	2,182	1,963	1,875	1,607	1,434	1,608	1,966	2,228	2,358	2,406	2,345

Figure 7.2: Average hourly profile during months in Global Solar Atlas (source [33]).

As outputs, the system calculates the energy produced annually and monthly, estimating the average hourly profiles for each month. In December is shown an average production of 2580 kWh.

7.4 Capital Cost Estimation (CAPEX)

In order to estimate the Levelized Cost Of Energy and to compare this type of plant with other renewable sources, it is necessary to consider the main cost items. Regarding the floating support structure, the material cost of the various components has been increased by 20% to consider all the manufacturing work, such as beam lamination and welding, to obtain the supporting structure. Table 7.6 summarises these items: the total cost of the complete platform is EUR

FEATURES	VALUE	UNIT OF MEASURE	N PIECES
Material cost HDPE	558	EUR	28
Material cost Al 5005	944.78	EUR	18
Material cost AISI 205	2678.4	EUR	14
Manufacturing work, assembly	20	%	
Total cost	84152.8	EUR	

Table 7.6: Overall cost estimation of the floating platform

Australia maintains some of the world most competitive solar installation costs due to high market maturity. Due to this, the price of the chosen solar module is around 90 €/unit purchased in bulk. According to the CSIRO [105] (reference for energy costs in Australia), the capital expenditure for utility scale project in Australia is approximately 950 – 1100 AUD/kW (around 580 – 670 €/kW). However, offshore or floating projects, such as the one proposed, incur significant "marine premiums" including specialized mooring systems, anchoring and submarine cabling to withstand tidal and saline conditions. These costs are challenging to evaluate due to the absence of projects of this size in a marine environment and the lack of public data: preliminary estimation data from offshore wind and ocean engineering are considered. Regarding the mooring system, an hybrid mooring configuration is adopted to optimize performance in the local marine environment. As illustrated in the reference study, the total cost for the steel chain section (C_{chain}) is calculated based on the weight (W_{chain}) and the local price of marine grade galvanized steel (C_{steel}), estimated in Australia at 4.70 AUD/kg (approx. 2.87 €/kg).

$$C_{\text{chain}} = W_{\text{chain}} \cdot C_{\text{steel}} \tag{7.2}$$

To enhance elasticity and reduce the structural load on the floating platforms, the system incorporates synthetic ropes (Polyester) [106]. In the Australian market, these specialized marine ropes are priced at around 20 AUD/m (approx. 12.60 €/m) [107]. For the project the helical anchor is chosen due to the seabed characteristics, where in the Queensland marine sector typically costs between 130 - 190 AUD/unit

(80 - 110 €/unit) [109], depending on the Maximum Breaking Load (MBL).

$$C_{\text{drag}} = MBL \cdot (0.052/9.81) \tag{7.3}$$

Electrical balance of system (BoS) costs for offshore applications in Queensland are estimated at 800 AUD/kW (approx. 450 €/kW) [108], while the submarine cable connecting the plant to the Dunwich grid is priced at 120 - 300 AUD/m (approx. 73 - 183 €/m) depending on section and armour [110].

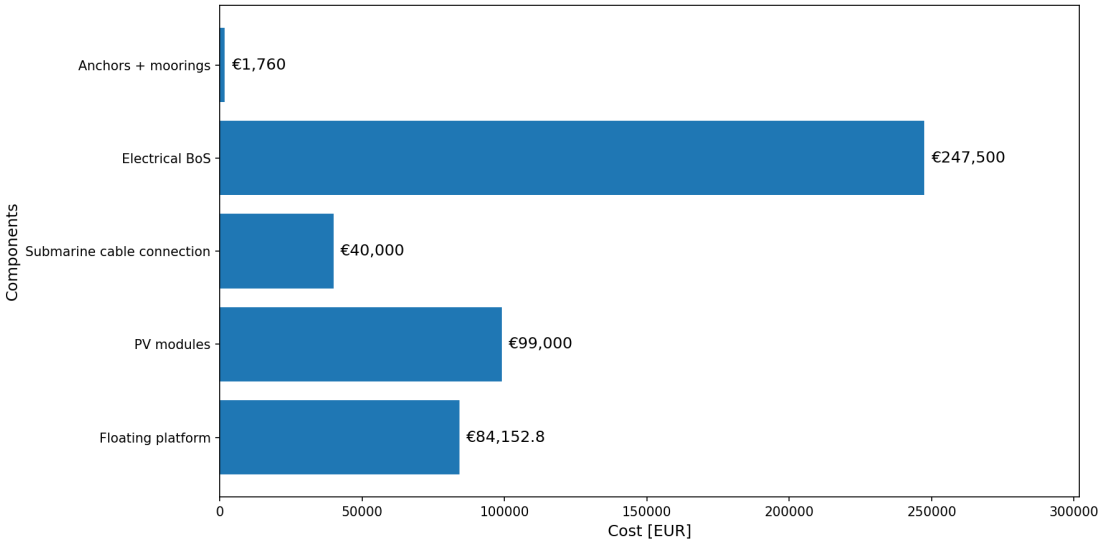

Figure 7.3: CAPEX Breakdown of the proposed FPV system (author's elaboration)

For the mooring system, a simplified rounded estimate is adopted by assuming a total mooring length of 30 m for each line, despite the local water depth being approximately 12 m, in order to account for the inclined configuration and the additional length required for proper anchoring behaviour. On this basis, the steel portion corresponds to about 6 m per line, leading to an estimated cost of approximately 72 € in total, assuming 3 €/m for four chains. The polyester portion corresponds instead to about 24 m per line, which, at an assumed unit cost of 13 €/m, results in approximately 1248 € for the four mooring lines. The total approximated mooring cost is therefore taken as 1320 €. For the anchoring system, a simplified estimate is also adopted by assuming 110 € for each helical anchor. Considering four anchors, this leads to a total anchor cost of 440 €. Accordingly, the combined cost of anchors and moorings was approximated at about 1760 €. For the Electrical BoS, a specific cost of 450 €/kW was considered, which, for a 550 kW system, gives the adopted value. Finally, for submarine cable connection,

a unit cost of 700 €/m is assumed over an estimated distance of 4000 m, since the proposed installation is located approximately 4 km from the shoreline.

7.5 Operation and Maintenance Cost Estimation (OPEX)

Operation and maintenance cost estimation for floating photovoltaic systems remains affected by a significant degree of uncertainty, particularly for offshore photovoltaic applications. FPV is still a recent technology and publicly available cost data for long term operation and maintenance are limited, fragmented or often not directly comparable across projects. For this reason, in this study the OPEX assessment is approached from a qualitative and functional perspective, identifying the main cost categories that are expected to contribute to the annual operational expenditure. In the present case, relevant O&M costs for the floating system include:

- saline humidity with corrosion risk;
- wave induced structural stress;
- periodic inspection of mooring and anchoring components;
- safe maintenant operation of electrical components.

Compared with land based PV systems, these aspects may require more specialised inspection procedures, dedicated safety protocols and more frequent replacement or servicing of selected components. From a budget perspective, the OPEX structure can be divided into several main categories.

Figure 7.4: FPV O&M costs breakdown (source [75]).

A first cost stream is associated with monitoring and inspection, including remote monitoring systems, sensor equipment and periodic visual inspections of both structural and electrical components. A second category concerns key component

inspections, such as the verification of PV modules, floating supports, joints, cable routing, inverters, combiner boxes and mooring connections, with the objective of detecting early degradation, displacement, corrosion or mechanical fatigue. A third category includes site management and cleaning of PV modules, removal of salt deposits or marine fouling where required and general maintenance of the floating structure and access paths. Additional costs arise from labour and logistics, particularly because offshore O&M activities may require trained marine personnel, small vessels, specialised safety equipment and weather dependent scheduling. Finally, soft costs and contingency allowances should also be considered, including insurance, regulatory compliance, emergency repairs and reserves for unplanned interventions. Due to the absence of data, in this study are considered fixed percentages for installation and decommissioning concerning the total Capex: offshore wind percentages are used indicatively from the Carbon Trust, which suggests values of 5% and 2%, respectively.

7.6 Levelised Cost of Energy Analysis (LCOE)

The Levelized Cost Of Energy is a ratio that calculates the cost incurred for the production of energy, taking into account the Capex and Opex of the plant and considering its entire life: it is typically expressed as EUR per MWh or kWh. The LCOE formula is defined as follows:

$$LCOE = \frac{I_0 + \sum_{t=1}^{n} \frac{A_t}{(1+f)^t}}{\sum_{t=1}^{n} \frac{M_{el}}{(1+f)^t}} \tag{7.4}$$

where:

- I_o is the capital expenditure expressed in thousands of euros corresponding to 472.41 k€;
- A_t is the value of the Opex for the single year t;
- M_{el} is the electricity produced each year expressed in MWh;
- i is the weighted average cost of capital (WACC), expressed as a percentage.

WACC takes into account many factors, including currency inflation and the level of investment risk: the higher this value is, the less value future cash flows have when discounted to the present.Revenue must be greater than the operating costs incurred each year, so a high value of i penalizes the LCOE ratio. In order to perform this calculation, the useful life of the photovoltaic plant of 20 years has been estimated and being a very innovative technology also has a high level of risk, equal to 5.5% [111]. The loss of productivity due to the panel degradation is

considered by including a decrease factor equal to 2% per year. In following Table the estimated LCOE is reported:

FEATURES	VALUE
CAPEX (k€)	472.41
OPEX (k€)	33.06
LCOE (€/MWh)	85
Annual Productivity (MWh)	1012.9

Table 7.7: Capex, Opex and LCOE for the system studied

While the LCOE demonstrates strong economic potential, but for a more accurate feasibility study must integrate cable landing point on the island and assessing the ease of grid interconnection.

7.7 Discussion of Techno-Economic Performance

The LCOE obtained in the present study, equal to 85 €/MWh, indicates that the proposed offshore floating photovoltaic configuration can be regarded as economically credible, although still more expensive than conventional land based solar technologies. In the Australian context, this result should be interpreted against the cost ranges reported for other renewable technologies. The latest CSIRO GenCost [105] assessment confirms that large scale solar PV remains one of the lowest cost forms of new build electricity generation in Australia, with indicative cost ranges below those of more complex technologies, while onshore wind also remains highly competitive. At the same time, GenCost notes that renewables can incur additional costs, estimated at about AUD 42–48/MWh in 2024 depending on the share of renewable energy in the system. At global level, IRENA reports the average LCOE values of 44 USD/MWh for utility scale solar PV, 33 USD/MWh for onshore wind and 75 USD/MWh for offshore wind [112]. Although these benchmarks are not directly comparable because of differences in scale, financing assumptions and system boundaries, they still show that the LCOE found in this thesis is higher than ground PV, already close to the same order of magnitude as offshore renewable technologies. This difference is consistent with the specific characteristics of the system analysed. Unlike ground mounted PV, the proposed configuration requires floating support structures, corrosion resistant materials, components, structural solutions, and labour specifically suited to the marine environment which inevitably increase both investment and operational costs penalising therefore the final LCOE. A similar trend has already been observed in Australian FPV literature: a recent feasibility study on floating PV in

New South Wales found that FPV systems involve about 20% higher initial costs than ground PV and around 9% higher LCOE, despite the benefits from improved thermal performance and lower module operating temperatures [114]. Therefore, the value obtained here is coherent with the Australian context, especially considering that the present case refers not to a sheltered freshwater reservoir, but to a coastal offshore environment where engineering requirements are more severe. Compared to the retail electricity prices for commercial consumers in South East Queensland, which frequently exceed 200 AUD/MWh according to the Queensland Competition Authority (QCA) [113], the project demonstrates a clear economic rationale for self consumption applications. The sensitivity of the model is heavily influenced by the conservative 2% annual degradation rate adopted. While this provides a prudent safety margin for a coastal deployment, utilizing the Jinko Tiger Neo's technical specification of 0.4% degradation would further compress the LCOE towards 78 €/MWh. Furthermore, the inclusion of Australian large scale Generation Certificates (LGCs) or potential capital subsidies for innovative marine renewables could further enhance the project's Internal Rate of Return (IRR). In conclusion, while offshore FPV currently faces a cost premium over terrestrial solar, its ability to bypass land use constraints on North Stradbroke Island and benefit from water induced cooling—potentially increasing yield by 5 - 10% positions it as a robust future contributor to the Moreton Bay renewable energy [**?**].

8 Conclusions and Future Research Perspectives

This thesis investigates the feasibility of an offshore floating photovoltaic system proposed for the semi-sheltered marine environment located west of North Stradbroke Island, in South East Queensland. The study was conceived as a preliminary feasibility assessment, with the aim of exploring whether a floating solar installation in coastal marine conditions could be developed as a credible and technically coherent in the Australian context. Unlike conventional photovoltaic design studies, which often rely on well established design standards and mature technological references, this work addressed a field in which offshore FPV applications remain only marginally explored, especially in relation to open marine environments. The limitation of the academic literature currently available is primarily related to the fact that offshore floating photovoltaic systems are still at an early stage of development within the renewable energy sector. As a result, the thesis evaluates the progressive construction of a new system. The most significant outcome of this research is therefore not only the identification of a potentially suitable installation area, although this remained an important part of the study, but above all the development of the floating platform concept itself. The central challenge of the thesis is the need to conceive the system from the ground up, in the absence of a consolidated body of literature specifically addressing offshore FPV platforms in marine Australian conditions. The available academic references are limited, since most existing studies concern inland reservoirs, calm water bodies or generic floating renewable structures rather than photovoltaic platforms exposed to real offshore environmental actions. Consequently, the design process required a strongly interpretative and engineering based approach, in which assumptions had to be introduced carefully and coherently in order to move from a theoretical idea to a physically plausible configuration. The proposed system was defined through a sequence of assumptions concerning geometry, buoyancy, structural mass distribution, mooring arrangement and environmental loading. This approach made it possible to transform an initially abstract concept into a floating system that could satisfy the essential requirements of hydrostatic balance and preliminary hydrodynamic feasibility. Reaching this result represented the main scientific and engineering challenge of the entire work. The platform had to be dimensioned and arranged by balancing multiple competing requirements through iterative processes. The design process has required a verification that the assumed system could remain physically stable, float at a realistic draft and maintain a coherent weight distribution under operating conditions. The fact that the final concept was able to satisfy these hydrostatic constraints is one of the strongest indicators that the design path

followed in the thesis is technically meaningful. Beyond hydrostatic equilibrium, the thesis also demonstrated a satisfactory preliminary hydrodynamic feasibility of the proposed system. Through numerical modelling, the platform was shown to respond in a regular and acceptable way under the wave conditions considered. This result is highly relevant because, in offshore floating photovoltaic applications, the transition from a static floating body to a dynamically viable energy platform is one of the key thresholds of feasibility. In this work, the modelling showed that the concept is not only able to remain afloat, but also to behave in a mechanically coherent way within the selected environmental framework. The hydrodynamic and structural modelling carried out in the thesis provided useful insight into the behaviour of the mooring platform system and the local load transfer mechanisms. The analyses indicate that the station keeping arrangement is able to maintain the platform in a stable configuration while transferring environmental loads without entering in critical conditions. At the same time, the simulations revealed areas where force concentrations and structural sensitivity may arise especially near local connections. From the energy perspective, the study confirmed that the selected marine area presents favorable solar potential for photovoltaic generation. The assessment showed that the proposed configuration could produce a good annual energy yield. The techno-economic assessment further supports the relevance of the proposed concept, even though it remains a preliminary evaluation. The estimated LCOE indicates that the system is more expensive than conventional land based photovoltaic solutions, which is expected given the additional requirements associated with marine deployment. However, the resulting value still suggests that the concept can be regarded as economically credible at feasibility level in an Australian offshore context, especially when interpreted as an experimental and pioneering project rather than a final commercial design. The thesis does not claim to resolve all uncertainties related to offshore floating solar deployment but rather, it provides a starting point from which those uncertainties can now be investigated with greater depth and precision. Future studies should investigate a broader spectrum of irregular sea states, combined wave wind and current loading for a more advanced structural and hydrodynamic analysis. Experimental validation should also represent a major objective of future research. Since the present work is based on conceptual modelling and engineering assumptions, the next logical step would be the development of a reduced scale prototype for physical testing. Such an activity would make it possible to compare numerical predictions with real behaviour, calibrate hydrodynamic and structural parameters. In an emerging field such as offshore FPV, this passage from conceptual modelling to experimental verification is essential for technological advancement. Further studies will also be required on the electrical integration of the system. The present thesis identified a technically reasonable export solution but a more detailed grid connection analysis will be necessary in order to verify the landing point of the cable and inverter

placement. Similarly, the economic assessment should be expanded once more reliable data become available especially regarding offshore OPEX. In conclusion, this thesis has demonstrated that the development of an offshore floating photovoltaic platform is feasible in the marine waters of Moreton Bay, successfully defining a system capable of showing promising hydrodynamic feasibility and energy production performance. For this reason, the thesis provides a basis for future research on offshore FPV in Australia.

8 Bibliography

[1] Z. He, W. Xu, Y. Sun, and X. Zhang, "A GIS-based techno-economic comparative assessment of offshore fixed and floating photovoltaic systems: A case study of Hainan," *Applied Energy*, vol. 391, Art. no. 125854, 2025. Available: https://www.sciencedirect.com/science/article/pii/S0306261925005847. doi: 10.1016/j.apenergy.2025.125854.

[2] International Energy Agency (IEA), *Snapshot of Global PV Markets 2024*, IEA-PVPS, 2024. Available at: https://iea-pvps.org/snapshot-reports/snapshot-2024/.

[3] Pv magazine, "Wood Mackenize forecasts 77GW of floating solar by 2033", 20 November 2024. Available: https://www.pv-magazine.com/2024/11/20/wood-mackenzie-forecasts-77-gw-of-floating-solar-by-2033/.

[4] K. Trapani and M. Redón Santafé, "A review of floating photovoltaic installations: 2007–2013," *Progress in Photovoltaics: Research and Applications*, vol. 23, no. 4, pp. 524-532, 2014.

[5] M. Al-Badawi et al., "Floating Photovoltaic Solar in Australia—A Feasibility Study," *Sustainability* (or relevant ResearchGate repository), 2024. Available:https://www.researchgate.net/publication/386490879_Floating_Photovoltaic_Solar_in_Australia-A_Feasibility_Study.

[6] S. Gadzanku, H. Mirletz, N. Lee, J. Daw, and A. Warren, "Benefits and Critical Knowledge Gaps in Determining the Role of Floating Photovoltaics in the Energy-Water-Food Nexus," *Sustainability*, vol. 13, no. 8, Art. no. 4317, 2021. Available: https://www.mdpi.com/2071-1050/13/8/4317.

[7] P. Conca and D. Tognetti, *Ricerca di una metodologia per la modellazione multibody di impianti fotovoltaici offshore*, Tesi di Laurea Magistrale, Università degli Studi di Genova, Scuola Politecnica, Dipartimento di Ingegneria meccanica, energetica, gestionale e dei trasporti, A.A. 2023-2024.

[8] R. Bugeja et al., "Floating Solar Energy Systems: A Review of Economic Feasibility and Cross-Sector Integration," *Journal of Marine Science and Engineering*, vol. 13, no. 8, 2025.

[9] Facebook post, "Helical Anchor System with Buoy,". Available: https://www.facebook.com/groups/371368279065178/posts/531339006401437/.

[10] M. Acharya and S. Devraj, *Floating Solar Photovoltaic (FSPV): A Third Pillar to Solar PV Sector?*, The Energy and Resources Institute (TERI), New Delhi, 2019. Available: https://www.teriin.org/sites/default/files/2020-01/floating-solar-PV-report.pdf.

[11] J. Solis-Chaves et al., "Potential Induced Degradation (PID) in Floating PV: Impacts of Humidity and Structural Design," *IEEE Journal of Photovoltaics*, vol. 11, no. 4, pp. 1022-1030, 2021.

[12] ITP Renewables, *Floating PV Technology Assessment and Market Analysis*, Australian Renewable Energy Agency (ARENA), 2020.

[13] International Renewable Energy Agency (IRENA), *Renewable Capacity Statistics 2025*, Abu Dhabi, 2025.

[14] World Economic Forum (WEF), *Fostering Effective Energy Transition 2025 Edition*, Geneva, 2025.

[15] World Bank Group, *Where Sun Meets Water: Floating Solar Market Report 2024*, Washington, DC, 2024.

[16] S. J. Stewart et al., "Environmental and Regulatory Barriers to Floating Solar in Australia," *Marine Policy*, vol. 155, 2023.

[17] F. S. Oliveira-Pinto and P. Stokkermans, "Assessment of floating solar photovoltaic potential in coastal areas: A case study of the Portuguese coast," *Renewable and Sustainable Energy Reviews*, vol. 135, p. 110414, 2021.

[18] T. Kjeldstad et al., "Cooling of floating photovoltaics and the importance of water temperature," *Solar Energy*, vol. 218, pp. 544-551, 2021.

[19] R. Claus and K. Lopez, "Operational and maintenance challenges for floating solar PV," *Renewable Energy Focus*, vol. 35, pp. 115-125, 2020.

[20] A. Sahu, N. Yadav, and K. Sudhakar, "Floating solar photovoltaic systems: An emerging technology," *Renewable and Sustainable Energy Reviews*, vol. 63, pp. 370-376, 2016.

[21] Moreton Bay Environmental Education Centre, *North Stradbroke Island (Minjerribah): Cultural and Environmental Importance*, Queensland Government, 2026. Available: `https://moretoneec.eq.edu.au/our-environment/north-stradbroke-island-minjerribah`

[22] Department of Climate Change, Energy, the Environment and Water (DCCEEW), *Moreton Bay Ramsar Site*, Australian Government, 2026. Available: `https://www.dcceew.gov.au/water/wetlands/australian-ramsar-wetlands/moreton-bay`.

[23] Geoscience Australia, "Marine," *Geoscience Australia Portal*. Available: `https://portal.ga.gov.au/persona/marine`.

[24] Tourism and Events Queensland, *Guide to North Stradbroke Island (Minjerribah)*, 2024. Available: `https://www.australia.com/en-in/places/brisbane-and-surrounds/guide-to-north-stradbroke-island.html`.

[25] Department of Resources (Queensland), *Queensland Coastal Waters and Islands Dataset*, Queensland Spatial Catalogue (QSpatial), 2023. Available: `https://spatial-qld-gov-au.s3.amazonaws.com`.

[26] Google, *Google Earth Pro*, Version 7.3, Google LLC, 2026. Available: `https://earth.google.com`.

[27] Maritime Safety Queensland, *Moreton Bay Navigation Charts: Dunwich and North Stradbroke Island (Series MB1)*, Department of Transport and Main Roads, 2022.

[28] Stephens, A. W., *Geology of Moreton Bay*, in: I. R. Tibbetts, P. C. Rothlisberg, D. T. Neil, and T. A. Himer (Eds.), *Moreton Bay and Catchment*, School of Marine Science, University of Queensland, 2010.

[29] Redland City Council, *North Stradbroke Island (Minjerribah) Economic Transition Strategy*, Infrastructure and Transport Planning Division, 2021.

[30] Queensland Government, *Marine Parks (Moreton Bay) Zoning Plan 2019*, Subordinate Legislation 2019 No. 175, Nature Conservation Act 1992, Department of Environment and Science, 2019. Available: `https://www.legislation.qld.gov.au`.

[31] Solargis, *Global Horizontal Irradiation Australia*, Solar Resource Map, 2019. Available: `https://solargis.com`.

[32] SolarGIS, *Solar resource map: Global Horizontal Irradiation (GHI), long-term average (2007-2020)*, 2021. Available: `https://solargis.com`.

[33] World Bank Group, *Global Solar Atlas 2.0*, Solar resource data: Solargis; Published by: Energy Sector Management Assistance Program (ESMAP), 2024. Available:`https://globalsolaratlas.info`.

[34] meteoblue AG, *Weather forecast and climate data (model-based) for Brisbane, Australia*. Available: `https://www.meteoblue.com/en/weather/week/-27.504N153.406E0_Australia%2FBrisbane`.

[35] Bureau of Meteorology (BoM), *Climate Statistics for Australian Locations: Monthly Wind Rose Data (Station 040520 - North Stradbroke Island)*, Australian Government, 2024. Available:`http://www.bom.gov.au`.

[36] Patterson, D. C., *Coastal Processes of Moreton Bay*, in: I. R. Tibbetts et al. (Eds.), *Moreton Bay and Catchment*, School of Marine Science, University of Queensland, 2013.

[37] Queensland Government, *Coastal Data System - Wave Monitoring: North Moreton Bay Station Annual Report 2024*, Department of Environment and Science, 2024. Available: `https://www.qld.gov.au`.

[38] Queensland Government, "Coastal Data System – Waves (North Moreton Bay)," *Queensland Open Data Portal*. Available: `https://www.data.qld.gov.au/dataset/coastal-data-system-waves-north-moreton`.

[39] Holthuijsen, L. H., *Waves in Oceanic and Coastal Waters*, Cambridge University Press, 2007.

[40] Lybolt, T., Neil, D., Zhao, J.-x., Feng, Y.-x., Yu, K.-F., and Pandolfi, J. (2011). Instability in a marginal coral reef: The shift from natural variability to a human-dominated seascape. *Frontiers in Ecology and the Environment*, 9, 154-161. Available: `https://doi.org/10.1890/090176`.

[41] Gibbes, B. et al., *Hydrodynamics of Moreton Bay*, in: *Moreton Bay and Catchment*, School of Marine Science, University of Queensland, 2014.

[42] Dennison, W. C. and Abal, E. G., *Moreton Bay Study: A Scientific Basis for the Healthy Waterways Campaign*, South East Queensland Regional Water

Quality Management Strategy, 1999.

[43] ISO 12944-2:2018, *Paints and varnishes — Corrosion protection of steel structures by protective paint systems — Part 2: Classification of environments*, International Organization for Standardization, 2018.

[44] W. Shi, C. Yan, Z. Ren, Z. Yuan, Y. Liu, S. Zheng, X. Li, and X. Han, "Review on the development of marine floating photovoltaic systems," *Ocean Engineering*, vol. 286, p. 115560, 2023. Available:https://strathprints.strath.ac.uk/87067/1/Shi_etal_OE_2023_Review_on_the_development_of_marine_floating_photovoltaic_systems.pdf.

[45] A. Ghigo, E. Faraggiana, M. Sirigu, G. Mattiazzo, and G. Bracco, "Design and Analysis of a Floating Photovoltaic System for Offshore Installation: The Case Study of Lampedusa," *Energies*, vol. 15, no. 23, p. 8804, 2022, doi: 10.3390/en15238804.

[46] Streamline Europe, *Solar panel cleaning and maintenance practices*. Available: https://www.streamline-eu.com/solar-panel-cleaning/.

[47] World Bank Group, ESMAP, and SERIS, "Where Sun Meets Water: Floating Solar Handbook for Practitioners,"Washington, DC: World Bank, 2019. Available:https://documents1.worldbank.org/curated/en/418961572293438109/pdf/Where-Sun-Meets-Water-Floating-Solar-Handbook-for-Practitioners.pdf.

[48] DNV, *DNV-RP-0584: Design, Development and Operation of Floating Solar Photovoltaic Systems*, DNV Recommended Practice, 2021. Available: https://www.dnv.com/.

[49] A. Sahu, N. Yadav, and K. Sudhakar, *Floating photovoltaic power plant: A review*, Energy Reports, vol. 6, pp. 241–258, 2020. Available: https://www.sciencedirect.com/science/article/pii/S2352484720313482.

[50] JinkoSolar, *Transparent Backsheet vs Dual-Glass: Advantages and Disadvantages*, PV Tech Industry Updates. Available: https://www.pv-tech.org/industry-updates/.

[51] P. J. M. Isherwood, "Reshaping the Module: The Path to Comprehensive Photovoltaic Panel Recycling," *Sustainability*, vol. 14, no. 3, Art. no. 1676, 2022. Available: https://www.mdpi.com/2071-1050/14/3/1676. doi: 10.3390/su14031676

[52] National Renewable Energy Laboratory (NREL), *Floating Photovoltaic Systems: A Review of Energy Potential, Environmental Impacts, and Design Considerations*, NREL Technical Report NREL/TP-6A20-83497, 2023. Available: https://docs.nrel.gov/docs/fy23osti/83497.pdf.

[53] Solarteknik, *STU Single Pile Ground Mounting Systems*, product datasheet, *ENF Solar Mounting System Directory*. Available: https://www.enfsolar.com/pv/mounting-system-datasheet/8082.

[54] Sahu, A., Yadav, N., and Sudhakar, K. *Floating solar photovoltaic systems: An applications guide*. Renewable and Sustainable Energy Reviews, vol. 63, pp. 816-824, 2016.

[55] Interesting Engineering, *Europe's largest floating solar farm is ready to produce power starting in July*, 2022. Available: https://interestingengineering.com/innovation/europes-largest-floating-solar-farm-july.

[56] International Electrotechnical Commission. *IEC 62790:2020 - Junction boxes for photovoltaic modules - Safety requirements and tests*. Geneva, Switzerland, 2020.

[57] International Electrotechnical Commission. *IEC 61701:2020 - Photovoltaic (PV) modules - Salt mist corrosion testing*. Geneva, Switzerland, 2020.

[58] Raj, B., Nordin, A. H., Othman, M. H., and Hwai, L. J., "Effect of UV exposure on bimodal HDPE floats for floating solar application,"*Energy Procedia*, vol. 100, pp. 278–281, 2016.Available: https://www.sciencedirect.com/science/article/pii/S2238785416302794.

[59] KOM Sistems, "Ponton,". Available: https://komsistems.ru/shop/izdeliya-iz-ps-polistirol/ponton-detail.html.

[60] Lee, J., Ko, H., Park, N., and Kang, G., "A Novel Accelerated Aging Test for Floats in a Floating Photovoltaic System,"*Coatings*, vol. 11, no. 11, Art. 1283, 2021. Available: https://www.mdpi.com/2079-6412/11/11/1283.

[61] Damen Shipyards Group, "HDPE Jetty 1203 – HDPE floating pontoon,"Damen, online technical product page, accessed Mar. 2026. Available: https://www.damen.com/vessels/pontoons-and-barges/hdpe-jetties/hdpe-jetty-1203.

[62] Y. Li, Z. Cheng, and Y. Gao, *Design and Analysis of Mooring Systems for Offshore Floating Structures*, Journal of Marine Science and Engineering, vol. 11, no. 1, p. 193, 2023. Available: https://www.mdpi.com/2077-1312/11/1/193.

[63] Lankhorst Offshore, *Deepwater mooring systems and synthetic fibre rope technology*. Available: https://www.lankhorstoffshore.com/markets/deepwater-mooring.

[64] SINTEF, *Floating Solar Photovoltaic Systems: Environmental and Technical Considerations*, SINTEF Energy Research, Norway. Available: https://www.sintef.no/en/publications/publication/0198cc807d44-df7ea3c2-5c6e-41de-89b8-753eb10eaf97/.

[65] Z. Cheng, Y. Gao, and Y. Sun, *Mooring System Design and Analysis for Floating Offshore Structures*, Journal of Marine Science and Engineering, vol. 8, no. 6, p. 431, 2020. Available: https://www.mdpi.com/2077-1312/8/6/431.

[66] Open Infrastructure Map, *Global energy infrastructure map*. Available: https://openinframap.org.

[67] University of Queensland, *Moreton Bay Research Station – Research Activities*. Available: https://moreton-bay.research.uq.edu.au/research.

[68] CIGRE Working Group B1.40. *TB 610 - Offshore Generation Cable Connections*. CIGRE, Paris, France, 2015.

[69] DCA (Drilling Contractors Association). *Technical Guidelines for Horizontal Directional Drilling (HDD)*. 4th Edition, 2017.

[70] International Electrotechnical Commission. *IEC 60502-2:2014 - Power cables with extruded insulation for rated voltages from 6 kV up to 30 kV*. Geneva, Switzerland, 2014.

[71] Worzyk, T. *Submarine Power Cables: Design, Installation, Repair, Environmental Aspects*. Springer Science & Business Media, Berlin, 2009.

[72] SolarPower Europe, *Floating PV Best Practice Guidelines, Version 1.0*, December 2023. Available: `https://helapco.gr/xoorigle/2023/12/Floating_PV_Best_Practice.pdf`.

[73] AccuSolar, *Solar PV Anchoring Explained: Critical Steps for Floating Systems*. Available: `https://www.accusolar.com/`.

[74] International Electrotechnical Commission. *IEC 62446-2:2020 - Photovoltaic (PV) systems - Requirements for testing, documentation and maintenance - Part 2: Grid connected systems - Maintenance of PV systems*. Geneva, Switzerland, 2020.

[75] IEA PVPS Task 13, *Floating PV Plants: Performance, Reliability and Operational Issues*, IEA Photovoltaic Power Systems Programme, Report IEA-PVPS T13-31:2025. Available: `https://iea-pvps.org/wp-content/uploads/2025/04/IEA-PVPS-T13-31-2025-REPORT-Floating-PV-Plants.pdf`.

[76] DNV. *DNV-RP-0584: Design, development and operation of floating solar photovoltaic systems*. Recommended Practice, Edition March 2021.

[77] The University of Queensland. *Moreton Bay Research Station (MBRS) - Facilities and Research Support Guidelines*. Available:`https://www.uq.edu.au`.

[78] AquaSim. *User Manual: Hydrodynamic Analysis of Floating Structures and Mooring Systems*. Aquastructures AS, Norway, 2023.

[79] Masters, G. M. *Renewable and Efficient Electric Power Systems*. 2nd Edition, John Wiley & Sons, Hoboken, NJ, 2013.

[80] Ueda, Y., et al. *Performance Analysis of PV Systems: Effect of Shading on Energy Yield*. Solar Energy Materials and Solar Cells, vol. 92, no. 11, pp. 1402-1408, 2008.

[81] International Electrotechnical Commission, *IEC 61215-1:2021 Terrestrial photovoltaic (PV) modules - Design qualification and type approval - Part 1: Test requirements*, Ed. 2.0, Geneva, Switzerland, 2021.

[82] W. Huang,"Research directions in synthetic fiber ropes applied as mooring lines for floating offshore wind turbines," *Renewable and Sustainable Energy Reviews*, vol. 225, p. 116183, 2026. Available: `https://doi.org/10.1016/j.rser.2025.116183`.

[83] Aquastructures, *AquaSim Theory Manual*, Available: https://aquasim.no/files/documentation/Theory_manual.pdf.

[84] DNV. *DNV-RP-0584: Design, Development and Operation of Floating Solar Photovoltaic Systems*. Recommended Practice, Edition March 2021. Available: https://www.dnv.com/.

[85] Y. Lian, Q. Chen, J. Zheng, J. Zhang, D. Sheng, L. Tao, S. Shu, W. Chen, M. Zhou, and S. C. Yim, "Effects of water level variation on the response of mooring systems for offshore floating photovoltaic platforms," *Ocean Engineering*, vol. 339, p. 122088, 2025. Available: https://doi.org/10.1016/j.oceaneng.2025.122088.

[86] A. L. N. da Silva, L. V. R. de Messano, D. M. da Cruz, H. F. M. Araújo, E. B. A. V. Pacheco, I. N. Bastos, A. Yao, R. Coutinho, and L. B. Zangalli, *Biofouling growth study in offshore mooring ropes*, Marine Pollution Bulletin, vol. 223, p. 118948, 2026. Available: https://www.sciencedirect.com/science/article/pii/S0025326X25014249.

[87] Aspiring Safety. *Rope Quality Standards*. Available: https://www.aspiring.co.nz/rope-quality-standards/.

[88] University of Southampton. *Ocean Engineering – Final Manuscript*. Available: https://eprints.soton.ac.uk/419455/1/Ocean_Eng_final_manuscript.pdf.

[89] L. H. Holthuijsen, *Waves in Oceanic and Coastal Waters*, Cambridge University Press, Cambridge, 2007.

[90] National Weather Service (NWS), *Explanation of Wave Height in the Nearshore Marine Forecast*, Available: https://www.weather.gov/dlh/WaveHeightExplanation.

[91] T. Sarpkaya and M. Isaacson, *Mechanics of Wave Forces on Offshore Structures*, Van Nostrand Reinhold, New York, 1981.

[92] R. G. Dean and R. A. Dalrymple, *Water Wave Mechanics for Engineers and Scientists*, World Scientific, Singapore, 1991.

[93] Rinnovabili.it, *Fotovoltaico galleggiante: guida al solare flottante*. Available: https://www.rinnovabili.it/energia/fotovoltaico/fotovoltaico-galleggiante-guida-solare-flottante/.

[94] Business Analytiq, *HDPE Price Index*. Available: https://businessanalytiq.com/procurementanalytics/index/hdpe-price-index/.

[95] Jinko Solar Australia. *Tiger Neo N-Type 72HL4-(V) Technical Datasheet*. Available: https://jinkosolar.com.au

[96] SolarQuotes Australia, *Jinko Solar Panels Review: Reliability and Market Performance in Australia*. Available: https://www.solarquotes.com.au.

[97] International Electrotechnical Commission. *IEC 61701:2020 - Salt mist corrosion testing of photovoltaic (PV) modules*. Geneva, Switzerland.

[98] Jinko Solar. *White Paper on N-type TOPCon Technology: Advantages in High-Temperature and High-Radiation Environments*, Jinko Solar Global Technical Division, 2023.

[99] F. M. Markos and J. Sentian, *Potential of Solar Energy in Kota Kinabalu, Sabah: An Estimate Using a Photovoltaic System Model*, Journal of Physics: Conference Series, vol. 710, no. 1, p. 012032, 2016. Available: https://doi.org/10.1088/1742-6596/710/1/012032.

[100] Australian Bureau of Statistics (ABS), *2021 Census QuickStats: North Stradbroke Island*. Available: https://www.abs.gov.au/census/find-census-data/quickstats/2021/301021550.

[101] Grouply, *Electricity Rates in North Stradbroke Island, QLD 4183*. Available: https://grouply.co/energy/compare-electricity-rates/north-stradbroke-island-qld-4183.

[102] SolarQuotes, *Solar Power Statistics for North Stradbroke Island (QLD 4183)*. Available: https://www.solarquotes.com.au/location/north-stradbroke-island-4183-qld/.

[103] Energex, *Peak Demand*. Available: https://www.energex.com.au/manage-your-energy/managing-electricity-demand/peak-demand.

[104] SolarQuotes, *Solar Power Statistics and Solar Irradiation Data for North Stradbroke Island (QLD 4183)*, Available: https://www.solarquotes.com.au/location/north-stradbroke-island-4183-qld/.

[105] CSIRO, *GenCost: Cost of Electricity Generation*. Commonwealth Scientific and Industrial Research Organisation, Australia. Available: https://www.csiro.au/en/research/technology-space/energy/gencost.

[106] Blue Economy CRC. (2026). *Offshore Renewable Energy Systems (ORES) Program: Floating Solar PV Research*. Available: https://blueeconomycrc.com.au.

[107] Bullivants. (2026). *Lifting & Rigging Equipment for the Marine Industry: Solutions for Offshore Mooring and Synthetic Ropes*. Available: https://www.bullivants.com/industry-innovations/marine.

[108] Graham, P., Hayward, J., & Foster, J. (2025). *GenCost 2024-25: Final report*. CSIRO, Australia. Available: https://doi.org/10.25919/yfbj-4k58.

[109] ABC Helical Piling. (2026). *Standard Unit Rates for Helical Anchors and Marine Piling Components*. Available: https://abchelicalpiling.com.au.

[110] Australian Energy Market Operator (AEMO). (2024). *2024 Integrated System Plan (ISP) for the National Electricity Market*. Available: https://www.aemo.com.au/energy-systems/major-publications/integrated-system-plan-isp/2024-integrated-system-plan-isp.

[111] L. Micheli, *Energy and economic assessment of floating photovoltaics in Spanish reservoirs: Cost competitiveness and the role of temperature*, Solar Energy, vol. 227, pp. 625–634, 2021.

[112] IRENA, *Renewable Power Generation Costs in 2023*, International Renewable Energy Agency, Abu Dhabi, 2024. Available: `https://www.irena.org/Publications/2024/Sep/Renewable-Power-Generation-Costs-in-2023`.

[113] Queensland Competition Authority (QCA), *Regulated Retail Electricity Prices for Regional Queensland 2024–25*, Queensland Competition Authority, Brisbane, 2024. Available: `https://www.qca.org.au/electricity/regional-prices/`.

[114] S. Deilami, H. A. Ozgoli, L. Callegaro, F. Taghizadeh and K. H. Kim, "Floating photovoltaic solar in Australia: A feasibility study," *Journal of Electronics and Electrical Engineering*, vol. 3, pp. 568–588, 2024,